The Role of Oscillatory Synchrony in Motor Control

By

Alexandros Georgios Androulidakis

Institute of Neurology
University College London

A thesis submitted to the University of London for a PhD in the Faculty of Science.

October 2008

Supervisor: Professor Peter Brown

ProQuest LLC
789 East Eisenhower Parkway
P.O. Box 1346
Ann Arbor, MI 48106-1346

ABSTRACT

Synchronized oscillations are manifest in various regions in the motor system. Their variable nature has increased the interest in the functional significance. Subcortical and cortical activity in the beta band is pathologically increased in Parkinson's disease (PD) – a state dominated by bradykinesia and rigidity. After the administration of the drug levodopa, beta activity and motor impairment are substantially decreased, while activity in the gamma band is increased. The function of beta bursts within the healthy motor system remains unknown. Recent evidence suggests that beta activity may promote the existing motor set and posture. In this thesis, with the use of positional hold tasks the role of beta activity on performance will be examined. It will be demonstrated that during bursts of beta synchrony in the corticomuscular system of healthy subjects there is an improvement in the performance of these tasks. The findings will argue that physiological fluctuations in the beta band in the motor system may be of behavioural advantage during fine postural tasks involving the hand. The present work will also examine the role of population oscillations in the parkinsonian basal ganglia. It will demonstrate that under levodopa treatment the pattern of movement-related reactivity in the subthalamic nucleus (STN) and the pedunculopontine nucleus (PPN) as well as the background activity in the PPN change significantly. It will be shown that levodopa suppresses movement-related beta activity around the time of self-paced movements and promotes the increase of movement-related gamma activity contralateral to the movement side, following the same pattern as in the non dopamine-depleted brain. This suggests that dopaminergic therapy restores a more physiological pattern of reactivity in the STN. In the untreated state, beta activity in the STN will be shown to be modulated during repetitive self-paced movements, reflecting a role in ongoing performance, but only when motor performance is maximal and not when bradykinesia occurs. Finally, it will be demonstrated that levodopa promotes alpha band activity in the PPN at rest and before movement suggesting a possible physiological role of this activity in this nucleus. These observations provide further insight in the function of neuronal synchronization in the motor system in health and disease.

Declaration of originality of thesis

Work towards this thesis was carried out at the Sobell Department of Motor Neuroscience and Movement Disorders of the Institute of Neurology, University College London under the supervision of Professor Peter Brown. The research projects were undertaken with the collaboration of other research fellows and clinicians as outlined in the acknowledgements and the authorship of publications arising from this work. The contents of this thesis are my own.

Signed:

Date:

PUBLICATIONS

Publications incorporated in this thesis

Androulidakis AG, Mazzone P, Litvak V, Penny WD, DiLeone M, Doyle-Gaynor LMF, Tisch S, Di Lazzaro V, Brown P (2008) Oscillatory activity in the pedunculopontine area of patients with PD. Exp Neurol 211(1):59-66.

Androulidakis AG, Brücke C, Kempf F, Kupsch A, Aziz T, Ashkan K, Kühn AA, Brown P (2008) Ampitude modulation of oscillatory activity in the subthalamic nucleus during movement. Eur J Neurosci 27(5):1277-1284.

Androulidakis AG, Khan S, Litvak V, Pleydell-Pearce CW, Brown P, Gill S (2008) Local field potential recordings from the pedunculopontine nucleus. Neuroreport 19(1): 59-62.

Androulidakis AG, Doyle LMF, Yarrow K, Gilbertson PT, Brown P (2007) Anticipatory changes in beta activity in the human corticospinal system and associated improvements in task performance. Eur J Neurosci 25(12): 3758-3765.

Androulidakis AG, Kühn AA, Chen CC, Blomstedt P, Kempf F, Kupsch A, Schneider G-H, Doyle LMF, Dowsey-Limousin P, Hariz M, Brown P (2007) Dopaminergic therapy promotes lateralized motor activity in the subthalamic area in Parkinson's disease. Brain 130(Pt2):457-68.

Androulidakis AG, Gilbertson T, Doyle LMF, Brown P (2006) Corrective movements in a postural hold task are more effective during periods of 13-35Hz oscillatory synchrony in the human corticospinal system. Eur J Neurosci 24(11): 3299-3304.

Additional published work during the PhD programme

Doyle Gaynor LMF, Kühn AA, Litvak V, Eusebio A, Pogosyan A, Androulidakis AG, Tisch S, Insola A, Mazzone P, DiLazzaro V, Brown P (2008) Suppresion of beta oscillations in the subthalamic nucleus following cortical stimulation in humans. Eur J Neurosci. In Press.

Kempf F, Brücke C, Schneider G-H, Kupsch A, Kühn AA, Chen CC, Androulidakis AG, Wang S, Vandenberghe W, Nuttin B, Aziz T, Brown P (2007) Involvement of human basal ganglia in off-line feed-back control of voluntary movement is modulated by dopamine. Curr Biol 17(15): R587-9.

ACKNOWLEDGEMENTS

My deepest gratitude and respect go to my supervisor Professor Peter Brown who believed in me and my abilities and gave me the opportunity to work with him. His inexhaustible enthusiasm, enduring guidance, and great effort to explain things clearly and simply make him the most interested and patient mentor I have known.

Special thanks to Dr. Louise Gaynor for her invaluable assistance with the experiments, her important contribution to my work, and her amazing personality.

Also, many thanks to Professor Marwan Hariz and Drs. Andrea Kühn, Tom Gilbertson, Elodie Lalo, Alek Pogosyan, Zoe Chen, Vladimir Litvak, Stephen Tisch, and Patricia Limousin for their valuable input to the work performed at the Institute of Neurology.

I am indebted to the collaborators from other universities, namely Professors Vincenzo DiLazzaro, Paolo Mazzone, Andreas Kupsch, Tipu Aziz, Steven Gill, and Keyoumars Ashkan for their support of the work that took place in Rome, Berlin, Oxford, Bristol, and London.

I am grateful to the A.G. Leventis Foundation and A.S. Onassis Foundation for their financial support.

Thanks to Leslie Goldmann, Keith Norman, and Vasiliki Zali for their moral support.

Finally, I would like to thank my parents for their love and encouragement during my long staying so far away from home.

TABLE OF CONTENTS

LIST OF FIGURES

LIST OF TABLES

ABBREVIATIONS USED

ACH	Acetylcholine	**LBT**	Low-beta trigger
CL	Confidence limits	**LFP**	Local field potential
CM	Corticomotoneuron	**MCP**	Metacarpophalangeal
CWT	Continuous wavelet transform	**MEG**	Magnetic resonance imaging
DBS	Deep brain stimulation	**MEP**	Motor eveoked potential
DA	Dopamine	**MPTP**	1-methyl-4-phenyl-1,2,3,6-tetrahydropyridine
EEG	Electroencephalography	**MRI**	Magnetic resonance imaging
EMG	Electromyography	**PD**	Parkinson's disease
ERD	Event-related desynchronization	**PET**	Positron emission tomography
ERS	Event-related synchronization	**PPN**	Pedunculopontine nucleus
FDI	First dorsal interosseous	**PSP**	Progressive supranuclear palsy
FFT	Fast Fourier transform	**SD**	Standard deviation
GABA	γ-aminobutiric acid	**SEM**	Standard error of the mean
GP	Globus pallidus	**SEP**	Somatosensory evekoed potentials

GPe	Globus pallidus externa
GPi	Globus pallidus interna
HBT	High-beta trigger
SMA	Supplementary motor area
SN	Substantia nigra
SNc	Substantia nigra pars compacta
SNr	Substantia nigra pars reticulata
STR	Subthalamic region
STN	Subthalamic nucleus
TANs	Tonically active neurons
TMS	Transcranial magnetic stimulation
VIM	Ventral intermediate nucleus of the thalamus
VTA	Ventral tegmental area

CHAPTER 1

Introduction

The last decade has experienced a renaissance in functional stereotactic neurosurgery for the treatment of patients with movement disorders. This has given scientists the opportunity to record deep brain activity from the permanently implanted stimulating electrodes and has shed more light on the physiology of deep brain structures such as the basal ganglia. For several years the explanation of the way the basal ganglia function and the pathophysiology of movement disorders had been heavily based on the Albin & Delong model which proposed the division of the basal ganglia into two distinct pathways that are differentially influenced by dopamine and have different effects on movement. More recently, concepts of basal ganglia function have considered that the basal ganglia as forming a network along with other structures around them such as the thalamus, the cortex, and the cerebellum and have proposed that it is the pattern of activity (i.e. neuronal synchronization) in this network that is the key concept behind the way these areas malfunction in disease.

The importance of oscillations and oscillating networks in motor behaviour has been extensively demonstrated in the literature. Oscillatory neuronal activity over different frequency bands has been found to be implicated in motor control in health as well as in motor deficits in movement disorders. The purpose of this thesis is twofold; on the one hand, to further understand the functional significance of neuronal synchronization between cortex and upper extremities in specific aspects of motor behaviour in health and, on the other hand, to elucidate the role of physiological oscillatory activity in basal ganglia nuclei that are therapeutic targets for functional neurosurgery, such as the subthalamic nucleus and the pedunculopontine nucleus, and their relation to parkinsonian symptomatology in on and off dopaminergic drug states. This introduction is aimed at providing a summary of the organization of the motor system in the cortex and basal ganglia and a literature review on the role of oscillatory activity in the motor system in health and disease.

1.1 The Cortical Motor System

The frontal lobe is formed by the prefrontal cortex which is related to cognitive functions and the motor cortex which is related to the control of movements. The

motor cortex constitutes of several distinct motor areas all of which are needed for motor control. Lesion of the motor cortex produces severe deficits in the voluntary movement of distal muscles in primates. The pattern of evolution among primates is an early development of cortical, voluntary control over the extremities for manipulation and exploration purposes. Additionally, in humans the highly developed motor cortex controls facial movements and vocalisation (Canedo, 1996).

The motor cortex sends projections to the ventral horn of the spinal cord through the pyramidal tract forming the corticospinal tract. Eighty percent of these neurons originate from the primary motor and premotor cortices. Additional corticospinal neurons from the primary and secondary somatosensory areas and the posterior parietal areas project to the dorsal horn of the spinal cord to regulate sensory inflow (Schieber and Baker, 2003). The pyramidal tract seems essential for the control of skilled locomotion, and the latter requires continuous sensory feedback and online postural corrections. The motor cortex has the ability to perform postural adjustments slightly before and during movement in response to sensory feedback because it has wide access to visual and somatosensory information via the pyramidal tract (Canedo, 1996). The motor circuit that links the cortex, the basal ganglia, and the thalamus is one of the five parallel pathways that have been identified as processing information between the cortex and the basal ganglia (Parent & Hazrati, 1995).

1.1.1 Primary motor cortex (M1)

The M1 area (or Broadman area 4) was the first cortical region to be associated with movement. It is considered to be the principal cortical region for voluntary motor execution. Lesions in that area produce force deficit and impairments in generating fractionated finger movements (Porter & Lemon, 1993).

The primary motor cortex consists of large pyramidal cells that, among other projections, connect monosynaptically to motoneurons in the spinal cord and use glutamate as their major neurotransmitter, and large basket cells (interneurons) that synapse pyramidal neurons and are mainly GABAergic. Forty percent of all pyramidal tract neurons originate in the M1, the majority of which project to the contralateral side of spinal cord and form direct monosynaptic connections with motor neurons that primarily innervate distal and proximal extremity musculature (Leonard, 1998). These cells, known as cortico-motoneurons (CM), have been shown to be

specialized for the use of distal muscles in movements requiring accuracy and not so much in automatic movements (Muir and Lemon, 1983). The CM connections can be classified as fast- and slow-conducting. The latter are usually more sensitive to peripheral feedback (Canedo, 1996). M1 neurons also project to brainstem, and from there to cerebellum, and to basal ganglia, and then to the thalamus, forming a cortico-thalamo-cortical loop.

The primary motor cortex receives input from the primary somatosensory area and from peripheral sensory afferents and subcortical structures via the thalamus. In fact, it is the target of somatotopically organized outputs from both the cerebellum and the basal ganglia (Hoover and Strick, 1999). The M1 is very responsive to this input and modifies or adjusts its output in relation to it, which indicates that it has the ability to operate via feedback mechanisms (Leonard, 1998).

In the mid-twentieth century, work conducted by Penfield with the use of electrical stimulation of M1 revealed a somatotopically organized representational map for muscles that resembled a deformed cartoon of the body (known as Penfield's homunculus). This implied that representations for each body part are orderly and point-to-point and that each part occupies non-overlapping cortical space. Later studies rejected the idea of a precise topography proposing that somatotopic organization of M1 is not a one-to-one mapping of body parts, muscles or movements but there is considerable overlap between muscle representations and that single M1 pyramidal neurons project to the spinal motoneuron pools of multiple muscles (Leonard, 1998; Schieber and Baker, 2003). A significant characteristic of this organization is that the majority of these cells innervate groups of either agonist muscles or antagonist muscles but rarely both. Pyramidal tract neurons appear to excite agonists and inhibit antagonists to the movement muscles via the inhibitory interneurons (Leonard, 1998). Such a functional organization is the basis of M1's capability for modification and plasticity (Sanes and Donoghue, 2000).

Populations of M1 neurons are in direct control of movement kinematics. Studies conducted by Evarts (1965, 1966) revealed that M1 pyramidal neurons of monkeys fired several hundred milliseconds before the monkey performed a wrist movement and in temporal relation to movement onset. Later on, Evarts showed that the neurons' firing rate varied in relation to changes in the exerted force applied on the wrist of the

monkey (Schieber and Baker, 2003). Subsequent studies demonstrated that these cells can change their level of activity based on speed or precision of movement, position of the limb, individual's intent, and complexity of the movement (Leonard, 1998). Because pyramidal neurons are active before movement, they appear to contribute to the establishment of the postural set required for the desired movement indicating that they can also operate in a feedforward mode. A recent study proposed that in fact posture and movement involve different neural control processes identifying two distinct populations of neurons in the primary motor cortex of the monkey that control either posture or movement (Kurtzer et al., 2005).

1.1.2 Premotor Areas

The frontal cortex of non-human primates contains at least six distinct premotor areas, the premotor cortex which can be functionally divided into the ventral and dorsal portions, the supplementary motor area (SMA), which can be divided into the caudal SMA (or SMA-proper) and the rostral SMA (or pre-SMA) and the cingulate motor area, which can be divided into the rostral, ventral and dorsal portions. Corresponding areas are also present in humans with the exception that the cingulate area is divided into the rostral and caudal zones. Premotor areas have some degree of somatotopic organization and project directly to the spinal cord. In fact, the number of corticospinal neurons in the premotor areas in primates has been reported to be equal or greater than the number of corticospinal neurons in the primary motor cortex. Neuronal efferents from the SMA-proper and cingulate cortex terminate in the ventral horn of spinal cord where the motoneurons are located (Dum and Strick, 2002).

Premotor areas are associated with activities that require series of goal-directed movements or remembered sequences. The dorsal premotor cortex is more directly involved in movements guided by sensory signals and due to its extensive interconnections with the M1 can influence the generation of movements. The ventral premotor cortex receives information on a motor target and sends output to achieve an action based on this information (i.e. control of hand movements required for the manipulation of objects) and even though it has little corticospinal projections by itself, it can still affect corticospinal output via it's connections with the M1 (Chouinard & Paus 2006; Hoshi & Tanji 2007). Cells within the premotor cortex respond to both visual and proprioceptive input from the upper extremities implying a

role of this region in proprioceptively or visually guide tasks and are active regardless of whether a movement is real or imagined (Leonard, 1998). Lesions in the premotor cortex produce weakness of proximal arm muscles and limb apraxia (Chouinard & Paus 2006).

The SMA-proper has been found to be active during motor tasks that require temporal sequencing, while pre-SMA is more closely related to processing or maintenance of relevant sensory information (Picard & Strick, 2001). Single neuron recordings in monkeys have shown that pre-SMA neurons are active when the monkeys are learning new movement sequences and well in advance of single movement initiation, while SMA neurons discharge during the execution of learned sequences (Rizzolatti & Luppino, 2001). Additionally, positron emission tomography (PET) studies in humans have shown that pre-SMA plays a role in movement preparation as it is usually active during self-initiated movements, while SMA-proper is a motor executive area as it is active during both self-initiated and externally-cued movements (Jenkins et al., 2000). Lesions in the SMA impair visuo-motor associative learning (Passingham et al., 2002). Finally, in humans the caudal cingulate cortex appears to be activated during simple motor tasks, whereas the rostral cingulate seems to be associated with tasks involving selection between two different responses (e.g. Go/No-Go tasks) and conflict monitoring (e.g. STOP tasks; Rubya et al., 2001; Picard & Strick, 2001).

The connectivity of premotor areas is a matter of ongoing study. There is a major subdivision between premotor areas according to their connectivity. The premotor cortex and SMA-proper receive their main cortical input from areas in the parietal lobe, connect with the primary motor cortex in a somatotopic manner, and send direct projections to the spinal cord. In contrast, pre-SMA receives its main cortical input from the pre-frontal cortex and does not send fibres to the M1 or the spinal cord, but connects with the brainstem. These anatomical data suggest that premotor cortex and SMA-proper receive abundant sensory input from the parietal lobe and use it to organise movement, while pre-SMA receives cognitive information from prefrontal cortex related to motor plans and use it in order to determine the conditions under which movement takes place (Rizzolati & Luppino, 2001).

1.1.3 Somatosensory Cortex

The primary somatosensory cortex (S1) is the main sensory receptive area for the sense of touch. It lies within Broadman areas 1, 2, and 3 and is composed of multiple sensory fields that exhibit somatotopy. Most neurons in S1 fire after movement onset in response to sensory feedback generated by the movement. Sensory input arrives to the S1 via the thalamus. The S1 projects to the M1, the premotor areas, the parietal sensory fields, the dorsal horn of the spinal cord, the brain stem, and the thalamus. The secondary somatosensory area (S2) lies within Broadman area 2 and responds to sensory input which is conveyed via the thalamus but, unlike S1, doesn't exhibit strict somatotopy. It has reciprocal connections with the S1, M1, and prefrontal cortex. Neurons in the S2 are involved in exploratory movements performed by hand and discrimination of objects' shape and texture (Leonard, 1998).

1.2 Anatomy of the Basal Ganglia

The basal ganglia consist of a group of neural structures that are highly interconnected and form reciprocal connections with large areas of cerebral cortex, the brainstem, and the thalamic nuclei. The striatum (caudate nucleus and putamen), the globus pallidus (GP), the substantia nigra (SN), and the subthalamic nucleus (STN) are agreed to be the principal components of the basal ganglia although the pedunculopontine tegmental nucleus (PPN) is lately referred to as part of them (Mena-Segovia et al., 2004, 2005). They have been historically thought of as being vital for movement yet they have no direct projections to the spinal cord (only via the brainstem and cortex) and receive no direct input from the periphery. By their projections to the thalamus, however, which receives sensory information from peripheral receptors, they can potentially influence all sensorimotor activity (Leonard, 1998). There is recent evidence that they also modulate cognitive and emotional information (Parent & Hazrati, 1995a; Leonard, 1998).

The basal ganglia are the largest subcortical structure in the human forebrain and a central part of a neuronal loop connecting most cortical areas with the frontal cortex (Bar-Gad et al., 2003). A simplified diagram of the connections of the basal ganglia would show a circuit that arises throughout the cortex and projects to the striatum and STN and from there via the GPi and SNr, the major basal ganglia output nuclei, to the thalamus and back to the cortex (Alexander et al., 1986; Parent & Hazrati, 1995a;

Nambu et al., 2005). It has been suggested that the majority of processing does not occur within the nuclei of the basal ganglia per se but in the synaptic interactions between them (Bar-Gad et al., 2003). In Figure 1.1 the anatomical connections within the basal ganglia – thalamocortical circuit are presented.

Figure 1.1 Anatomical connections of the basal ganglia. Black arrows depict inhibitory connections and red arrows excitatory connections. Adapted from Gatev et al., 2006.

1.2.1 The basal ganglia nuclei

1.2.1.1 Striatum

The striatum is the primary input structure of the basal ganglia and is divided into the dorsal and ventral striatum. The dorsal striatum forms the caudate nucleus and the putamen. The ventral striatum consists of the nucleus accumbens, the medial and ventral portions of the caudate and putamen. It receives excitatory glutamatergic input from most parts of the cerebral cortex (Parent & Hazrati, 1995a) and the thalamus (McFarland and Haber, 2000). The striatum consists mainly of GABAergic medium spiny neurons that form synapses with both intrinsic striatal neurons and afferent neurons from cortex, thalamus, and mesencephalon (Tisch et al., 2004) and of cholinergic interneurons (or tonically active neurons; TANs) that are associated with

reinforcement and incentive behaviour. Projecting spiny neurons are classically divided into those that express D1 dopamine receptors and those that express D2 receptors.

Due to its extensive connectivity with the entire cortical mantle, the striatum is functionally divided into sensorimotor, limbic, and associative areas. The sensorimotor area, which occupies the dorsolateral putamen and a small part of the caudate, receives input from primary motor cortex, primary somatosensory cortex, premotor cortex, and supplementary motor area (Parent & Hazrati, 1995a). The associative territory, which comprises mostly the caudate and the rostral putamen, receives input from areas of the frontal and temporal cortex, and from parietal, preoccipital and parahippocampal areas. The limbic area, which occupies the ventral striatum, receives input mainly from amydgala and hippocampus (Tisch et al., 2004).

The striatum also receives information from the intralaminar thalamic nuclei and small afferents from other thalamic nuclei. Among the intralaminar thalamic nuclei, the centromedian and parafascicular nuclei send the most prominent thalamic projections to the striatum using mainly glutamate as their major neurotransmitter. The sensorimotor territory receives input from the centomedian nucleus, which in turn receives input from the motor cortex, and the associative territory from the parafascicular nucleus, which receives input from the premotor cortex (Parent & Hazrati, 1995a).

The third major striatal input is from the midbrain dopaminergic cells from the SNc and the ventral tegmental area (VTA). The majority of nigrostriatal neurons make synapses with the medium spiny neurons that receive cortical afferents. Such an arrangement implies that dopaminergic input not only interacts with excitatory cortical input but also modulates it and the site of interaction is the striatum and the medium spiny neurons (Parent & Hazrati, 1995a; Tisch et al., 2004). In order to be able to understand the effect of dopamine on the striatum it is critical to mention the electrophysiological properties of the striatal neurons. In physiological conditions medium spiny neurons move between two membrane states, the down-state, where neurons are governed by inwardly rectifying K^+ currents and are kept hyperpolarized, and the up-state, where the neurons are depolarized in response to temporally coherent excitatory cortical input. Weak excitatory synaptic input typically fails to cause an up-

state transition and the neuron maintains its resting, down-state. When the neuron is in the down-state, dopaminergic activity is said to make the transition to the up-state more difficult by suppressing the response to weak excitatory input. In this way, dopamine helps striatum to filter out uncorrelated and "noisy" cortical input. On the other hand, when the neuron has achieved enough depolarization to switch to an up-state due to strong excitatory input, activation of dopaminergic receptors appears to enhance evoked activity. Also, dopamine is said to modulate striatal cholinergic interneurons because of its impact on acetylcholine release. D2 receptor agonists have been reported to decrease ACh release whereas D1 receptor agonists enhance it (Nicola et al., 2000).

In contrast to its diversity of its inputs, the striatum sends projections mainly to the globus pallidus (both interna (GPi) and externa (GPe)) and substantia nigra pars reticulata (SNr). Neurons from the sensorimotor territory project mainly to the pallidum, neurons from the associative territory project to the SNr, and neurons from the limbic territory to the ventral pallidum (Parent & Hazrati, 1995).

1.2.1.2 Subthalamic nucleus

The second major input structure of the basal ganglia is the STN which lies between the zona incerta dorsally and the cerebral peduncle ventrally. It consists of glutamatergic tonically active projection neurons and a small number of interneurons (Yelnik, 2002). Despite its size, the STN receives massive excitatory glutamatergic input from the motor and premotor cortex. The dorsolateral part, the sensorimotor territory of STN, receives input from the primary motor cortex and exhibits somatotopy with a clear organization of the face and upper and lower limbs cortical regions. This part is mostly implicated in skeletomotor behaviour and constitutes 80% of the STN. Its cells have also been shown to respond to somatosensory stimulation. The ventromedial part which is considered to be the associative territory receives afferents from the premotor and prefrontal cortex and is mostly implicated in associative aspects of movement. The medial tip of the STN is targeted by limbic cortices (Parent & Hazrati, 1995b).

Afferents also arise from the GPe to the rostrolateral part of the STN and they are mostly GABAergic and inhibitory (Parent & Hazrati, 1995b; Tisch et al., 2004). These projections seem to modulate STN's responsiveness to its other afferents and

especially those from the motor cortex. GPe by inhibiting STN cells keeps the subthalamic afferents inactive. This inhibition can only be overcome, if a strongly synchronized flow of information from multiple sources, such as the cortex, arrives (Parent & Hazrati, 1995b). Thalamic inputs to the STN involve glutamatergic projections from the parafascicular and centromedian nuclei; the former innervates the sensorimotor territory of the STN and the latter the associative one (Parent & Hazrati, 1995b). Finally, dopaminergic afferents arise from the SNc and cholinergic afferents from the PPN.

The STN exerts excitatory efferents to the globus pallidus in the form of parallel bands; one band that starts from the associative territory of the STN innervates GPi and another band that arises from the dorsolateral territory of the STN sends projections to GPe. Both bands seem to be linked with one another through short fibers. Substantia nigra is another target of STN efferents. Outputs from the ventrolateral STN are mainly innervating SNr, but some of these fibres would reach dopaminergic neurons of the SNc that invade the SNr suggesting that the STN affects both dopaminergic and non-dopaminergic cells in the substantia nigra. The functional and anatomical subdivision of the STN shows that it processes different types of cortical information simultaneously and conveys them to the rest of the basal ganglia in separate channels (Parent & Hazrati, 1995b). It was very recently shown that in the healthy human the STN may have connections with the PPN and via the brainstem extend down to the spinal cord (Aravamuthan et al., 2007).

1.2.1.3 Globus Pallidus

The globus pallidus lies medial to the putamen and rostral to the hypothalamus. It is functionally devided in sensorimotor, associative and limbic territories and anatomically separated into an internal segment (globus pallidus internus or GPi) and an external segment (globus pallidus externus or GPe) by a fiber tract, the internal medullary lamina (Mink, 2003; Tisch et al., 2004). Virtually all pallidal neurons use GABA as their major neurotransmitter. Although these neurons display the same anatomical, physiological, and biochemical characteristics (Bar-Gad et al., 2003), data on their connectivity clearly suggest that the pallidal segments are distinct entities (Parent & Hazrati, 1995a). The GPi is one of the major output nuclei of the basal

ganglia, while GPe is viewed as an intrinsic nucleus which is closely associated both physiologically and anatomically with the STN.

Globus Pallidus Internus

The GPi receives excitatory glutamatergic input from the STN, inhibitory GABAergic input from the striatum and the GPe, and dopaminergic input from the substantia nigra. Afferents from the striatum are the most abundant. Input from the STN is highly divergent such that each axon from the STN ensheathes many GPi neurons (Mink, 2003). The output from GPi is inhibitory and GABAergic. Axons from the GPi project to thalamic relay and intralaminar thalamic nuclei (Parent & Hazrati, 1995a; Bar-Gad et al., 2003). These efferents maintain the division of motor, associative and limbic information and project to the thalamus and from there to primary motor and premotor cortices (Tisch et al., 2004).

Globus Pallidus Externus

The GPe is part of the basal ganglia's intrinsic circuitry. Its inputs are GABAergic projections from the striatum and glutamatergic ones from STN and its outputs GABAergic projections to STN, striatum, SNr, and GPi. Thus, GPe not only forms reciprocal connections with the two input structures of the basal ganglia providing feedback inhibition to striatum and STN, but is also able to exert inhibitory effects on the main output nuclei of the basal ganglia providing feedforward inhibition (Mink, 2003). This circuitry suggests that GPe may act to control the effect of the striatal and subthalamic projections to GPi/SNr and hence control basal ganglia's output to the thalamus.

1.2.1.4 Substantia Nigra

Like the globus pallidus, the substantia nigra is divided into two segments, the densely cellular part called pars compacta (SNc) and the sparsely cellular part called pars reticulata (SNr).

Substantia nigra pars compacta

The SNc consists of large dopaminergic cells. These cells along with neurons from the VTA form the midbrain dopaminergic cell group (Bar-Gad et al., 2003). Midbrain dopaminergic neurons are divided into the dorsal tier, which consists of the dorsal

cells of SNc and the VTA, and the ventral tier, which consists of the densocellular group and the cells that project down to the SNr. This structure is very important for movement as these are the cells that degenerate in PD. The SNc receives inhibitory GABAergic input from the striatum and glutamatergic input from the dorsolateral part of the STN. It projects mainly to the striatum and to a lesser extent to the GP and the STN (Smith and Kieval, 2000). The division between sensorimotor, associative, and limbic information is maintained within the nigrostriatal network since the three territories of the striatum (see section 1.2.1.1) are innervated by the relevant territories of the midbrain dopaminergic cell group.

Substantia nigra pars reticulata

The SNr is the second major output structure of the basal ganglia. It is usually seen as an extention of the GPi but the two structures are separate entities. Like the GPi, the SNr consists of large inhibitory GABAergic projection cells. They project mainly to thalamic relay nuclei, superior colliculus, and the dopaminergic neurons of SNc (Tisch et al., 2004). The SNr receives afferent inhibitory input from the caudate nucleus and excitatory input from the STN (Bar-Gad et al., 2003).

1.2.1.5 Pedunculopontine Nucleus

The PPN lies in the upper brainstem limited rostrally by the SN and caudally by the locus coeruleus. It has not been traditionally considered to be part of the basal ganglia but recent studies suggest that the relationship between basal ganglia and PPN is unique compared to other structures as it can influence their activity substantially (Mena-Segovia et al., 2004). Hence, in this thesis, the PPN will be regarded as a functional part of the basal ganglia. The PPN is one of the main components of the reticular activating system and forms a part of the mesencephalic locomotor region. It plays important role in arousal, attention, learning, reward, locomotion, and in the generation and maintenance of REM sleep.

The PPN is divided into two parts, the pars compacta and the pars dissipatus. It is composed of cholinergic neurons that account 50% of the neuronal population of the PPN, glutamatergic, GABAergic, and dopaminergic neurons (Mena-Segovia et al., 2004, 2005). The cholinergic neurons have larger somata than the non-cholinergic. It has strong reciprocal connections with the STN, SN, and GP (Mena-Segovia et al.,

2005) and projections to the thalamus and spinal cord via the brainstem (Aravamuthan et al., 2007). Cholinergic and glutamatergic neurons of the PPN receive afferent inhibitory GABAergic input from the SNr and GPi. In turn, the PPN sends back cholinergic and glutamatergic projections to the SN and GP (Mena-Segovia et al., 2004, 2005). [It has to be noted that a recent study did not confirm a connection between PPN and SN in the healthy human (Aravamuthan et al., 2007)]. The STN sends glutamatergic efferents to the PPN which, in turn, provides cholinergic, glutamatergic and GABAergic innervations back to the STN. Efferents to the spinal cord are primarily from glutamatergic neurons in the pars dissipatus and efferents to the thalamus are primarily from cholinergic neurons (Pahapill & Lozano, 2000). Finally, connections with the motor cortex have been recently demonstrated in healthy humans (Aravamuthan et al., 2007). This extensive connectivity suggests that the PPN is a route for sensory input to thalamus and basal ganglia and, in turn, mediates their output and that it is engaged by corticostriatal and thalamic systems (Alderson & Winn, 2005).

1.2.2 The physiology of basal ganglia

Microelectrode recordings in normal primates have demonstrated tonic activity in all basal ganglia nuclei at rest albeit at a low level in striatum. Most basal ganglia neurons fire in an irregular, non-oscillatory manner and independent of the activity of surrounding neurons. Only a small percentage of basal ganglia neurons in the normal primate have been shown to discharge in an oscillatory mode implying that oscillatory activity in the basal ganglia is a weak but possibly normal phenomenon (Tisch et al., 2004). In awake performing primates, examination of the firing patterns of basal ganglia neurons has revealed that alterations in their activity occur with movements of different body parts, changes in specific elements of movement such as direction, velocity, and amplitude and in relation to passive versus active movements and movement onset versus rest. There is, of course, a considerable overlap of activity between cortical and basal ganglia structures during movement. It needs to be stressed, however, that movement-related changes in the neuronal activity of the basal ganglia tend to occur after the relevant alterations in cortical activity implying that much of the activity in the "motor circuit" may be initiated in the cortex (Alexander & Crutcher, 1990). The very small amount of electrophysiological studies of the animal PPN that have appeared in the literature have proposed that neurons in the PPN

change their firing rates in response to voluntary movement and the majority of them appear to fire in an irregular manner (Matsumura 2005). A recent study conducted in human PD and PSP patients reported similar electrophysiological characteristics for PPN neurons as previously documented in vitro and in vivo animal studies (Weinberger et al., 2008).

The relationship between basal ganglia activity and movement has been a subject of debate. Some studies have suggested a role for the basal ganglia in programme selection and movement planning rather than movement initiation itself, while others have highlighted a modulatory role for the basal ganglia in facilitation of desired motor programmes and cancellation of the non-desired ones (Tisch et al., 2004). Nevertheless, most basal ganglia neurons increase their firing rates after movement onset. Neurons in the basal ganglia have also been shown to respond to environmental signals that can be cues for movement responses or stimuli with emotional valence.

1.2.3 Basal ganglia- thalamo-cortical loop

The basal ganglia are involved in the processing of motor, associative, and limbic information through different circuits, all of which have a similar basic structure. They all originate from a specific cortical area depending on the type of function, pass through a distinct non-overlapping striatal area, project to the output structures of the basal ganglia (GPi and SNr) and then project back to the original cortical area through specific thalamic nuclei (Tisch et al., 2004). The connections from striatum to GPe, from GPe to STN and from STN to GPi are referred to as the "indirect" striatopallidal pathway to GPi to distinguish it from the "direct" striatopallidal pathway that runs from striatum to GPi (Alexander and Crutcher 1990).

The medium spiny neurons that constitute the indirect pathway are anatomically topographical, receive major projections from the cortex, and preferentially express D2 dopamine receptors. The population of striatal neurons that form the direct pathway express D1 dopamine receptors and they appear to be targets of the intralaminar thalamic nuclei (Wichmann & DeLong, 2003a). The distinction between the two subtypes of dopamine receptors has been particularly important for the pharmacological characterization of these pathways. Striatal dopamine activates the direct pathway and inhibits the indirect. Recent studies, however, have suggested that neurons projecting to the GPi and SN also can send axon collaterals to the GPe

(Nicola et al., 2000) and that striatal neurons can co-express different subtypes of dopamine receptors, implying that the two pathways are not as segregated as previously believed (Bar-Gad et al., 2003). The functional significance of this co-localisation of the receptor subtypes remains uncertain.

Activation of the indirect pathway results in inhibition of the thalamus and hence decreased input from the thalamus to the cortex. On the other hand, activation of the direct pathway disinhibits the thalamic nuclei and facilitates cortical drive. In addition to the cortico-striato-pallidal pathways, recent studies also emphasized the importance of the connections from cortex to STN and from STN to GPi, also known as the "hyperdirect" pathway, which is purely glutamatergic and has shorter signal conduction time from the cortex than the other two (Nambu, 2004; Nambu et al., 2005).

The basal ganglia-thalamo-cortical loop and motor control

The loop that links the motor cortex with the basal ganglia is vital for the control of voluntary movement. Since the beginning of the 1980s there have been efforts to explain the role played by basal ganglia in motor control in health and disease. Early models of basal ganglia focused on the segregated versus convergent processing of cortical information along the pathway. The former claimed that information that comes from different cortical areas is being processed separately through the pathway, while the latter suggested that the anatomical structure of the basal ganglia lead to an inevitable convergence of cortical information (Parent & Hazrati, 1995). The emerging evidence of the complexity of basal ganglia connectivity could not be accounted for by these early models. Albin and DeLong proposed that central to the function of these nuclei is the balance between the direct and indirect pathways whose activation depends on the action of dopamine and differentially affects information processing. Later modifications of this model tried to incorporate the role of inter-nuclei and intra-nuclei communication in the selection of single actions or action sequences (Bar-Gad et al., 2003). However, these theories fail to explain findings from electrophysiological and lesion studies on oscillations and synchronization and their complex association with PD symptoms (Section 1.3).

Motor Control and Functional Imaging Studies

In vivo patterns of cortical and subcortical connectivity have also been investigated with the use of imaging techniques such as tractography. These studies confirm specific cortico-basal ganglia connections (Behrens et al., 2003; Lehericy et al., 2004) and provide evidence of coexisting segregated and integrative basal ganglia-thalamo-cortical circuits (Draganski 2008). Functional imaging due to its excellent spatial resolution has been extensively used to study brain function during motor control and show how brain areas participate differentially in the control of movement and the processing of information. It has become evident from the previous sections that motor areas work in a networked cooperative manner to achieve meaningful movement. Regardless of the complexity or the characteristics of the motor tasks used in fMRI studies, multiple brain areas are activated. From the simplest to the most complex motor task, the participation of many cortical and subcortical brain areas is crucial in the planning and execution of the movement. For example, during simple motor tasks such as repetitive finger tapping, fMRI images reveal activation of the M1, premotor areas and the SMA, the basal ganglia (Reichenbach et al., 1998; Moritz et al., 2002), the thalamus (Moritz et al., 2000; Toma & Nakai, 2002), and the cerebellum (Reichenbach et al., 1998; Toma & Nakai, 2002). Therefore, prior knowledge of the anatomical connections between motor-related brain areas is necessary in order to understand functional imaging data.

Functional imaging has been successfully used to give important information on the temporal organization of motor areas and their involvement in the processing of different parameters of movement. Richter et al. (1997) proposed that during a delayed, cued complex finger movement task M1, premotor areas, and SMA were active during both movement preparation and movement execution but the intensity of activity in the M1 was weaker during movement preparation than during movement execution while activity in premotor areas and SMA was similar during both periods. Samuel et al. (1998) demonstrated that activation of prefrontal and premotor cortex was greater at the initiation of motor planning and preparation, but that significant activity in these areas was not maintained during continued repetitive movements with a joystick. In contrast, significant activation in contralateral sensorimotor cortex was maintained throughout the task Activation of the sensorimotor cortex has been correlated with basic movement parameters such as frequency and has been shown to

increase with the number of fingers used to perform a movement but stay unaffected by the complexity of the movement task (Sadato et al., 1996). In the same study premotor areas were shown to be activated with sequential movements and their activation correlated with movement frequency. On the contrary, prefrontal cortex has been shown to participate more in tasks requiring learning (Jueptner et al., 1997) and its activation is not modulated by basic movement parameters.

Basal ganglia activation has been inconsistently observed in functional imaging studies in humans. Activation of the putamen has been associated with performance of a simple repetitive joystick task (Samuel et al., 1998), learned sequences of finger movements (Juptner et al., 1997; Lehericy et al., 2006) and bimanual coordination (Kraft et al., 2007). Sequential movements and motor learning have been shown to recruit the striatum (Juptner et al., 1997). Lehericy and colleagues (2006) have also reported activation of the caudate nucleus, the STN, and the ventrolateral thalamus mainly when subjects were performing complex sequences of finger movements or externally paced high frequency finger tapping and not so much during simpler tasks. Finally, in a recent study where planning-related brain activity was tested under external and internal initiation modes, it was revealed that activation of the putamen occurs early and is much higher during the planning phase of the internally initiated rather than the externally initiated motor task similar to the activation patterns of the premotor cortical areas. This finding underlines the crucial role of the cortico-basal ganglia-thalamo-cortical network for self-initiated motor behaviour. In contrast, activation of the substantia nigra was observed under both, internally and externally guided conditions, strengthening theories of dopaminergic gating of motor sequence control (Boecker et al., 2008).

1.3 The Nature of Oscillations

Oscillation is a periodic feature of spontaneous neuronal activity that is usually detected by autocorrelation or power spectrum analysis (Boraud et al., 2002). A single cell or a neuronal network can oscillate in synchrony or out of synchrony with another cell or neuronal network. Hence, *oscillation* and *synchronization* are distinct properties of neuronal networks. Synchronized oscillations are responsible for the brain's ability to perform tasks that require the cooperation of different and separate brain areas (Boraud et al., 2005).

Neuronal network oscillations are prominent large-scale events generating bursts of neuronal firing at frequencies mainly between 1-200Hz. They have received considerable attention because they are implicated in interneuronal and long-range interareal communication. Their functional significance depends on their frequency content, anatomical location, and mechanisms of generation (Connors and Amitai 1997). Neuronal functions that seem to involve oscillatory activity include sleep-wakefulness cycle, cognitive functions, such as memory formation, perception, and attention, and motor control (see review by Schnitzler and Gross 2005). Neuronal oscillations are associated with the segregation of distributed neurons into coherent assemblies for combined processing and hence coordinated communication between different brain areas. The emergence of oscillations and their frequencies depend on cellular pacemaker mechanisms and neuronal network properties. In general, high frequency oscillations originate from a smaller neuronal population whereas low frequency oscillations include larger populations (Buzsáki and Draghun 2004).

Neuronal communication can be best investigated at the level of population activity by recording local field potentials (LFPs), which depict the average change in extracellular ionic currents generated by subthreshold and, to a lesser extent, suprathreshold depolarisation and hyperpolarisation in large groups of neurons close to the recording electrode. The LFP, i.e. a single oscillating population signal, implies that the local electrical elements in a group of cells must be synchronised to produce that oscillation. LFPs cannot record unsynchronized activity. Two oscillating populations of cells can be time locked, implying large scale synchronisation. LFP recording is an invasive technique which involves implantation of electrodes in the brain and is mostly used in animal studies or in studies with patients that undergo functional neurosurgery for the treatment of neurological disorders. Non-invasive investigation of oscillatory activity involves spatially summated LFP recordings by the use of electroencephalogram (EEG) and magnetoencephalogram (MEG). According to the classical nomenclature, oscillatory activity has been classified into distinct frequency bands: delta (<4Hz), theta (4-7Hz), alpha (7-12Hz), beta (13-35Hz), gamma (>40Hz), fast (100-200Hz) and ultra-fast (200-600Hz) activity (Schnitzler and Gross 2005).

1.3.1 The generation of LFPs in the cortex and basal ganglia.

The origin of the EEG, the spatially summated cortical LFP activity, is thought to be the synaptic currents in the dendrites of pyramidal neurons. The reason for this is because pyramidal neurons are more probable to produce macroscopic field potentials than other neurons due to their elongated morphology, columnar organization, and their cortico-cortical and thalamocortical connectivity. The polarity of the excitatory and inhibitory currents and the layer in which they are elicited produce positive and negative deflections in the EEG. A pyramidal neuron can be seen as a dipole source. The apical dendrites of pyramidal cells in the cerebral cortex are aligned perpendicular to the cortical surface and receive a diverse range of synaptic inputs. When an excitatory potential is initiated on the apical dendrite, current flows into the dendrite creating a current sink. Sequentially, the flow of the current along the dendrite and back out across the membrane at other sites creates a current source. The voltage fluctuations recorded at the surface of the brain are, in fact, the summed macroscopic sinks and sources created by the pyramidal cells in response to the balance of their inhibitory and excitatory input (Kandel and Schwartz, 2000).

In contrast to the well-characterized nature of LFP in layered structures, the neural basis of LFPs generated in non-layered structures such as the basal ganglia is not well-understood (Boraud et al., 2005). Cytoarchitectural investigations in human and animal STN and pallidum reveal elliptic dendritic fields which in the STN are aligned along the axis of the primary neuron and in the pallidum are orientated parallel to the lateral body of the nucleus (Brown and Williams, 2005). In spite of this anatomical organization that would predict to oppose the generation of strong fields, LFPs have been recorded from structures of the basal ganglia such as the STN, GPi, and striatum and they have been shown to reflect synchronous discharges in large populations of neurons. The fact that basal ganglia LFPs are linked to neuronal activity has been evidenced in rats (Magill et al., 2004) and healthy primates (Courtemanche et al., 2003) as well as in alert parkinsonian patients (Levy et al., 2002; Kühn et al., 2005). Authors such as Wennberg and Lozano (2003) have argued that it is possible that basal ganglia LFPs partially reflect volume conduction rather than subthreshold and suprathreshold activities of local networks. There is evidence, however, that would argue against this notion. Firstly, recording with the use of a bipolar montage seems to minimize the effects of volume conduction. Moreover, LFPs recorded across basal ganglia nuclei can exhibit a phase shift and/or polarity reversal which is not expected

for volume-conducted potentials (Brown et al., 2001; Boraud et al., 2005). Finally, strong coherence between single unit activity and LFP activity has been shown in many studies thus proving that LFPs are generated locally and are not the product of neuronal activity from distant structures (Kühn et al., 2005).

1.3.2 Oscillations in the LFP

The oscillatory activity in the EEG is determined by the intrinsic properties of the neurons and the co-operativity between neuronal corticocortical and thalamocortical networks. Neocortical neurons have the ability to generate oscillatory signals at certain frequencies or frequency bands. Such intrinsically generated oscillatory potentials have been recorded in frontal cortical pyramidal cells (Gray and McCormick, 1996) and interneurons in animals (Llinas et al., 1991). Neocortical neurons are also able to preferentially respond to sensory input that arrives at the same frequencies (Gutfreund et al., 1995). This latter property of neurons, called resonance, characterizes the frequency at which neurons respond best to inputs and indicates that a neuron can discriminate between its inputs frequency-wise and produce a response according to its frequency preference. Resonant neurons produce large responses only when they receive inputs near their resonant frequency (Hutcheon & Yarom, 2000). Pyramidal cells in animals have been found to exhibit two resonant frequencies depending on whether they are at rest or depolarized (Gutfreund et al., 1995; Hutcheon et al., 1996). Similar intrinsic properties have also been found in thalamocortical cells (Puil et al., 1994) and they appear to be crucial for the EEG changes that occur during sleep – wakefulness cycle. Thalamocortical cells can also modulate cortical activity by transmitting changes in basal ganglia oscillatory activity that reach the thalamus via GPi/SNr.

Co-operativity between inhibitory and excitatory neuronal networks is also thought to be another cause behind the generation of oscillations seen in the LFP. For example, studies in the olfactory system of rats have suggested that two populations of interacting neurons, as in the olfactory system, can produce oscillatory dynamics in which the inhibitory population lags the excitatory by a quarter of a cycle (Eeckman and Freeman, 1990). Similarly, research in the hippocampal formation in animals has suggested that inhibitory interneurons produce gamma oscillations in response to

excitatory drive and, in turn, entrain the pyramidal neurons to oscillate in the gamma band as a result to the imposed inhibition (Whittington and Traub, 2003).

Likewise, oscillatory activity seen in the basal ganglia LFP is determined by intrinsic properties of neurons and the co-operativity between neuronal populations within the basal ganglia or in the basal ganglia – cortical network. Studies in rats have shown that intrinsic currents and membrane properties are responsible for the low-frequency oscillations seen in STN neurons. Additionally, Magill et al (2001) have demonstrated that urethane-anaesthetised rats display coherent low-frequency oscillatory activity between STN and GPi which is coupled with slow-wave cortical activity. Ipsilateral cortical ablation abolishes the spontaneous oscillatory activity in the two basal ganglia structures suggesting the important role of the cortex for the generation of these oscillations.

In summary, the data from these studies confirm that oscillatory activity seen in the LFPs is a consequence of the intrinsic oscillatory characteristics of neurons within the population as well as the interconnection of neuronal populations that are not necessarily intrinsically oscillatory. Scalp EEG studies and, more recently, basal ganglia LFP studies have demonstrated that oscillatory synchronization is likely to play a role in motor functioning.

1.3.3 Oscillatory activity in the motor system

1.3.3.1 Oscillations in the alpha band

Rhythms in the alpha frequency band (7-13Hz) were firstly witnessed in the human scalp EEG by Hans Berger. It has been described as the most prominent oscillatory activity in the alert but mentally inactive brain, an "idling" rhythm that reflects a level of cortical inhibition and attenuates with increased attentiveness. However recent studies have started questioning the validity of this theory (Palva & Palva, 2007), but this will be discussed in chapter 7.

Sensorimotor Cortex

In the motor cortex, activity in the 7-13Hz band represents the alpha component of the mu rhythm. Studies in human subjects with no movement impairments have consistently demonstrated power suppression in this band during tasks activating the

sensorimotor cortex (Pfurtscheller 1989; Crone et al., 1998a). Because the change in alpha power has been diffuse and generalized without much somatotopical specificity during movement of different body parts and with no clear laterality during movement of different sides, it has been suggested that alpha suppression might reflect a widespread neuronal phenomenon that is not necessarily critical to movement but rather a supporting mechanism (Crone et al., 1998a).

Periphery

Alpha oscillations in the peripheral musclulature can be found in the form of motor fluctuations between 8 and 12 Hz, called physiological tremor. Physiological tremor is a complex somatomotor phenomenon caused by a combination of mechanical, reflex, and central mechanisms and is traditionally know to peak at ~10Hz at rest. Peak oscillation frequencies have also been reported at ~20Hz (frequency range 13-30Hz) during postural contractions against elastic resistance (see section 1.3.3.2; McAuley et al., 1997; Halliday et al., 1999). The occurrence of physiological tremors requires both motor unit synchronization and cortical drive to the muscle (Freund 1983).

Basal ganglia

Consistent with the previous findings in the motor cortex, it is uncertain whether neuronal synchronization in the alpha band plays a proper role in subcortical motor processing. Hence, it might be that movement-related changes predominantly obtained for beta-oscillations further extend to oscillatory activity as low as 8Hz (Brown and Williams, 2005), resulting in one broad frequency band.

1.3.3.2 Oscillations in the beta band

Activity in the beta band was first recognized in intracortical recordings of human motor cortex by Jasper and Penfield in 1949. They described a brain rhythm of ~20Hz whose amplitude was reduced before and during voluntary movement but remained intact at rest and during postural contraction. Recent studies confirm that synchronized oscillatory activity in the beta band is a common feature at various levels of the central motor system.

Sensorimotor Cortex

Microelectrode recordings in monkey sensorimotor cortex have demonstrated 20-30Hz oscillations (Murthy and Fetz, 1992; Sanes and Donoghue, 1993; Murthy and Fetz, 1996a; Baker et al., 1997; Donoghue et al, 1998; Fetz et al, 2000) that occur in bursts of about 4 – 30 cycles duration (Murthy and Fetz, 1996a) and are capable of synchronization over distances of up to 14mm (Murthy and Fetz, 1996a; Sanes and Donoghue, 1993) and between cerebral hemispheres (Murthy and Fetz, 1996a). This activity was mainly evident in the preparation period before movement onset but seemed to decrease during movement.

In the human motor cortex transcortical and intracortical recordings have demonstrated a peri-rolandic beta rhythm at about 20Hz which is decreased during self-paced movement execution but increases again 1s after movement (Crone et al., 1998a; Pfurtscheller and Lopes da Silva., 1999; Pfurtscheller et al., 2003). These movement-related fluctuations, termed event-related desynchronization (ERD) and event-related synchronization (ERS) respectively, constitute changes in synchrony in the beta band (power) of the underlying neuronal populations and exhibit somatotopical specificity according to the body part moved (Crone et al., 1998a). The suppression of beta band activity occurs in the sensorimotor cortex contralaterally prior to movement but becomes bilateral during movement, while the rebound in beta activity occurs contralaterally after movement (Crone et al., 1998a; Pfurtscheller and Lopes da Silva., 1999; Pfurtscheller et al., 2003). These findings suggest that temporal changes in oscillatory synchronisation are likely to have functional significance in motor control.

Periphery

Cortical beta activity has also been recorded indirectly in the periphery as a corticospinally driven synchronization within and between muscles both in primates (Baker et al., 1997) and in humans (Farmer et al., 1993; Conway et al., 1995; Gibbs et al., 1995; Salenius et al., 1997; Kilner et al., 1999). It has been demonstrated that these oscillations observed in the periphery are coherent with the motor cortex and are modulated in a task-dependent way (see section 1.3.4; Kilner et al., 1999; Kilner et al., 2000).

Beta activity can also be recorded in the form of physiological tremor or microtremor. It has been shown that microtremor at ~20Hz can be attributable to motor unit

synchronization (McAuley et al., 1997; Halliday et al., 1999) which in turn is likely to be caused by synchronization due to common input to efferent fibres from the motor cortex (Farmer et al., 1993; Baker et al., 2001). It should be noted, though, that motor unit synchronization can also occur due to peripheral resonance phenomena independently of oscillatory drive by the cortex (Moritz et al., 2005; Christou et al., 2006).

Basal Ganglia

Oscillations in the striatum have a strong relationship to activity in the cortex. Beta oscillations have been observed in the striatum of freely moving rats (Berke et al., 2004) and awake behaving monkeys demonstrating a task-related specificity (Courtemanche et al., 2003). It has also been shown that EEG activity can be closely linked to single-neuron or LFP activity in the STN in rats (Magill et al., 2000, 2004) and in monkeys (Wichmann et al., 2002) and in GPe in monkeys (Gatev et al., 2006). LFP recordings from the STN in PD patients undergoing functional neurosurgery have demonstrated prominent beta oscillations (see section 1.3; Brown et al., 2001; Levy et al., 2002; Williams et al., 2002; Silberstein et al., 2003, 2005) which have been found to be locked to the discharge of neurons in the STN (Levy et al., 2002; Kühn et al., 2005). In these studies, subthalamic beta oscillations are coherent with cortical beta activity and their power fluctuates during movement.

Although it is very likely that the oscillatory activity in the STN LFP is locally generated, this does not imply that it is autonomous. Previous studies have demonstrated coherence between activities at various nodes in the basal ganglia-cortical loop (Brown et al., 2001; Cassidy et al., 2002; Williams et al., 2002; Fogelson et al., 2006) and have concluded that there is a net drive to the STN from the cortex in the beta band. However, it should be stressed that these findings are derived from analyses of spectral phase, which do not allow for bidirectional flow (Cassidy and Brown, 2003), and have only considered resting patterns of functional connectivity. The predominant direction of information flow may of course change with state, as has been demonstrated in rats (Magill et al., 2006).

Other motor areas

Beta oscillations also occur in the primary sensory cortex (Brovelli et al., 2004), the parietal areas (Murthy and Fetz, 1992; Brovelli et al., 2004), the thalamus (Paradiso et al., 2004) and the cerebellum (Courtemanche et al., 2003) during isometric contraction and movement preparation.

1.3.3.3 Oscillations in the gamma band

Rhythmic activity in frequencies above 30Hz, the so called gamma band, was first described by Jasper and Andrews in 1938. It has mostly been implicated in "top-down" sensory processing (Tallon-Baudry and Bertrand, 1999; Engel et al, 2001; Buzsáki and Draguhn, 2004) and motor behaviour (Pfurtscheller et al., 1993; Salenius et al., 1996; Crone et al., 1998b; Pfurtscheller et al., 2003). Recent studies suggest that oscillations in the gamma band can be recorded at various levels of the motor system.

Sensorimotor Cortex

The oscillatory activity that has mostly been studied in the human EEG/MEG in the gamma band is the 40Hz activity, which has been found to increase in the sensorimotor cortex slightly before and during self-paced finger movements (Pfurtscheller et al., 1994; Salenius et al., 1996) and during tactile discrimination tasks (Sauvé 1999). Intracortical LFP recordings have furthered the above findings by suggesting that not only low (~40Hz) but also high gamma (70-90Hz) ERS may also be observed during a motor response (Crone et al., 1998b; Pfurtscheller 2003). These studies have shown lateralization and appropriate somatotopy during movement of different body parts and they have pointed to possibly independent neurophysiological mechanisms between low and high gamma bands. Gamma oscillations have also been observed in the LFPs in primates performing self-paced grasping movements or visually-guided reaching tasks (Murthy and Fetz, 1996a; 1996b). EEG and MEG are extremely limited tools for the investigation of the gamma band oscillatory activity above 40Hz because of very poor signal to noise ratios due to the inverse relationship between frequency and amplitude of oscillations.

Periphery

Low gamma (~40Hz) oscillations can been recorded in the EMG of contralateral forearm muscles during maximal contraction and slow extension movements of the wrist. It has been shown that this activity, also called the Piper rhythm, is coherent

with the sensorimotor MEG signal with appropriate somatotopy and movement-related modulation (Brown et al., 1998).

Basal Ganglia

LFP recordings from the STN in PD patients on levodopa medication have demonstrated gamma oscillations (Brown et al., 2001; Cassidy et al., 2002; Williams et al., 2002; Obeso et al., 2004; Fogelson et al., 2005) that are coherent with gamma activity in the GPi and cortex before and during motor response (Brown et al., 2001; Cassidy et al, 2002). LFP oscillations in this band have been found to be synchronized with the discharge of neurons in the upper STN and bordering zona incerta confirming their physiological role in the basal ganglia (Trottenberg et al., 2006). In further support of this, gamma oscillations have been recorded in the basal ganglia of healthy rats during task performance (Brown et al., 2002; Masimore 2005; DeCoteau et al., 2007a). Previous studies have demonstrated that gamma activity in the STN has a temporal lead over that in cortex (Williams et al., 2002) but this finding is based upon analyses that assume unidirectional flow.

1.3.4 Physiological significance of oscillations in the motor system

Beta oscillations in muscle activity represent the reverberations of synchronized cortical oscillatory activity over this band (Schnitzler & Gross, 2005). During maintained isometric contractions cortico-muscular coherence in the beta range has been found to be enhanced (Conway et al., 1995; Salenius et al. 1997; Baker et al., 1999). Kilner et al. (2000) demonstrated that coherence occurred only during the hold phase of a precision grip task but not during the ramp phase and that its increase scaled with the level of compliance experienced in the succeeding holding contraction. Although initially proposed that the degree of phase locking between the lower and upper motoneurons in the beta range was dynamically modulated according to the properties of the object being manipulated (Kilner et al., 2000), Riddle and Baker (2006) later suggested that it was not the compliance of the object being gripped but the size of the movement of the finger during the ramp phase that correlated most with the phase relationship (and coherence) between cortex and muscle. The larger the movement of the digit was, the higher the cortico-muscular coherence during the forthcoming hold phase. Should that be the case, then cortico-muscular coherence may be a sensorimotor, not solely motor, process and may be

defined by a mixture of afferent and efferent phenomena (see also Riddle and Baker, 2005; Baker et al., 2006). It has to be noted, however, that any parametric relationship between beta activity and load compliance and/or digit displacement was demonstrated in the presence of confounding changes in peripheral feedback.

Together these observations suggest that beta activity might have a physiological role in tonic contractions by actively promoting processing related to postural activity, while compromising local motor processing related to new movements. This hypothesis received recent support from an experiment in healthy subjects in which movements triggered during or slightly after periods of elevated beta band synchrony in the finger microtremor were slowed, while transcortical (M2) stretch reflexes that may reinforce existing posture were potentiated (Gilbertson et al, 2005). Up-regulation of the transcortical stretch reflex would be expected to promote an effective postural motor response, but this was not explicitly demonstrated in this study.

The increase in the M2 component of the stretch reflex during periods of beta bursts in the cortico-spinal system could be due to changes in motor and/or sensory processing, suggesting a role for beta activity in the sensorimotor integration. This was supported by Lalo and colleagues (Lalo et al., 2007) who showed that the amplitude of the N20 and P30 components of the centro-parietal SEP elicited by median nerve shocks was increased during periods of bursts of beta activity in the EEG and increased cortico-muscular coherence in the same band.

Thus, cortical oscillations in the beta band may play a role in sensorimotor integration, reinforcing the postural contraction by up-regulating the effects of sensory inputs, such as stretches or peripheral nerve shocks. However, no behavioural advantage of beta bursts was established in the above mentioned studies and the behavioural context in which beta bursts occur remain unclear.

➡ Aim: To investigate the behavioural circumstances under which the beta bursts occur in the healthy corticospinal system and their functional significance in motor control.

The physiological significance of gamma oscillations has mainly been studied with relation to cognitive functions. In the motor system, oscillatory activity at 40Hz has been recorded during maximal contraction, while activities at higher frequencies

(>60Hz) occur during self-paced movement (section 1.1). Recent studies have indicated that gamma oscillations in the motor system support normal movement and are essentially prokinetic, but this will be discussed in more detail in section 1.6.

1.3.5 Physiological significance of coherence in oscillatory activity in the motor system

The ability of neuronal populations to oscillate in synchrony is the key mechanism behind neuronal communication (Fries 2005). Oscillations tend to show coherence between functionally related but spatially distant sites and, hence, link single neuron activity to behaviour (Buzsaki & Draguhn 2004). This characteristic of oscillations allows distant neuronal networks to become temporally coupled and then trigger a physiologic output. Several studies have demonstrated coherence between areas involved in visuo-motor tasks where the cooperation between early visual areas, parietal cortex, motor cortex, and spinal cord is essential. For example, Schoffelen and colleagues (2005) recently showed that the strength of gamma band coherence between cortex and spinal cord neurons, but not the gamma band cortical motor power, was highly correlated with subjects' performance in a simple reaction-time task thus confirming that changes in local and inter-regional oscillatory coupling are likely to have a role in determining physiologic motor output. Pascal Fries (2005) has also proposed that neuronal communication is rendered not only more efficient but also more selective through coherence. Neuronal ensembles involved in a task are entrained to the selected or preferred rhythm and, at the same time, are rendered "deaf" to the non-preferred ones. Finally, the same research team has recently highlighted the importance of phase relations in effective connectivity suggesting that neuronal groups have greater influence on each other when neuronal synchrony in one group is in phase with neuronal synchrony in another group (Womelsdorf et al., 2007).

In sum, these findings suggest that regional and coupled changes in oscillatory activity in the motor system are likely to be of functional significance. It is therefore possible that abnormal alterations in oscillatory activity in the motor system are highly possible to contribute to the symptomatology seen in movement disorders, such as Parkinson's disease.

1.4 Parkinson's Disease

Parkinson's disease (PD) was first described by James Parkinson in 1817. It is a debilitating, chronic, neurodegenerative disorder that affects more than six million people worldwide and 1.5 million people in Europe. The average age of onset is in the sixth decade, but early onset is seen in cases of juvenile parkinsonism even from the third decade. It is characterized by motor disturbances such as tremor, rigidity, bradykinesia or akinesia, and non-motor features, such as dementia, depression, and dysautonomia especially in advanced stages of disease. It is associated with progressive neuronal loss of the substantia nigra pars compacta. Early diagnosis is important if patients are to be relieved of symptoms with currently available therapies.

At present there is no biological hallmark for the diagnosis of the disease, so its diagnosis is based on clinical manifestations. Tremor features in the majority of cases and usually begins unilaterally. It is present at rest with a frequency of 4-6Hz but a faster tremor of around 8-10 Hz may appear on action or during postural contraction. Rigidity is reported as stiffness and cramp-like pains in the limbs and if it coexists with tremor, it may appear as the "cog-wheel effect". Bradykinesia describes slowness of movement and is often the most disabling feature of PD. The diagnosis of PD can be made if two of those features coexist. Although this sounds straightforward, the differential diagnosis versus other forms of parkinsonism can be difficult, especially early in the disease when signs and symptoms of different forms of parkinsonism tend to overlap. Clinical subgroups can be divided into tremor-predominant and akinetic/rigid-predominant variants. Decline is more rapid in older than in middle-aged onset patients, and bradykinesia, rigidity, and balance problems predominate over tremor. Also, progression of motor deficits is slower in tremor-predominant patients than in akinetic/rigid patients, and young-onset patients have more preserved cognitive function and fewer falls than subjects with late disease onset. The prominent axial symptoms such as gait disturbance (initiation, execution, and termination), gait freezing, and postural instability that usually occur in elderly patients have been suggested to be accounted for by additional non-dopaminergic processes. However, they may also occur early in the disease.

1.4.1 Pathology

The main pathological finding in PD is the loss of pigmented neurons in the midbrain, more specifically those in the SNc with the presence of Lewy bodies. These are intracytoplasmic eosinophilic inclusions that consist of proteins such as alpha-synuclein and ubiquitin. Loss of dopaminergic neurons in SNc leads to a considerable loss of striatal dopamine content. Deficiency of striatal dopamine is the major biochemical feature of PD and is thought to account for the motor symptoms seen in PD. Dopamimenrgic denervation is also evident in other structures of the basal ganglia such as the STN and the GPi, the thalamus, and the cerebral cortex (Quinn, 2003). Oxidative stress is thought to be critical in the neurodegeneration caused in PD. It has been proposed that nigral cells in PD are more prone to oxidative stress since they contain high levels of iron, which is known to facilitate oxidation, and low levels of glutathione, which is know for its antioxidant effects (Fukae et al., 2007).

1.4.2 Pathophysiology

It was mentioned earlier (section 1.2.2) that the cortico – basal ganglia – cortical pathway is a feedback loop that is essential to stabilize motor control. Excitatory glutamatergic input connections run from the cortex to the striatum which in turn sends nerve fibers to dopaminergic neurons in the SNc. The dopaminergic neurons connect back to the striatum which projects down to the GPi and STN. From there, nerve fibers project to the motor cortex via the thalamus. All the nerve fibers leading from the striatum to the pallidum and from there to the thalamus are GABAergic. Neurotransmission from the striatum to the SNr also involves GABA at the SN nerve terminals. This feedback loop works through a finely tuned balance of excitatory and inhibitory neurotransmitters.

Destruction of the striatonigral dopaminergic neurons causes immediate dopamine deficiency and leads to excessive excitation by acetylcholine. The imbalance between inhibition and excitation is also enhanced by the fact that medium spiny neurons have higher probability of depolarization during the up-states probably due to the absence of modulation of their inwardly rectifying K^+ currents by dopamine (Nicola et al., 2000). All these augment the inhibitory GABAergic output of the striatum increasing the activity in the indirect pathway and decreasing it in the direct. This results in the disinhibition of the STN and GPi/SNr and the pathological increases in the firing rate of STN neurons and GABAergic output neurons. As a consequence, the activity of the

thalamocortical feedback loop is markedly reduced, leading to impaired motor function (Wichmann & DeLong 2003b). By the time the first clinical symptoms (e.g., tremor or hypokinesia) become obvious, 80% of these dopaminergic cells have already been destroyed (Schatton & Lyssy, 2000).

The excessive excitation of the basal ganglia output neurons seen in PD due to dopaminergic deficit is also enhanced by the constant glutamatergic cortical input that reaches the STN through the hyperdirect pathway. It has been shown that under normal conditions STN neurons fire in response to cortical input without necessarily affecting the discharge rates of GP and SNr neurons (Magill et al., 2000). In PD, processing at the level of STN integrates two pieces of information, i.e. excitation that comes from the hyperdirect pathway and disinhibition that comes from the direct and indirect pathways, confirming the importance of a wider network in the generation of PD pathophysiology (Hammond et al., 2007). According to the dynamic model of cortico - basal ganglia functions (Nambu et al., 2005), when a voluntary movement is about to be initiated by cortical mechanisms, aberrant increased activity through the hyperdirect and indirect pathways prevails and suppresses not only unwanted motor programs but also the selected motor program. Additionally, due to the decreased activation of the direct pathway, smaller areas of the thalamus and cortex are disinhibited for shorter period of time than in the normal state. Thus, the selected motor program cannot be released, resulting in bradykinesia / akinesia.

Brainstem areas such as the PPN are also directly involved in the development of PD. Akinesia and gait freezing that develop in later stages in PD are thought to be the result of PPN degeneration. In the MPTP-treated primate, the overactive inhibitory GABAergic projections from the GPi and SNr suppress the activity of the PPN leading to hypokinesia (Pahapill & Lozano, 2000; Mena-Segovia et al., 2004). In agreement with this, experimental lesions of the PPN in normal monkeys caused parkinsonian akinesia (Kojima et al., 1997), while pharmacological blockade of the inhibitory input to PPN reduced akinesia in MPTP-treated primates (Nandi et al., 2002a). On the other hand, PPN neurons were shown to exhibit increased activity in dopamine-depleted parkinsonian rats and this was attributed to the hyperactivity of the STN, as a subsequent lesion of the STN restored baseline levels of neuronal activity in the PPN (Breit et al., 2001). It is still unknown which PPN neurons increase their firing in response to increased input from STN and which neurons decrease their

firing in response to increased input from SNr and GPi and how these inputs affect the functions of different types of PPN neurons (Mena-Segovia et al., 2004). That dopaminergic neurotransmission affects PPN function was demonstrated by Mena-Segovia & Giordano (2003) who showed that amphetamine, a dopaminergic agonist, injected in the striatum of rats could produce PPN disinhibition.

Electrophysiology

Microelectrode recordings have demonstrated that dopaminergic deficiency in MPTP-treated primates is associated with an increase in the firing frequency in the STN, GPi and SNr and an increase in the number of bursting cells in the STN and GPi. Reinstitution of dopamine produced a decrease in the firing rate of the GPi and SNr cells and reduced the number of bursting GPi neurons confirming the previous finding. Similar results have also been reported by studies with patients that undergo surgical treatment for PD (Boraud et al., 2002). Microelectrode recordings of STN and GPi units after administration of the non-selective dopaminergic agonist apomorphine have shown a similar increase in the mean rate of GPi units but no change in the rate of units in the STN (Levy et al, 2001). Furthermore, oscillatory temporal patterns of single neurons in STN and GPi with the same frequency regimen as that of the tremor or its higher harmonics have been noted to emerge with the onset of tremor in the MPTP-treated monkey but there was no covariation between oscillatory synchronization and tremor reported (Bergman et al., 1994; Raz et al., 2000).

On the other hand, electrophysiological recordings in GPe have had more inconsistent results with some studies reporting decrease in the firing frequency of GPe neurons in the MPTP-treated primate (Raz et al., 2000) and in human patients and some others reporting no change in the MPTP-treated primate (Boraud et al., 2001). Again, dramatic increases in oscillatory activity in GPe at tremor frequencies have been found but without significant covariation between the average frequency of oscillations and tremor (Raz et al., 2000). Similarly, simultaneous recordings of neurons in the GP and the cholinergic striatal TANs have revealed an increased rate of synchronized oscillatory bursts at double the tremor frequencies which was then reduced after reinstitution of dopamine. There have been no conclusive results from

studies on the electrophysiological characteristics of the SNc of primates that could shed light on the physiology of this nucleus in PD (Boraud et al., 2002).

1.4.3 Aetiology

The cause of PD is not known. At the beginning of the 20th century due to a pandemic of encephalitis lethargica it was proposed that it might be caused by a virus but such a suggestion was never confirmed. Environmental factors that have been implicated with the disease include toxins such as the pesticide paraquat and the 1-methyl-4-phenyl-1,2,3,6-tetrahydropyridine (MPTP). MPTP itself is not an active toxin but it is converted by monoaminoxidase B into MPP (1 – methyl – 4 – phenylpyendinium) which is taken up into dopaminergic neurons and leads to oxidative stress and cell death. This model of PD shows that environmental toxins can cause selective nigral cell death (Quinn 2003).

At least 10% of the PD cases have been linked to a genetic defect. Initial clinical studies showed no inheritance pattern between identical twins, one of whom had PD. Later studies however in which both twins were subjected to PET scans revealed that abnormalities in both clinically normal and PD sufferer twin pairs (Quinn 2003). Several genes and chromosomal loci have been shown to account for familial forms of parkinsonism and designated as PARK1 to 13. Five autosomal dominant (PARK1, 3, 5, 8, and 13), four recessive (PARK2, 6, 7, and 9), one X-linked (PARK12), and two forms with a still unknown mode of transmission (PARK10, 11) have been found to date. Moreover, mutations in some other genes have been linked to parkinsonism in a small number of families or in individual cases but have not been given a PARK locus number. They have all been shown to be responsible for abnormal protein production. Although the exact function of the implicated proteins might still be obscure, they all seem to be involved in the degeneration of dopamine-releasing axon terminals in the striatum and of corresponding neurons in the substantia nigra (Klein & Schlossmacher 2007).

1.5 Parkinson's disease and its treatment

Treatment methods in PD involve only symptomatic relief that improves the patient's quality of life for a significant period of time but it does not appear to retard progression of the disease. These involve pharmacological treatment that aims to

restore the chemical imbalance caused by the destruction of dopaminergic neurons and deep brain stimulation (DBS) of basal ganglia nuclei with implanted macroelectrodes. The latter has enabled direct recordings from the human basal ganglia.

1.5.1 Pharmacological Treatment

The only available pharmacological treatment for PD aims to reduce the severity of symptoms and maintain motor function as long as possible. Reinstitution of dopaminergic neurotransmission seems to be the only effective form of treatment. Among the drugs that regulate dopamine, levodopa, the biochemical precursor of dopamine, remains the gold standard and is used by most patients. Usually, l-dopa is administered with extracerebral decarboxylase inhibitors such as carbidopa, which is combined with levodopa in Sinemet, and benserazide, which is combined with levodopa in Madopar, in order to reduce peripheral side effects that might occur due to conversion of l-dopa to dopamine in the periphery. However, up to 80% of patients develop severe motor complications, such as levodopa-induced dyskinesias, after five to ten years of l-dopa use, which clearly limits the therapeutic efficacy of the drug (Alonso-Frech et al., 2006). In addition, with time, the immediate effects of levodopa last for shorter periods leading to increasing fluctuations in disability throughout the day in relation to the timing of levodopa intake (Quinn 2003). Finally, there have been studies to show that l-dopa might contribute to the oxidative stress in PD and hence in the progression of cell death (Jenner, 2003).

Drugs that are usually administered in combination with levodopa in order to promote its action are the monoamine oxidase B inhibitor Selegiline and the catechol-O-methyltransferase (COMT) inhibitor, Entacapone. The former has mild symptomatic effect in PD and can prolong the duration of action of l-dopa doses in some patients. The latter enhances the delivery of levodopa to the brain by blocking the degradation of l-dopa in the periphery allowing more l-dopa to reach the brain. It eventually augments its action, but it can also enhance the occurrence of dyskinesias. Dopaminergic agonists are also considered possible drugs of choice, but they are sometimes given in combination with levodopa. The most common are Bromocriptine, Pergolide, Pramipexole and Ropinirole. These are relatively D2 dopamine receptor selective and are less likely to induce dyskinesias. They have

longer half life than l-dopa, but they are not as efficient and they carry higher risks of inducing cognitive side effects (Wooten 2003).

Motor fluctuations can be a persistent problem in dopaminergic antiparkinsonian therapy and, in spite of the adjunctive use of agents that reduce their occurrence, some patients might still suffer from them. Parenterally available apomorphine, a dopamine agonist, can be added in order to efficiently reverse off-periods and control motor fluctuations by achieving serum levels which maintain the patient in the on state without dyskinesias. Finally, amantadine, an antiviral agent that was found by chance to be of benefit in PD, has been shown to have mild antiparkinsonian effects and reduce levodopa-induced dyskinesias.

Before the advent of levodopa, the original drugs that used to be administered for PD were the anticholinergics. This was reasonable considering that PD is characterized by the imbalance between the dopaminergic and cholinergic neurotransmission in the striatum in the direction of cholinergic dominance. Today, such drugs are generally used in early onset PD cases to reduce tremor. They have modest effects in about two-thirds of patients, but they can cause side effects, such as dryness of mouth, nausea, visual disturbances, and even memory impairment and personality change.

The severe side effects, especially the motor complications that dopaminergic therapy causes, have led to the resurgence of interest in functional neurosurgery. DBS is considered an effective symptomatic treatment that maintains function and quality of life and alleviates motor complications.

1.5.2 Deep Brain Stimulation

High-frequency DBS has become a widely used method to treat successfully the parkinsonian motor symptoms. It involves the stereotactic implantation of stimulating electrodes in deep brain structures. These electrodes are connected to a subcutaneous stimulating device, which delivers a square wave pulse to the target nucleus and can be modulated by an external electromagnetic device. Electrodes consist of four platinum-iridium (1.27mm diameter and 1.5mm length) cylindrical surfaces with a centre to centre separation of 3mm (model 3387) or 1.5mm (model 3389). The stimulation parameters differ according to the targeted nucleus and the symptoms. In

general, stimulation voltage ranges from 1-5V, pulse width from 60-450μV and frequency from 130-220Hz.

For the treatment of PD, three nuclei have been the target of neurosurgeons, the STN, the GPi, and the ventral intermediate nucleus of the thalamus (VIM). Stimulation in all these nuclei has been clinically effective but STN DBS has been proven to be most beneficial. Specifically, VIM DBS provides a good clinical effect on tremor but shows no other antiparkinsonian or antidyskinetic effects. Therefore, it is considered the appropriate target for patients that suffer from non-parkinsonian tremor. Stimulation in the GPi is considered useful for the treatment of rigidity and levodopa-induced dyskinesias but not for bradykinesia and gait disability. In fact, it was shown to worsen akinesia and gait disturbance cancelling out the effects of levodopa therapy. On the other hand, STN DBS improves rigidity, bradykinesia, tremor, and levodopa-induced dyskinesias in the majority of patients, and, only in some cases, gait and postural problems. These effects are long-lasting and they are accompanied by a 50% reduction of the levodopa dose. Hence, STN DBS is preferred to GPi because of the greater anti-parkinsonian efficacy and drug reduction afforded by the procedure.

Despite its remarkable clinical efficacy, DBS's neurobiological mechanism is unclear. In vitro studies have shown that STN DBS silences STN neuron activity and replaces it by activity entirely driven by the stimulation producing, in that sense, an effect equivalent to a lesion. However, in vivo studies have suggested that STN DBS acts not only by causing silencing of the aberrant STN activity or lesion-like effects but also by reshaping/resetting the abnormal activity and the firing patterns of the STN as well as those of the GPi and SNr (Maurice et al., 2005; Meissner et al., 2005). This raises the possibility that some of the therapeutic effects of DBS might be due to driven activity that mimics the synchronization in the gamma frequency range similar to the one reported in the basal ganglia after levodopa administration (Hammond et al., 2007). Such an argument, of course, has not been confirmed to date.

The procedure is not without disadvantages however. Recent studies have argued that the motor benefits gained by DBS depend upon the state of the patients and their baseline performance at the time of the study. In patients with poor task performance STN DBS improves simple finger tapping, but in patients with good task performance stimulation causes deterioration by about 10% (Chen et al., 2006). This suggests that

there can be slight motor deficits following functional neurosurgery in motor tasks probably because physiological functioning that would otherwise promote motor processing is also knocked out by high-frequency stimulation of the STN (Brown & Eusebio 2008).

The PPN as a new target for stimulation

Although STN is the preferable target nucleus for DBS for the treatment of parkinsonian motor symptoms, it has only a moderate and short term effect in improving axial symptoms such as gait freezing and postural instability. The PPN has been introduced as a new therapeutic target for DBS in PD patients who suffer from severe gait and postural impairments that are refractory to other forms of treatment (Pahapill & Lozano 2000; Mazone et al., 2005). The PPN is an integral component of the midbrain locomotor region and plays an important role in walking behaviour. Its important role in the mechanisms of movement disorders was only lately revealed when it was shown that experimental lesions of this nucleus produce parkinsonian akinesia in primates (Kojima et al., 1997; Aziz et al., 1998). It's been proposed that abnormalities in gait and posture may reflect neuronal loss and suppression of activity in the PPN.

Earlier research in cats and rats had shown that mid-frequency electrical stimulation of this brain stem structure can elicit locomotion and muscle tone (Garcia-Rill & Skinner, 1988), while high-frequency stimulation can suppress it (Lai & Siegel, 1990). In agreement with this, recent studies by Aziz and colleagues demonstrated that in normal monkeys stimulation of PPN at frequencies above 30Hz can elicit mild akinesia, while high-frequency (>60Hz) stimulation can cause loss of postural control (Nandi et al., 2002b). On the other hand, low-frequency (10Hz) stimulation of the PPN in MPTP-treated monkeys alleviated akinesia (Jenkinson et al., 2004) and increased motor activity in addition to, but independently of, levodopa therapy (Jenkinson et al., 2006). This contrasts with other basal ganglia targets, such as the STN and GPi, where stimulation must be delivered at frequencies above 100 Hz to be therapeutic. Just how and why this unique stimulation regime should work in the PPN in PD and how it might be related to the unexplored neurophysiological properties of this nucleus remains unclear.

➡ Aim: To investigate the electrophysiological properties of PPN in PD by recording LFP activity directly from DBS leads from PD patients implanted in the PPN both at rest and during movement before and after levodopa treatment.

1.6 Pathology of oscillations

Abnormal neuronal synchronization has been associated with many psychiatric and neurological disorders, including movement disorders, such as PD. Our understanding of the pathophysiology of PD in humans has been greatly advanced by the recent renaissance in functional neurosurgery. Such surgery makes it possible to record neuronal activity from basal ganglia targets during awake neurosurgery and LFP signals directly from the macroelectrodes used for DBS in the few days between implantation and subsequent connection to a subcutaneous stimulator. Thus LFPs can be investigated in different pharmacological and behavioural states. Overall, three different bands of neural synchrony have been identified in the LFP signals recorded from the basal ganglia, < 8Hz, 8-30Hz, and > 30Hz. In most parts of this thesis activity in the 8-30Hz frequency range will be termed as basal ganglia "beta band", although it is acknowledged that it does not exactly correspond to the classical EEG beta band.

Oscillations at tremor-related frequencies (i.e. < 8Hz), although common in microelectrode recordings (see section 1.4.2), are not consistently detectable in LFP recordings in PD patients, probably because neurons oscillating at these frequencies have variable phase relationships (Brown & Williams 2005). However, synchronization of basal ganglia neurons at these frequencies evident in the LFP is usually observed in dystonic patients and – recently – in a PD patient with levodopa-induced dyskinesias (Foffani et al., 2005c). In addition, GPi and STN LFP activity at frequencies below 8Hz has been found to be increased after administration of levodopa in PD patients (Silberstein et al., 2003; Priori et al., 2004). These observations led to the suggestion that low-frequency synchronization in the treated parkinsonian state might be associated with hyperkinesias, which in PD are caused by chronic levodopa administration (Priori et al., 2004).

Perhaps the most important observation in depth recordings to date in PD has been the propensity for neuronal synchronisation in the STN and GPi in the 8-30Hz frequency band in patients withdrawn from antiparkinsonian medication (Brown et al., 2001;

Cassidy et al., 2002; Levy et al., 2002; Priori et al., 2002; Williams et al., 2002; Silberstein et al., 2003; Amirnovin et al., 2004; Kühn et al., 2004; Priori et al., 2004; Williams et al., 2005; Kühn et al., 2005; Alonso-Frech et al., 2006; Devos et al., 2006; Fogelson et al., 2006; Wingeier et al., 2006). Similar observations in the MPTP model of PD have confirmed that, in the diseased state, low-frequency oscillatory activity in the basal ganglia is enhanced (Wichmann et al., 1994). At this point it needs to be stressed that MPTP-treated primates exhibit oscillations at a lower frequency range than the humans which might be due to the increased severity of symptoms seen in the MPTP model of PD (Brown 2008). In addition, in PD patients LFP activity recorded from the basal ganglia has been found to be coupled with cortical activity in the beta band (Marsden et al., 2001). Neuronal oscillations and cortico-basal ganglia coherence over the beta range are reduced in preparation for and during voluntary movement (Cassidy et al., 2002; Doyle et al., 2005) and these reductions in STN beta synchronization correlate with reaction time after cued movements (Kühn et al., 2004). Additionally, the duration and magnitude of the amplitude modulation, specifically amplitude reduction, of beta activity in the STN prior to cued movement relates to the amount of processing necessary for motor preparation (Williams et al. 2005) and the latency and power of the movement-related beta power reduction in untreated PD patients inversely correlate with the degree of motor impairment (Doyle et al. 2005). However, it still remains unclear whether there is any modulation of beta power during ongoing repetitive movement in the untreated parkinsonian brain and how it might be related to time-evolving bradykinesia.

➡ Aim: To investigate patterns of amplitude modulation of beta activity during sustained or repetitive movements and examine their role on motor performance.

On the other hand, antiparkinsonian dopaminergic medication reduces neuronal oscillations and cortico-basal ganglia coherence over the beta range (Brown et al., 2001; Marsden et al., 2001; Levy et al., 2002; Priori et al., 2002, 2004; Kühn et al., 2006b; Alonso-Frech et al., 2006) and promotes synchronization at higher frequencies and coupling of activities between basal ganglia structures and between them and the cortex in the gamma band, particularly during voluntary movement (Cassidy et al., 2002; Williams et al., 2002; Alegre et al., 2005; Obeso et al., 2004; Foffani et al., 2005b; Fogelson et al., 2005; Alonso-Frech et al., 2006; Devos et al., 2006), with STN and GPi leading the cortex. In fact, some studies have proposed that it might be

the activity in the lower beta band (<20Hz), at frequencies closer to the ones seen in the MPTP model of PD, that is sensitive to dopaminergic treatment (Priori et al., 2004) suggesting that probably these are the activities that are pathologically synchronized in PD and that upper beta band activities (>20Hz) are distorted by a harmonic of the lower beta (Marceglia et al., 2006). Levodopa, which ameliorates bradykinesia, has also been shown to increase the additional suppression of beta band activity that occurs prior to and during voluntary movement (Doyle et al., 2005; Devos et al., 2006) and enhance synchronization in the gamma band. The latter has been reported for a frequency range from 60-90Hz (Brown et al., 2001; Alegre et al., 2005; Devos et al., 2006) and for very high frequencies at around 300Hz (Foffani et al., 2003). Gamma oscillations, on the other hand, are attenuated in the untreated Parkinsonian state probably suggesting the possibility that neurons in the basal ganglia-cortical loop oscillate at high frequencies when dopaminergic neurotransmission is restored. At this point it is important to note that gamma synchronization was observed during a motor response in the cortical LFP of epileptic patients with no movement disorders or dopaminergic deficiencies. In fact this physiological cortical gamma ERS appeared strictly contralateral with respect to movement side (Crone et al., 1998b; see section 1.3.3.3). Is it possible that subcortical movement-related gamma activity follows the same pattern in PD after levodopa treatment?

➡ Aim: To elucidate the nature of beta and gamma activity in the basal ganglia and the effect of levodopa on amplitude modulation of frequencies over these bands before and after movement.

In line with this, stimulation of the pallidum of the cat at frequencies over the beta band range lead to immediate termination of voluntary movement (Hassler & Diekmann, 1967). Similarly, in PD patients stimulation of the STN and GPi at around 20Hz has been shown to deteriorate motor performance by exacerbating bradykinesia (Fogelson et al., 2005; Chen et al., 2007; Eusebio et al., 2008), while stimulation at frequencies above 70Hz improve it (Limousin et al., 1995). Clinically effective stimulation frequency (~130Hz) or levodopa therapy have also been proven to reduce the degree of cortico-cortical coupling over the beta range, which is strongly related to the severity of the disease, and degree of clinical improvement (Silberstein et al., 2005). The degree of suppression of synchronization in the beta band at the cortex and

STN caused by levodopa therapy and/or DBS stimulation correlates with clinical improvement in rigidity and bradykinesia, but not with the degree of improvement in rest tremor (Brown et al., 2004; Silberstein et al., 2005; Kühn et al., 2006).

All these have led to the idea that beta activity is related to the bradykinetic state, which it may serve to promote (Brown, 2003; Dostrovsky and Bergman, 2004; Brown and Williams, 2005), and oscillations in the gamma band might resemble the normal state and support normal movement (Brown et al., 2001). For this purpose, gamma activity has been termed prokinetic and beta antikinetic. It should be noted though that it is not the beta activity per se that is linked to the expression of the disease symptoms but the excessive amount of neuronal synchronization in this band within the cortico-basal ganglia circuit as lower degrees of beta synchrony can be seen in healthy humans (Gilbertson et al., 2005; see section 1.3). In this sense, it is possible that the amount of desynchronization that is necessary to "release" movement can not be achieved and/or extreme synchronization under 30Hz prevents resonance of neuronal populations at higher frequencies that are directly involved in information transfer (Brown 2006). When the levels of dopamine are restored, pathological beta synchrony is suppressed and, hence, the neurons can efficiently engage in functions that underlie processing of movement information (Brown 2008). Another not mutually exclusive possibility is that dopaminergic deficiency causes loss of functional segregation in the basal ganglia subcircuits making the striatopallidal network unable to keep its activity independent (Bergman et al., 1998; Marceglia et al., 2006). This once again shows that the emergence of synchronized neuronal oscillations reflects the major changes at the network level of the basal ganglia circuitry in PD.

Oscillations and basal ganglia in motor control

It has become yet quite clear that the findings from microelectrode and LFP recordings and the remarkable effectiveness of DBS surgery in treating PD cannot be fully explained by the "direct/indirect pathway" models (see section 1.2.3) as it shows that the neurons in these structures do not follow the response to dopaminergic or electric stimulation predicted by these models. Failure of some studies to report hypoactivity of the GPe in dopamine-deficient basal ganglia and increase in the firing rates of the STN as a result of apomorphine administration (see section 1.4.2) as well

as the unexpected finding that lesioning of the GPi and STN does not lead to akinesia but in contrast improves it have served to stress the importance of the pattern of basal ganglia activity in PD and not the effect of the inhibited thalamocortical facilitation. These have led to the hypothesis that PD leads to a noisy pattern of basal ganglia activity that disrupts normal function within the basal ganglia and between basal ganglia and the cortex and that DBS suppresses this noisy signal (Brown & Eusebio, 2008).

1.7 Aims of the thesis

The primary aim of this thesis is to further understand the physiological mechanisms of synchronized oscillatory activity in the cortex and basal ganglia. On the one hand, elucidating the features of beta oscillations in the normal human brain will afford additional knowledge on the relationship between this rhythm and the generation of the bradykinetic parkinsonian symptoms. On the other hand, understanding the way oscillations over different frequency bands are represented in basal ganglia nuclei such as the STN and PPN in disease will provide further insight into their role in the basal ganglia and in motor functioning and their relationship with each other.

The main objectives of this thesis are:

Normal Conditions

- To demonstrate a behavioural context in which beta bursts occur in the healthy cortico-spinal system and elucidate the functional role of the beta-range coherence (Chapters 3 and 4).

Parkinson's Disease

- To clarify the relationship between beta and gamma oscillatory activity in the basal ganglia in PD patients and how it is affected by levodopa treatment (Chapter 5).
- To investigate the role of beta oscillations in the STN of untreated PD patients on performance during a sustained, repetitive motor task (Chapter 6).

- To describe the neurophysiology of the human PPN in the dopamine-depleted PD brain and examine its possible relationship with parameters of movement (Chapter 7).

CHAPTER 2

Materials and Methods

This chapter presents details of the methodology that is common in all experiments included in this thesis. Additional elements specific for each experiment are mentioned in the respective chapters.

2.1 Subjects

The participants in the following experiments were either healthy volunteers or - in the case of LFP recordings - patients that have undergone DBS surgery for treatment of PD and tremor. Experiments with healthy volunteers were principally performed in laboratories of the UCL Institute of Neurology, Queen Square. Depth recordings from the STN were obtained from patients in five surgical centres: 1) The National Hospital for Neurology and Neurosurgery, London, U.K., 2) Department of Neurosurgery, Charité Campus Virchow, Humboldt University Berlin, Germany, 3) Department of Neurosurgery, King's College London, U.K., 4) Department of Neurological Surgery, Radcliffe Infirmary, Oxford, U.K., 5) Department of Neurosurgery, University Hospital of Northern Sweden, Umea, Sweden. Depth recordings from the PPN were obtained from patients treated in 1) the Operative Unit of Functional and Stereotactic Neurosurgery, CTO "A. Alesini" Hospital, Rome, Italy and 2) the Institute of Neurosciences, Frenchay Hospital, University of Bristol, Bristol, U.K. Patients were recorded during the post-operative period prior to implantation of the stimulator while DBS leads were still external. All participants gave their informed written consent and all studies were approved by the local ethics committees.

2.2 Data acquisition

For the experiments in healthy subjects (chapters 3 and 4), the signals were amplified with a Digitimer 160 (Digitimer Ltd, Welwyn Garden City, Hertfordshire, UK), digitized with 12-bit resolution by a 1401 analog-to-digital converter (Cambridge Electronic Design, Cambridge, U.K.) and sampled at 1 kHz using a PC running Spike2 software (Cambridge Electronic Design). For the LFP experiments, amplification was performed using a Digitimer amplifier or a custom-made battery-operated portable high impedance amplifier (previously described in Kuhn et al., 2004) and then recorded using a 1401 analogue-to digital converter. LFP signals were

sampled at a minimum rate of 625 Hz up to 2.5 kHz across patients and then interpolated to a common sampling rate. In some cases (chapter 6), signals were initially collected with a Biopotential Analyzer Diana (St Petersburg, Russia) and, in one case (chapter 7), with a PsyLab SAM Contact Precision Amplifier (Contact Precision Instruments, Boston, Massachusetts, USA) and then exported for processing in Spike 2 and MatLab.

Analogue bandpass filtering was performed on all signals in the following experiments. This process allows the rejection of very high or very low frequencies from the signal so that the frequencies of interest are recorded without distortions. Bandpass filtering uses a low-pass filter (i.e. signals higher than the cut-off frequency are attenuated) and a high-pass filter (i.e. signals lower than the cut-off frequency are rejected). After analogue filtering the data pass to the analog-to-digital converter. This process converts the continuous signals to discreet digital numbers at discreet intervals of time. The rate at which the digital numbers are sampled from the analogue signal is defined by the sampling rate. The higher the sampling rate the higher the resolution of the recorded signal. In order to reliably reproduce the analogue signal, the sampling rate must be equal to or higher than twice the highest frequency to be resolved. This is called the Shannon-Nyquist sampling rate. Aliasing occurs if the analogue signal changes much faster than the sampling rate producing thus spurious signals. It is for this reason that the analogue signal needs to be low-pass filtered at less than half the original sampling rate (anti-aliasing filter).

2.2.1 Electroencephalography (EEG)

In the experiments with healthy subjects (chapters 3 and 4), EEG was recorded using Ag-AgCl electrodes attached to the scalp surface using collodion. One electrode was placed over the motor cortex hand area referenced to one placed 2.5 cm anterior to the hotspot, in the case of the bipolar recordings, or referenced to an electrode attached to the earlobe, in the case of monopolar recordings. An additional ground electrode was also placed on the forehead. The motor cortex hand area was defined by TMS. Before attaching the electrodes, the skin was cleaned with alcohol and conducting jell (Sigma, Parker Laboratories, New Jersey, USA) was applied to the base of the electrodes. In the experiments with PD patients that were implanted in the PPN for the treatment of PD (chapter 6), EEG activity was recorded using a needle electrode that

was placed over the Fpz area according to the 10-20 system. The EEG signals were amplified (x 100,000) and band-pass filtered at 1-100 Hz.

2.2.2 Local Field Potentials (LFP)

LFPs were recorded from patients that have undergone functional neurosurgery for the treatment of PD or tremor. Deep brain activity was either recorded bipolarly from the adjacent four contacts of each DBS electrode (0-1, 1-2, 2-3), or digitally converted offline to contiguous bipolar derivations where recordings were performed monopolarly (chapters 6 and 7). Data were amplified (x 100,000) and, in the PD patients that were implanted in the STN, pass band filtered at 1-250 Hz (chapters 5 and 6), in the PD patients that were implanted in the PPN, bandpass filtered at 1-500 Hz and in one case at 0.1-200 Hz (chapter 7) and, in the two tremor patients, band pass filtered at 1-90 Hz and 1.5 - 200 Hz, respectively (Biopotential Analyzer Diana, St Petersburg, Russia).

2.2.3 Electromyography (EMG)

EMG was recorded from the first dorsal interosseous (FDI) of the right (dominant) hand using 9-mm silver – silver chloride electrodes with one electrode over the muscle belly and a second electrode over the first metacarpo-phallangeal (MCP) joint. An additional ground electrode was attached on the wrist. Again, the skin was cleaned with alcohol and conducting jell was applied to the base of the electrodes. EMG signals were amplified (x 10,000) and band-pass filtered at 16-300Hz.

2.2.4 Goniometry

A goniometer is a sensor that is designed for the measurement of angular joint movement. A single axis electric goniometer F35 (Biometrics Ltd., Gwent, U.K.; see figure 2.1), as the one used in this thesis, consists of two endblocks that are connected to each other with a spring. It is usually attached across the joint employing double-sided medical adhesive tape between the endblocks and skin, and single sided adhesive tape is placed over the top of the endblocks. The goniometer is connected to an analogue amplifier (K100) which consists of a small subject unit and a large base unit. The analogue output from the K100 amplifier was then connected to the 1401 analogue-to-digital converter. In these series of experiments, the goniometer was used in order to record angles of excursion of the finger at the first metacarpophalangeal

joint. Biometrics' goniometer F35 permits the measurement of angles in one plane. Angles are measured when rotating one endblock relative to the other.

Figure 2.1: A single axis electric goniometer F35 (Biometrics Ltd., Gwent, U.K.).

2.2.5 Accelerometry

A miniature single axis accelerometer (EGAXT-50; Entran, Fairfield, New Jersey) was used to measure finger microtremor and acceleration of movements. It was usually taped to the distal phalanx of the right index finger. This device consists of a suspended cantilever beam which is connected to a transistor which allows the acceleration profile to be represented as a simple analogue signal.

2.2.6 Transcranial Magnetic Stimulation (TMS)

TMS was used in order to functionally localize the FDI area, for subsequent positioning of electrodes for EEG recordings. Single-pulse TMS was performed with a Magstim 200 magnetic stimulator (Novametrix Medical Systems Inc., Wallingford, CT, USA) using a figure-of-eight shaped coil (diameter 70mm) with current in the coil flowing in an anterior-to-posterior direction. The TMS coil was held tangentially over the left motor cortex and minor adjustments of coil position were made in order to find the hotspot on the scalp at which TMS evoked the most consistent motor evoked potential at the lowest stimulation intensity in the right FDI.

2.3. Data Analysis

All data analyses were performed off-line using cross-correlation or Fourier-based methods in Spike2 and wavelet-based methods in MatLab v.7 (The Mathworks Inc., Lowell, MA, USA).

2.3.1 Fourier Transform

The Fourier transform of a signal is achieved by multiplying its segments with the sine and cosine values of the frequencies of interest. The results can be used to derive information about the frequency spectrum $d(\lambda)$ of $x(f)$.

$$d(\lambda) = \int_{-\infty}^{\infty} x(f) e^{-j2\pi\lambda f} df \qquad \text{equation 1}$$

However, the signals that were analysed here were discrete periodic signals that change their frequency and period discretely. In this case, application of the FFT can give flawed results. The Discrete Fourier Transform (DFT) is the preferred method to apply for the calculation of the Fourier series coefficients for a discrete periodic signal. In the following experiments, Fourier analysis was performed by dividing each time series into disjoint segments (L) of length T (512 data points in the case of EEG and EMG (chapters 3 and 4) and 1024 (chapter 5 and 7) and 512 (chapter 6) data points in the case of LFP recordings), as described in Halliday et al. (1995). Let $x(t)$ to be sequence of T sampled values of $x(f)$, the discrete Fourier transform (DFT) was performed on the l^{th} segment at frequency λ, defined as:

$$d_x^T(\lambda, l) = \int_{(1-l)T}^{lT} x(t) e^{-2\pi\lambda t / N} dt \qquad \text{equation 2}$$

, where dt is the sampling interval of the signal $x(t)$, i is the imaginary unit $i = \sqrt{-1}$, and e is the exponential function of the Fourier transform $e^{it} = \cos(t) + i \sin(t)$. The term i is important for the extraction of the phase estimates and the term e produces a waveform of frequency λ which is multiplied with the signal $x(t)$ to produce the complex spectral estimate $d(\lambda, l)$.

Based on these equations estimates of power, phase, and coherence could be extracted. The significance of power and coherence could be calculated according to the equation $\hat{z} \pm 1.96x\sqrt{(\mathrm{var}\{\hat{z}\})}$, where $\hat{z}$ is a given estimate and $(\mathrm{var}\{\hat{z}\})$ its variance. The frequency resolution of $d(\lambda, l)$ is equal to the sampling rate sr divided by the number of samples in the DFT window of length T (sr/T). Hence, the higher the values of T are, the better the frequency resolution but the lower the temporal

resolution of power and coherence estimates. Therefore, a compromise between frequency and temporal resolution must be made.

Power spectrum and Coherence

The power spectrum or autospectrum (*fxx*) measures the amount of energy of a signal x at a given frequency λ based on the variance of the signal at λ frequency after DFT has been performed

$$f_{xx}(\lambda) = \frac{1}{2\pi LT} \sum_{l=1}^{L} d_x^T(\lambda, l)\overline{d_x^T(\lambda, l)} \qquad \text{equation 3}$$

, where L is the total number of disjoint segments of T length and $\overline{d_x^T(\lambda, l)}$ a complex conjugate. The power spectra can therefore reveal the frequency of locally synchronised electrical events and measure the statistical strength of this synchronisation. Unsynchronized events tend to cancel out in population measures such as EEG, LFPs, or EMG. The cross-spectrum measures the correlation between two signals x and y with respect to their phase and power.

$$f_{xy}(\lambda) = \frac{1}{2\pi LT} \sum_{l=1}^{L} d_x^T(\lambda, l)\overline{d_y^T(\lambda, l)} \qquad \text{equation 4}$$

All time series were assumed to be realisations of stationary, zero-mean time series (Brillinger, 1981). A stationary time series is one whose statistical properties such as mean, variance, autocorrelation, etc. are all constant over time. They were further assumed to satisfy a mixing condition, whereby sample values widely separated in time were independent. This assumption results in asymptotic normality of parameter estimates, allowing confidence limits to be constructed (Halliday et al., 1995).

In nearly all experiments, a Hanning window filter was used for spectral analyses (Halliday et al., 1995). Hanning windowing is a smoothing procedure that cuts the data into N discrete blocks. With the application of the FFT, the periodogram (estimate of power spectral density) of each separated block is then computed and an average of them is calculated. This method is introduced as a means to control the variance of the power spectrum estimate (Challis & Kitney, 1991). However, Hanning windowing still suffers from limitations regarding the trade-off between the number and the length of the blocks. Increasing block number introduces less variance, while

using time sequences of smaller length always has poorer frequency resolution, larger bias, and frequency leakage. In the first part of chapter 7 the 'multitaper method' was used for frequency analysis. The multitaper method is a multiple windows spectrum estimation scheme for low bias and low variance estimation and uses discrete prolate spheroidal sequences as tapers instead of conventional tapers such as Hanning. Instead of cutting the time data into a number of blocks, this method computes the periodogram for entire windowed time sequence, and then averages the results. For this purpose, a set of orthogonal time windows is employed, the discrete prolate spheroidal sequences. They optimally concentrate the spectral power of the signal over the desired bandwidth parameter W (in the interval $[-W, W]$; Mitra & Perasan, 1999).

The auto-spectra and cross-spectrum can be combined to give coherence $R_{xy}(\lambda)$, a measure of the linear association (correlation) between two signals x and y at a given frequency λ.

$$\left|R_{xy}(\lambda)\right|^2 = \frac{\left|f_{xy}(\lambda)\right|^2}{f_{xx}(\lambda)f_{yy}(\lambda)} \qquad \text{equation 5}$$

Coherence is therefore proportional to the square of the cross-correlation of the two signals in question and inversely proportional to the product of their individual autospectra. It is the ratio of the two auto-spectra and their cross-spectra and measures the consistency of the phase and amplitude of the two signals across frequencies. It is a bounded measure taking values from 0 to 1, where 0 indicates that there is no linear association (i.e. that one process is of no use in linearly predicting another process) and 1 indicates a perfect linear association. If two brain areas are coherent, then they probably receive common synaptic input and the phase of the oscillations produced by those areas should be related because they are being driven by the same input. Therefore, coherence is the ratio of the phase locked power between two signals to the total amount of power that both signals possess between them. For the calculation of the CL variance estimates can not be used as they are inaccurate with low coherence levels. Hence, the derivation of the CL is based upon the number of segments L (Halliday et al, 1995). This defined the upper 95% confidence limit as $1-(0.05)^{1/(L-1)}$.

Phase

If the coherence between two signals is significant, then their phase difference can be used to calculate the conduction delay over a given frequency range assuming unidirectional flow. The phase spectrum, in radians, between the two time series is given by the argument of the cross spectrum:

$$\phi_{xy}(\lambda) = \tan^{-1} \frac{\sum_{n=1}^{N} \Re|R_{xy}(\lambda)|}{\sum_{n=1}^{N} \Im|R_{xy}(\lambda)|} \qquad \text{equation 6}$$

, where $\Re$ and $\Im$ are the real and imaginary products of these transforms. Over frequency ranges with significant coherence, the time lag/lead between two signals can be calculated from the slope of the phase estimate, having fitted a line by linear regression. A significant positive or negative gradient indicates a lag or lead by the input channel respectively relative to the reference channel, at a latency given by: $\Delta\phi / (\Delta frequency \times 2\pi)$.

2.3.2 Directed Transfer Function

The directed transfer function (DTF) was applied in order to investigate the direction of the information flow between two signals (Kaminski & Blinowska, 1991). The determination of the direction of flow of the brain activity is crucial for the understanding of information processing. The DTF takes into account all channels simultaneously and makes possible estimation of activity flow in a given direction as a function of frequency. It is based on the concept of Granger causality according to which an observed time series *x(n)* causes another series *y(n)* if the knowledge of *x(n)*'s past significantly improves prediction of *y(n)*. The latter relationship between time series is not reciprocal, i.e. *x(n)* may cause *y(n)* without *y(n)* necessarily causing *x(n)*. This lack of reciprocity enables the evaluation of the direction of information flow between structures. This method of analysis utilizes a multivariate autoregressive (MAR) model so as to best describe the signals that come from the regions of interest. The MAR methodology is essential for the DTF, as the DTF is built directly from the MAR coefficients.

As a first step a MAR model is fitted to the data. All the data channels are treated as members of one system, are analyzed simultaneously, and their mutual influences are taken into account. (Kaminski & Blinowska, 1991). The MAR model is formed using

coefficients constructed by autocorrelation, whereby a value at time t is based on a linear combination of prior values. The model therefore measures the ability to predict the value of time t based on preceding observations. The model order is the number of previous values that are incorporated into the coefficient at each time point. A MAR model predicts the next value in a d-dimensional time series x as a linear combination of the p previous values plus a noise contribution:

$$x_t = \sum_{i=1}^{p} x_{t-i} a_i + e_t \qquad \text{equation 7}$$

, where $x_t = (x_t(1), x_t(2),\ldots x_t(d))$ is a row vector containing the values from the d-dimensional time series x at time t, $e_t = (e_t(1), e_t(2),\ldots e_t(d))$ is a row vector of residual errors which are assumed to be Gaussian, and a_i is a d-by-d matrix of coefficients. This model can be considered and reformulated as a multivariate linear regression model (Penny & Harrison, 2006). In such case the maximum likelihood estimation method can be used in order to calculate the best prior values (i.e. model order) that fit the data. Here, in order to determine the MAR coefficients that best represent the entire time series a Bayesian methodology was applied as detailed in Cassidy and Brown (2002). This approach is similar in form to the maximum likelihood estimation approach but it also incorporates a prior precision term (the precision of the Gaussian prior distribution from which the coefficients are drawn; Penny & Harrison, 2006).

The autoregressive coefficients can be used to construct a bounded, normalised measure (the DTF) that provides information on the effective direction of coupling. In order to estimate the spectral properties of the investigated process the signal has to be expressed in the frequency domain. This is performed by z-transforming the MAR equation:

$$X(z) = H(z)E(z) \qquad \text{equation 8}$$

, where $H(z)$ is the transfer function and z^{-1} is a unit delay operator. In the frequency domain, the transfer function $H(f)$ contains information about the spectral properties and interrelation between channels. The element $H_{xy}(f)$ of $H(f)$ describes transmission from channel y to channel x in the frequency domain. The DTF is constructed from the normalized version of the transfer function:

$$DTF_{xy}(f) = \frac{|H_{xy}(f)|^2}{\sum_{m=1}^{d} |H_{xm}(f)|^2}$$ equation 9

, where H_{xm}(f) is all the elements of the relevant mth row. The difference between DTF_{xy} and DTF_{yx} suggests an asymmetric information flow (Kaminski & Blinowska, 1991).

This approach is preferred to FFT/DFT when information on directionality is needed. Usually, with the FFT approach when coherence is strong across a given frequency band, the phase lag/lead between two signals can be calculated by using the slope of the phase estimate (radians/Hz) across the coherent frequency range, with a positive or negative gradient indicating that the one signal is lagging or leading the reference signal respectively. The phase estimate, however, might lead to spurious results as it can reflect a mixture of coherent activities with both lags and leads. DTF, on the other hand, has the ability to provide information about coherent activity in both directions giving a result which reflects the relative strength of coherence in each direction rather than an absolute lag or lead (Cassidy & Brown, 2003).

2.3.3 Continuous Wavelet Transform (CWT)

Wavelets are simple oscillating amplitude functions of time, like the sine and cosine waves used in Fourier transforms. However, unlike the sines and cosines which are precisely localised in frequency but extend in time infinitely, wavelets are localised in both the frequency and time domains. Also, they are composed of a relatively limited range of frequencies (Samar et al., 1999). This means that wavelets can be adjusted according to the time and bands of interest.

Wavelet analysis is a common tool for analysing time series that contain non-stationary power at many different frequencies. Wavelet transforms can detect temporal interactions between two anatomically distinct neuronal populations. Here, the Morlet wavelet $\psi_0(\eta)$, a Gaussian-modulated sine wave, was used which has previously been used for EEG, EMG, and microtremor analysis (Samar et al., 1999; Strambi et al., 2004; Gilbertson et al., 2005; Li et al., 2006):

$$\psi_0(\eta) = \pi^{-1/4} e^{i\omega_0 \eta} e^{-\eta^2/2}$$ equation 10

where η is the non-dimensional time parameter and ω_0 is the wavelet central angle frequency (or mother wavelet), here taken to be 6 in order to adjust/compromise the time-frequency resolution (Farge, 1992).

The continuous wavelet transform ($W_n(s)$) can decompose a time series x_n into a set of functions by fitting a constant waveform at time n by varying the wavelet scale s and shifting this along by equal intervals for a specific number of points in the time series (N).

$$W_n(s) = \sum_{n'=0}^{N-1} x_n \psi^* \left[\frac{(n'-n)}{s} \right]$$ equation 11

, where * denotes the complex conjugate. The wavelet scale s, which can basically denote any frequency, can be changed in order to match the band of interest (e.g. beta band) with a frequency resolution defined by the interval between scales. By fitting a waveform like this to a neuronal signal at time η and sequentially shifting this along by equal time intervals, the frequency content at a single frequency can be derived from all time points of interest. In order to improve the speed of transformations, all coefficients were normalized across scales and derived in Fourier space, as outlined in Torrence and Compo (1998).

Power spectrum, Coherence, and Phase

Here, the Morlet wavelet transform was used in order to obtain the wavelet power Wx of a time series x_n at wavelet scale s:

$$Wx = |W_n^x(s)|^2,$$ equation 12

the wavelet coherence $Coh_n^{xy}(s)$ of two signals x and y at wavelet scale s:

$$Coh_n^{xy}(s) = \frac{\sum_T |(W_n^{xy}(s))|^2}{\sum_T (|W_n^x(s)|^2) \cdot \sum_T (|W_n^y(s)|^2)}$$ equation 13

and the instantaneous phase ϕ_n at wavelet scale s at sample n:

$$\phi_n(s) = \tan^{-1}\left(\frac{\Re(W_n^x(s))}{\Im(W_n^x(s))}\right) \qquad \text{equation 14}$$

, where $\Re$ and $\Im$ are the real and imaginary products of these transforms. This is a true representation of a signal's phase as it evolves in time. In order to confirm that the phase of two signals is stationary, the Rayleigh statistic of uniformity ($\overline{R}_n(s)$) was used. This defines the distribution of T angles, formed by the real and imaginary products of the wavelet transform, at any sample time point n and at wavelet scale s:

$$\overline{R}_n(s) = \frac{\sqrt{\left(\sum_{t-1}^{T}\left(\cos\phi_{n,t}(s)\right)\right)^2 + \left(\sum_{t-1}^{T}\left(\sin\phi_{n,t}(s)\right)\right)^2}}{N} \qquad \text{equation 15}$$

2.4 Triggering

2.4.1 Online Analogue Triggering

The microtremor signal was amplified and filtered on-line using a custom-built 16th-order elliptic 13-35 Hz bandpass electronic filter (stopband attenuation of 60dB) with an output delay of 50 ms. The signal was used to trigger a rising voltage threshold in a Schmitt circuit. The voltage threshold was defined empirically during a 30–60 s calibration period at the start of each session and equivalent to two to three times the root-mean square amplitude of the bandpass filtered signal.

2.4.2 Online Wavelet-based Triggering

An online wavelet-based template matching algorithm for detecting bursts of oscillatory activity in the EEG was used in order to deliver the triggered stimulus in the same burst (Gilbertson et al., 2005). This script assumes that beta oscillations occur in phasic bursts lasting several cycles of approximately constant frequency and fits a wavelet of the same frequency to a cycle in the middle of a beta burst. This algorithm delivered a given output 2-3 ms after the triggering cycle. Bipolar EEG was sampled at 1 kHz using a 1401 analog-to-digital converter interfaced with MatLab v.7 using MATCED32 (written by Jim Colebatch). For the wavelet analysis the data are sampled in non-overlapping windows with a width corresponding to the period of the modelled waveform (e.g. for 20 Hz a window of 50 ms duration, i.e. 50 data samples)

and the convolved wavelet transform of Torrence and Combo (1998) at a single wavelet scale (pseudo-frequency) is used in order to minimise computational delay. The appropriate pseudo-frequency was established by identifying the pseudo-frequency with the peak wavelet power in a test sequence of data.

The EEG recorded during the test sequence was then averaged with respect to the algorithms output times. In order to ascertain satisfactory fit of the wavelet to the signal, at least half of the real values of the wavelet transformed samples in the sampled window had to be above a threshold. This threshold was empirically derived from the averaged EEG of the test sequence (see Results Fig 3.2.2A). To ensure stationarity of phase between those windows containing oscillations meeting the criterion specified above, the script allowed triggering to only occur when the peak of the oscillation was in the centre of the sampling window.

2.5 Functional Neurosurgery

PD patients

The patients that participated in the experiments had undergone surgical implantation of DBS electrodes for therapeutic stimulation. The PD patients were implanted in the STN (chapters 5 and 6) and in the PPN (chapter 7). Clinical details of the patients are presented in the respective chapters.

Implantation was performed under local anesthesia using Leksell's Frame (Eleka, Sweden) or the Riechert–Mundinger Frame (patients in Berlin). The DBS electrode used was model 3389 (Medtronic Neurological Division, Minnesota, USA) with four platinum-iridium cylindrical surfaces (1.27 mm diameter and 1.5 mm length) and a centre-to-centre separation of 2 mm. Contact 0 was the lowermost and contact 3 the uppermost. The intended coordinates for STN were 12 mm lateral from the midline, 3 mm behind the midcommissural point, and about 4 mm below the AC-PC line. Adjustments to the intended surgical coordinates were made according to the direct visualization of STN on individual pre-operative stereotactic T2-weighted magnetic resonance imaging (MRI; Hariz et al., 2003) and, in patients from Berlin, ventriculography and intra-operative microelectrode recordings. Intra-operative electrical stimulation and immediate post-operative stereotactic MRI were performed in all patients in order to confirm targeting.

The techniques used for implanting electrodes in the PPN were different in the two surgical centres. In Bristol, the position of the dorsal boundary of the PPN was defined lateral to the decussation of the superior cerebellar peduncle as visualized on an axial MRI slice acquired in a plane passing through the dorsal portion of the inferior colliculus and the dorsal most border of the pons. The ventral portion of the PPN was identified on a parallel slice 2.4mm below this. Fine plastic guide tubes and stylettes (Renishaws plc, UK) were first implanted to the targets. After the intra-operative MRI confirmation of accurate stylette placement, the latter were withdrawn from the indwelling guide tubes and replaced with DBS leads advanced to the same location. The middle two contacts of each DBS lead were positioned in the substance of the PPN bilaterally via a transfrontal trajectory that was parallel to the aqueduct of Sylvius (Plaha and Gill, 2005). In Rome, electrode implantation was performed in the target areas by means of a stereotactic double arch system "3P Maranello" (CLSSRL-Italy; Stefani et al., 2007). To target the PPN, the trajectory was performed strictly parallel to the floor of the IVth ventricle (parallel to the brainstem axis) and the angle was about 80–82° in the coronal plane. The coordinates for PPN surgery were 13mm lateral to the midline, 12.5/13mm below posterior commissure. After surgery, the definitive electrode locations were verified by brain MRI or CT-scan (Stefani et al., 2007).

Tremor Patients

Two non-PD patients with non-parkinsonian tremor participated in the study. Case 1 underwent simultaneous unilateral dual implantation of DBS macroelectrodes as part of a comparative clinical study of the efficacy of stimulation at different sites for essential tremor (ET) at the University Hospital of Umeå, Sweden. The first DBS electrode was aimed to target the nucleus ventralis intermedius thalami (Vim) with the caudal contact within Zona incerta (Zi). The second electrode was aimed to target STN. Case 2 was implanted in London with an electrode bridging posterior STN (rostral contact 3) and the preleminiscal radiation on the left for treatment of dystonic tremor in the right upper limb.

CHAPTER 3

Corrective movements in response to displacements in visual feedback are more effective during periods of 13-35 Hz Oscillatory Synchrony in the Human Corticospinal system.

Synchronised oscillatory activity in the beta band (~ 20 Hz) is a common feature at various levels of the human central motor system (Murthy and Fetz 1992; Sanes and Donoghue 1993; Baker et al.. 1997; Marsden et al., 2000; Brown et al., 2001; Levy et al., 2002; Williams et al., 2002; Silberstein et al., 2003; Courtemanche et al., 2003; Paradiso et al., 2004; Schoffelen et al., 2005). It is most readily recorded from the cerebral motor cortex, either directly in the form of the electrocorticogram and the more accessible scalp EEG, or indirectly, in the periphery, either as the cortico-spinally driven synchronization of motor units within and between muscles (Farmer et al., 1993; Conway et al.. 1995; Gibbs et al., 1995; Baker et al., 1997; Salenius et al. 1997; Kilner et al., 1999) or as microtremor, -the mechanical product of such synchronization (Halliday et al., 1999; McAuley et al., 1997; Gilbertson et al., 2005).

Yet the function of the beta activity in the motor cortex remains unclear. Recent studies have argued that oscillatory activity in the beta band is particularly increased during holding contractions but are attenuated by voluntary movements (Pfurtscheller, 1981; Sanes and Donoghue, 1993; Baker et al. 1997; Kilner et al., 1999; Schoffelen et al., 2005). In PD, elevation of beta activity in the basal ganglia has been linked to the patients' bradykinetic symptoms. This has lead to the suggestion that beta activity may actually penalize processing related to voluntary movement (Brown, 2003; Brown and Williams, 2005). Gilbertson et al. (2005) expanded on this hypothesis in relation to cortical beta activity in healthy subjects. They argued that physiological levels of beta activity penalize movement, while actively promoting processing related to postural activity, including tonic holding contractions. Although they showed that movements were slowed during bursts of physiological beta activity in the corticospinal system, they failed to demonstrate a behavioural advantage of the high beta state during postural contraction. They showed only a simultaneous potentiation of transcortical stretch reflexes that might support a postural motor response (see Chapter 1).

The core question addressed in this chapter is the following: If increased beta

synchrony promotes processing related to existing motor set and posture, then subjects should be able to have better performance in tasks that require postural control during and immediately after a burst of beta synchrony. In other words, if beta activity is related to processing information regarding posture, then there should be an improvement in the control of postural tasks during periods of beta bursts.

The following experiments were designed in order to test the hypothesis that performance during a manual positional hold task is improved following spontaneous bursts of beta synchrony in the cortico-spinal system. For this purpose, we designed a visual task that biased the timing of subject's motor responses to coincide with stochastic oscillatory events. Specifically, the task consisted of the holding of a particular position of the forefinger with visual feedback of position on a PC screen. The subjects were asked to keep their finger position as steady as possible and make corrections in case they deviate from this position. Every so often very small positional steps were made in the feedback signal, too small to be detected as externally imposed displacements and instead appreciated as part of the inherent noise in the task. In the first experiment, these displacements were triggered following beta bursts in finger microtremor (Gilbertson et al, 2005) or triggered randomly. In the second experiment beta bursts in EEG were used in order to provide the trigger. It was predicted that the corrective responses to steps would be larger after beta bursts than when steps were triggered randomly. Accordingly, we sought a promotion of the processing relevant to the control of positional hold tasks sufficient to affect motor behaviour during periods of increased beta synchrony.

3.1 Experiment 1

3.1.1 Materials and Methods

Subjects

Thirteen right-handed healthy volunteers (7 males; mean age 30 yrs, range 25 - 45 yrs) participated in the study.

Recordings

Surface EMG was recorded from the first dorsal interosseous (FDI) of the right hand. An electric goniometer attached to the medial aspect of the metacarpal and proximal

phalanges of the right index finger recorded abducting-adducting movements of the finger at the first metocarpo-phallangeal (MCP) joint. This goniometer signal was amplified and low-pass filtered at 20 Hz. Finger microtremor was detected by a miniature accelerometer taped to the distal phalanx of the right index finger. The accelerometer signal was amplified and split so that it was either low-pass filtered at 100 Hz or separately filtered on-line using a 13-35 Hz bandpass filter in order to generate triggering events (see chapter 2). Fig 3.1.1 shows examples of rectified EMG and raw accelerometer signals, one surpassing the triggering threshold applied to the beta bandpass-filtered acceleration and one failing to reach this threshold. Filtering and gain settings are as specified in chapter 2.

Behavioural Task

The participants sat in a quiet room with their forearms rested horizontally and their right hand pronated by their side. The paradigm was designed to investigate the effect of cortically projected microtremor oscillatory activity on the size and efficiency of corrective movements to step displacements. Subjects were instructed to keep their right index finger voluntarily extended and concentrate on a PC screen that was placed directly in front of them and displayed the goniometer output, which, with the hand pronated and the index finger extended, corresponded to the horizontal position of the finger. The goniometer signal was represented on-screen as a continuously updating time series of the current and recent (last 3 s) horizontal position of the finger. Horizontal position was displayed at high gain, so that displacements subtending a visual angle of 3 degrees on screen corresponded to changes in abduction/adduction of ~100 arc minutes at the first MCP joint. Two horizontal cursors were provided on screen and the subject asked to maintain finger position between these cursors. These cursors marked ± 1 degree excursions of the right index finger from the chosen target position. Unbeknown to the subjects, small positional step displacements in the feedback signal (but not the finger), lasting 5 s, were triggered by beta bursts (high beta trigger, HBT) in finger microtremor and again 10s latter (Fig 3.1.1A,B). The second trigger was therefore not time-locked to spontaneous beta bursts in finger microtremor (low beta trigger, LBT). Further beta triggering could not occur for an interval of 20s from the last HBT. The mean standard deviation of horizontal position (excluding imposed steps) was equivalent to 48.0 ± 4.7 arc minutes of adduction/abduction at the first MCP joint. The step displacements

in the visual feedback corresponded to changes in adduction of 24 arc minutes at the first MCP joint, to which the expected motor correction would have been abduction. These spurious steps in the visual feedback signal were therefore both very small and of a similar order of magnitude to the spontaneous variation in horizontal position of the finger. Thus subjects had no explicit knowledge of the timing of the imposed steps. Two recording sessions of 10 minutes duration and one session of 5 minutes, each separated by 3 minutes rest, were performed in each subject.

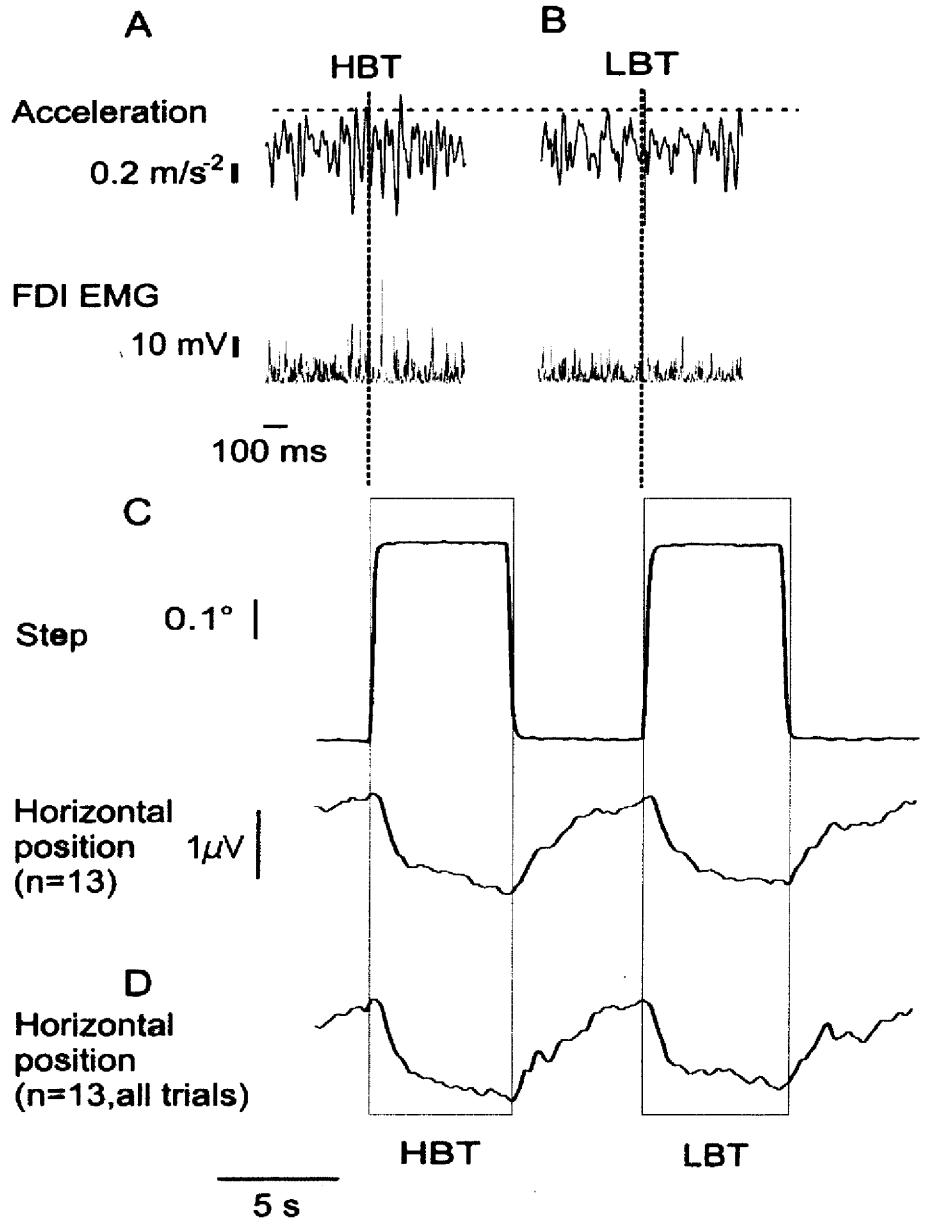

Figure 3.1.1 Microtremor triggering, imposed displacements, and responses. Acceleration and FDI EMG signals 500ms before and after the [A] HBT and [B] LBT trials, respectively. Note the bursts of microtremor in the accelerometer trace and the corresponding EMG bursts around 50ms before the HBT trial onset. On the other hand, before LBT, EMG signal is desynchronized and there is little microtremor in the finger. HBT and LBT onset are given by the dotted vertical lines. [C] Group averages (n = 13 subjects) of externally imposed step displacements in the visual feedback signal and

degrees abduction of the MCP joint of the right index finger. The first displacement of the feedback signal was time-locked to HBT and the second displacement (LBT) was presented 10 s later. Goniometer signal low-pass filtered at 20 Hz and then averaged with respect to HBT trials for a duration of 22s with a 2s offset. The first corrective movement was made in response to a change in the visual feedback triggered by a transient increase in the beta-band microtremor. The second corrective movement was made in response to a randomly-triggered visual step displacement 10s later. [D] The same goniometer signal as in C, but this time averaged with respect to all trials (including those that were rejected as movement artifacts). Note that the effect does not change due to the rejection of the trials.

Analysis

The first step was to reject HBTs triggered by large movements rather than microtremor and to also reject large spontaneous voluntary movements occurring before or after the HBT that might mask any small corrective displacements. Spurious triggering could be recognised as it involved abrupt non-oscillatory waves with much larger amplitude than the background acceleration activity. Accordingly, any trials with a triggering acceleration which exceeded 4 x SD of the mean acceleration over the 22 s period starting 2 s prior to the HBT were rejected as movement artefacts. In addition, residual trials in which any changes in goniometer signal exceeded 3 x SD of the mean goniometer signal were rejected as due to spontaneous voluntary movement rather than small corrective displacements. An average of 42 ± 17 trials were analyzed in the 13 subjects after an average of 48% of trials were rejected based on the above criteria.

Goniometer signals were low-pass filtered off-line at 20 Hz (3dB down at 23 Hz) and then averaged with respect to HBT for a duration of 22s with a 2s offset, so that both HBT and LBT trials were captured in the same average (Fig 3.1.1C). The magnitude of corrective movements was measured by subtracting the mean goniometer signal over the 2s period before the triggered displacement from the mean level during the 5s of the triggered step change. The imposed step in visual feedback (expressed as equivalent abduction/adduction of the MCP joint of the index finger) was likewise averaged with respect to HBT for a 20s duration with a 2s offset. The magnitude of corrective movements was then expressed as the percentage of the corresponding mean step displacement in the visual feedback (e.g. the second trace in Fig 3.1.1C was expressed as a % of the first trace over the boxed areas).

To confirm that the analysed HBTs were indeed triggered by bursts of beta band microtremor, spectral estimates of the power in the acceleration signals were derived using the FFT for blocks of 512 data points (frequency resolution ~ 2 Hz) centred on

each trigger and the average power within the beta range (13-35 Hz) estimated.

Finger microtremor in the beta band has been considered to be the mechanical product of synchronization of motor unit activity within muscles, which itself is due to synchronization within the beta activity in the corticospinal system (McAuley et al., 1997; Halliday et al., 1999; Gilbertson et al., 2005). To confirm that periods of elevated beta band microtremor were accompanied by increased descending drive at similar frequencies in this paradigm we extracted matrices of event-related coherence for each frequency within the beta band (13-35 Hz, frequency resolution ~2 Hz) for each subject between EMG and microtremor. Spectral analysis was performed using overlapping blocks of 512 data points, shifted by 2 ms and significance levels ($p = 0.05$) calculated as described elsewhere (Halliday et al., 1995). The value of 10 was attributed when coherence was significant at a particular frequency and time and the value of 0 when it was not. These values were then averaged across all frequencies in the beta band and across all subjects to give a single mean event related coherence score at each time point. This non-parametric approach ensured that the data would not be dominated by possible outliers.

3.1.2 Results

Adequacy of triggering

The acceleration signal revealed bursts of microtremor in the beta (13-35 Hz) band just before the HBT step change but not before the LBT step displacement (Fig 3.1.1). The average microtremor power in the beta band was substantially higher in HBT than LBT trials ($t = 5.16$, $p < 0.001$; Fig 3.1.2A) confirming the adequacy of the triggering.

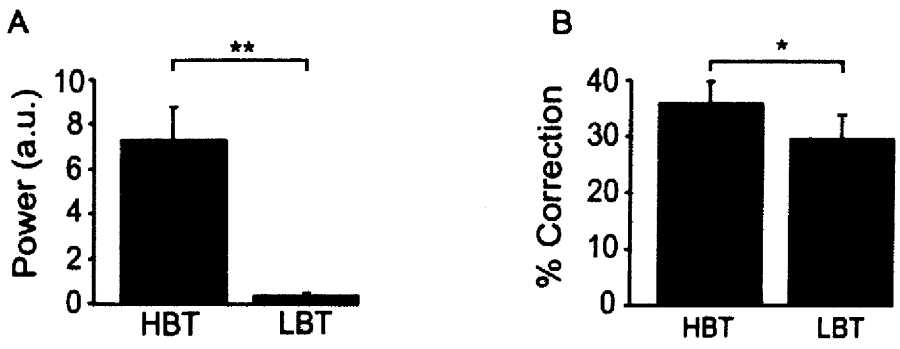

Figure 3.1.2 Adequacy of microtremor triggering of step displacements and percentage of corrections achieved. [A] Power spectral estimates of the accelerometer trace in the beta band 300ms

before and after the HBT and LBT trials, respectively. **p<0.001. [B] The percentage of the corresponding mean step displacements achieved following HBTs and LBTs, respectively. Error bars represent SEM. *p<0.05

Behavioural Data

The mean amplitude of corrective movements following each trigger after removal of spurious voluntary movements (see methods) is illustrated in fig 3.1.1C. The percentage of the step displacement achieved following HBTs was higher (36.1% ± 3.7) than following LBTs (30.0% ± 3.9; $t = 2.4$, $p < 0.05$; Fig 3.1.2B). Larger corrective movements were still seen even if no trials contaminated by spurious voluntary movement were rejected before averaging (Fig 3.1.1D). The onset latencies of the corrective movements did not differ between the two conditions (0.69s ± 0.08 in HBT trials and 0.74s ± 0.08 in LBT trials).

Significance of bursts of beta microtremor

In order to show that the coherence between EMG and microtremor was substantially higher within the beta band, coherence values were averaged across subjects for each frequency. The coherence spectrum exhibited a clear peak in the 20-30Hz range (Fig 3.1.3A). Fig 3.1.3B demonstrates the mean event-related coherence between FDI EMG and microtremor 2s before to 20s after HBT. There is clear coherence just before the HBT step displacement but not at any other time point during the trial, confirming that the triggering burst of microtremor is likely to be driven by muscle activity.

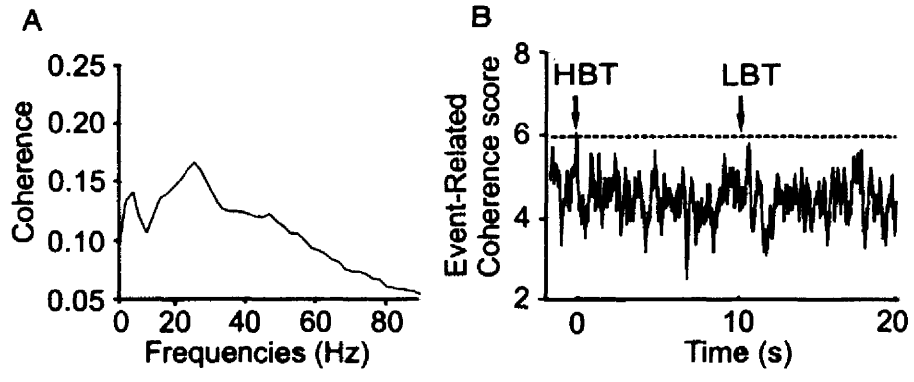

Figure 3.1.3 Coherence and event-related coherence between FDI EMG and microtremor. [A] The spectrum of the FDI EMG – accelerometer coherence across frequencies. There is a clear peak at 20-30Hz. [B] Plot of FDI EMG – microtremor coherence averaged across all subjects with respect to

HBT trials for a duration of 22s with 2s offset. Ninety-nine percent confidence limits are illustrated by the dotted horizontal line. Note that coherence is significant before HBT but not before LBT.

3.1.3 Discussion

This experiment demonstrated that the bursts of beta microtremor used to trigger the changes in visual feedback were associated with larger and more appropriately scaled corrective responses. The interpretation of these results rests on the assumption that bursts of beta band microtremor in the finger are a surrogate marker of phasic increases in beta activity in the cortico-spinal system (McAuley et al., 1997; Halliday et al., 1999; Gilbertson et al., 2005). In line with this we found a marked increase in the coherence in the beta band between EMG and microtremor during bursts of beta microtremor used to trigger step displacements in the visual feedback signal.

However, these data were subject to important limitations. First, no EEG was recorded so as to show that finger microtremor was indeed attributable to a synchronized oscillatory signal descending from the motor cortex. Second, the time difference between the HBT and LBT trials was not adequate for the finger to return to baseline before the LBT trials (see Fig 3.1.1.C). This could have confounded the results in favor of the HBT displacements resulting in higher estimations of the corrections achieved during the HBT. Finally, due to the high sensitivity of the accelerometer to minor jerks about half of the trials had to be rejected on the basis of spurious triggering. Of course, the result remained the same even when these trials were included in the analysis (see Fig 3.1.1D) but the exclusion of the 48% of the trials weakened the reliability of the results. Hence, the experiment was repeated but this time using beta bursts in EEG, rather than microtremor, as a trigger and prolonging the delay between the HBT and LBT step changes.

3.2 Experiment 2

The material presented here has previously been published (Androulidakis, A.G., Gilbertson, T., Doyle, L.M., Brown, P. (2006). Corrective movements in a postural hold task are more effective during periods of 13-35Hz oscillatory synchrony in the human corticospinal system. European Journal of Neuroscience. 24(11): 3299-3304).

3.2.1 Materials and Methods

Subjects

The participants were 11 right-handed healthy volunteers (5 males; mean age 30 yrs, range 25 - 45 yrs).

Recordings

The recording of EMG, goniometer and accelerometer signals was the same as in Experiment 1. Bipolar electroencephalogram (EEG) was recorded using a pair of silver – silver chloride electrodes, one over the motor hotspot (as defined by single-pulse TMS) referenced to one placed 2.5 cm anterior to the hotspot. The EEG signal was amplified and filtered as described in chapter 2. In order to trigger the visual step displacements a wavelet-based online triggering method was used (see Chapter 2).

Behavioral Task

The behavioral task was the same as before, but this time each trial lasted for 24s, rather than 20s, with the LBTs occurring 12s after the HBTs allowing thus for a 7s pre-LBT period. Unlike with the previous set-up, the 7s delay between HBT and LBT ensured that after HBT subjects made full corrective finger movements returning to and maintaining baseline levels for 2-3s before the LBT displacement occurred (see Fig 3.2.1). The magnitude of corrective movements was measured by subtracting the mean goniometer signal over the 3 s, rather than 2s, period before the triggered displacement from the mean level during the 5 s of the triggered step change. To contrast the efficiency of corrective movements made to the step displacements, the imposed step in visual feedback was likewise averaged with respect to HBT for 24 s duration with a 3 s offset. The magnitude of corrective movements was then expressed as the percentage of the corresponding mean step displacement in the visual feedback (e.g. the second trace in Fig 3.2.1C was expressed as a % of the first trace

over the boxed areas).

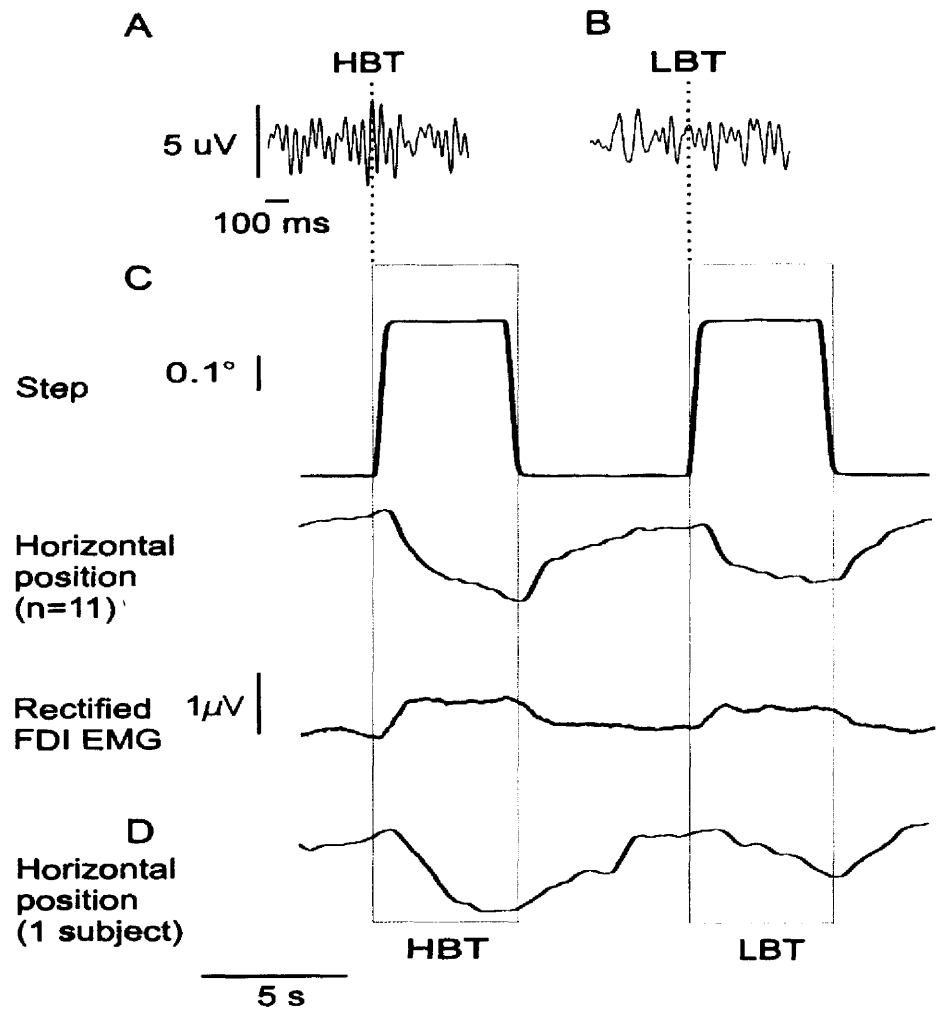

Figure 3.2.1. EEG triggering, imposed displacements, and responses. [A] Example of raw EEG signal in HBT trial. Note bursts of beta oscillations. [B] Example of raw EEG signal in LBT trial. [C] Group averages (n = 11 subjects) of externally imposed step displacements in the visual feedback signal and degrees abduction of the MCP joint of the right index finger and smoothed rectified surface EMG from the FDI. The first displacement of the feedback signal was time-locked to HBT and the second displacement (LBT) was presented 12 s later. [D] Example of mean event related abduction of the MCP joint of the right index finger from one subject.

Analysis

Triggered displacements in the feedback that coincided with scalp EMG contaminated parts of the EEG (high frequency activity with an amplitude of the signal exceeding 25μV) were excluded from the analysis. In addition, remaining trials in which any changes in goniometer signal exceeded 4 x SD of the mean goniometer signal occurring before or after the HBT and LBT were rejected as due to spontaneous

voluntary movements rather than small corrective displacements. An average of 57 ± 13.1 trials were analyzed in the 11 subjects after an average of 12.3 % ± 4.9 of trials were rejected based on the above criteria.

To confirm that the analysed HBTs were indeed triggered by bursts of beta EEG activity, spectral estimates of EEG power were derived using the FFT for blocks of 512 data points (frequency resolution ~ 2 Hz) centered on each trigger and the average power within the beta range (13-30 Hz) estimated.

We also tested whether beta bursts bunched in time, i.e. are more likely to occur after the last beta burst. For this purpose we used the EEG data obtained from the preliminary test sequence. We performed an interval histogram of the algorithms' output times using a width of 12 s and a bin size of 0.2 s.

Event related coherence was estimated between EMG and EEG from 0.5 s before to 0.5 s after the HBTs and the LBTs. Spectral analysis was performed using overlapping blocks of 512 data points, shifted by 2 ms and significance levels ($p = 0.05$) calculated as described elsewhere (Halliday et al., 1995) and matrices of event-related coherence were extracted for each frequency and for each subject. For the coherence analysis the same non-parametric approach was again used attributing the value of 10 and the value of 0 to significant and non-significant coherence values, respectively. Coherence peaked between 15-25 Hz in HBT trials (see results) so all scores were averaged across all frequencies in the 15-25 Hz band and across all subjects to give a single mean event-related coherence score at each time point for HBT and LBT trials. Scores were normalized using z-score transforms in a 1 s period starting 0.5 s before the trial onset.

3.2.2 Results

Adequacy of triggering

The adequacy of triggering was confirmed as the averaged EEG power in the beta band was found significantly higher in HBT than in LBT trials ($t = 4.77$, $p < 0.001$; Fig 3.2.3A). An example of the raw (non-pass band filtered) EEG signal is shown in Fig 3.2.1A,B. There is a clear burst of beta activity just before the HBT step change (Fig 3.2.1A) but not before the LBT step displacement (Fig 3.2.1B). Figure 3.2.2 confirms that there was no difference in the averaged EEG derived from the test

sequence and the EEG averaged with respect to HBT trials.

Figure 3.2.2 Adequacy of EEG triggering. Group EEG signals averaged [A] according to the algorithms' output times from the test sequence, [B] with respect to HBT trials, [C] with respect to LBT trials. There was little difference between A and B.

Behavioural data

The percentage of the step displacement achieved following HBTs was higher (41.7 ± 4.9 %) than following LBTs (31.5 ± 6.8 %; t = 2.46, p = 0.033; Fig 3.2.3B,C). The onset latencies of the corrective movements again did not differ between the two conditions (0.76 ± 0.08 s in HBT trials and 0.84 ± 0.14 s in LBT trials, t = -0.47, p = 0.6).

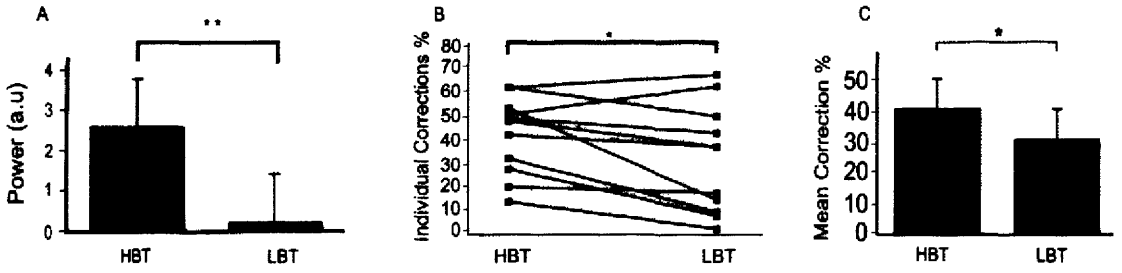

Figure 3.2.3 Power of EEG triggering and percentage of corrections to step displacements achieved. [A] Group mean power of EEG in the beta band at the time of HBT and LBT trials. Error bars represent SEM. **p<0.001. [B] Individual and [C] group average percentage of step displacement achieved during corrective movements made following HBTs and LBTs. Error bars represent SEM. *p<0.05

Significance of bursts of beta EEG

In order to demonstrate that the coherence between EMG and EEG was substantially higher within the beta band at the time of triggering, coherence values were averaged

across subjects for each frequency. Figure 3.2.4 demonstrates the mean event related coherence between FDI EMG and EEG 0.5s before and after HBT and LBT trials. There is clear coherence at the outset of the HBT step displacement but not upon onset of the LBT. Note that both the triggering burst of beta activity in the EEG (Fig 3.2.1 and 3.2.2B) and the accompanying burst of corticomuscular coherence (Fig 3.2.4) occurred simultaneously with the beta-triggered step perturbation, whereas EMG activity first began to increase, albeit very slightly, at about 200 ms later. Thus changes in the level of EMG activity were delayed (Fig 3.2.1 and 3.2.4C) and could not account for the phasic increase in cortico-muscular coherence.

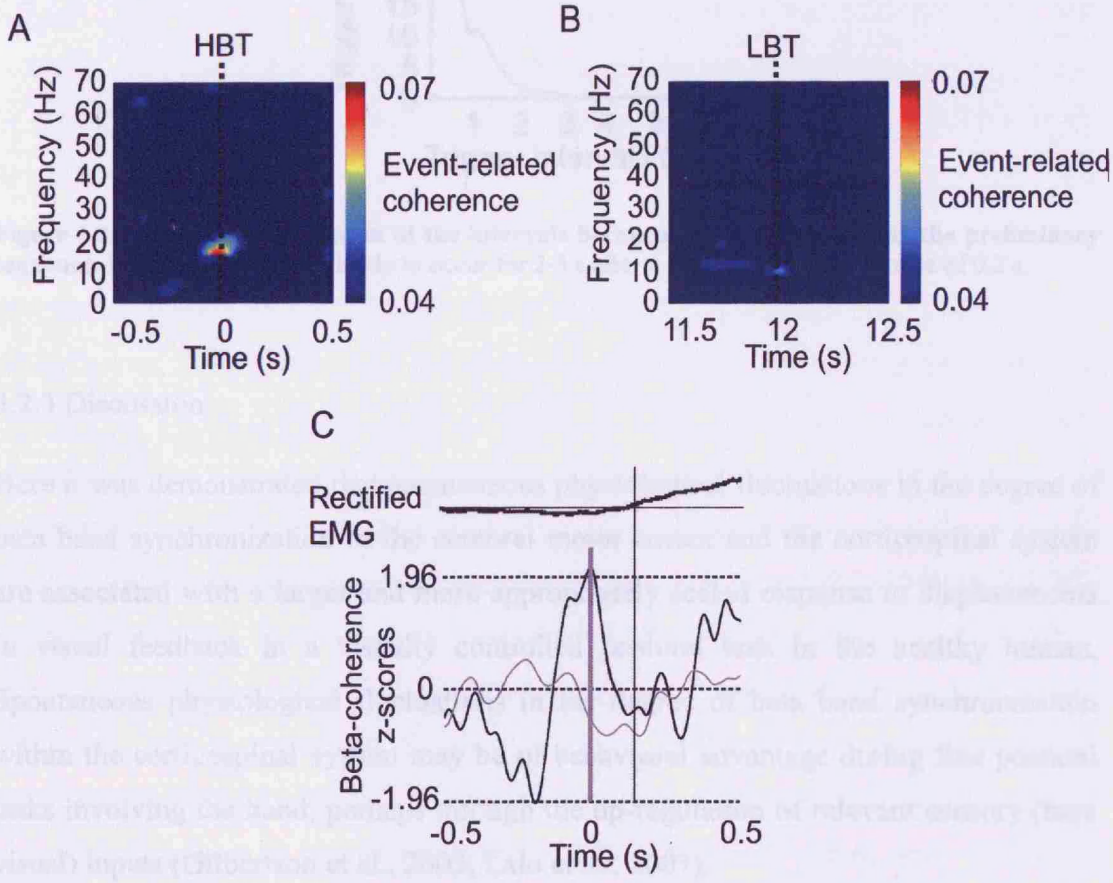

Figure 3.2.4. Corticomuscular synchrony. [A] Average event-related coherence across all subjects from 0.5s before to 0.5s after the HBTs. [B] Same for LBTs (with time being given from last HBT). [C] Average across all subjects and both triggering phases of the z-scores obtained from the number of bins at each time point with significant EEG – EMG coherence within the 15-25 Hz band with respect to HBTs (black line) and LBTs (grey line) trials. 95 % confidence limits are illustrated by the upper and lower dashed lines. Event-related coherence reaches significant levels around at the HBT event (marked by thick gray vertical line at t = 0). Smoothed rectified surface EMG from the first dorsal interossseous has been plotted above the coherence z scores. The thin black vertical line represents the point at which EMG begins to rise. This follows the peak in corticomuscular coherence.

Finally, the temporal relationship between beta bursts was delineated by plotting a frequency histogram of the intervals between triggerings made during the preliminary sequence (without displacements of the visual feedback signal) across the subjects (Fig 3.2.5). This indicated that further beta bursts were likely to follow within 2-3 s of a given triggering burst.

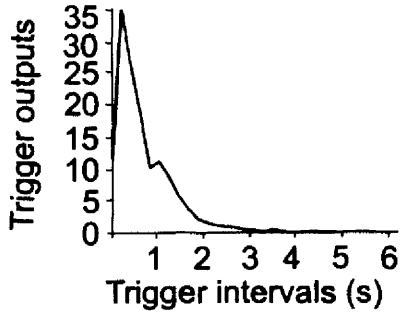

Figure 3.2.5 Frèquency histogram of the intervals between beta triggers during the preliminary sequence. Beta bursts are more likely to occur for 2-3 s after a given beta burst. Bin size of 0.2 s.

3.2.3 Discussion

Here it was demonstrated that spontaneous physiological fluctuations in the degree of beta band synchronization in the cerebral motor cortex and the corticospinal system are associated with a larger and more appropriately scaled response to displacements in visual feedback in a visually controlled postural task in the healthy human. Spontaneous physiological fluctuations in the degree of beta band synchronization within the corticospinal system may be of behavioral advantage during fine postural tasks involving the hand, perhaps through the up-regulation of relevant sensory (here visual) inputs (Gilbertson et al., 2005; Lalo et al., 2007).

A major assumption in the present study is that learning, whether explicit or implicit, did not occur during the task as, although HBT displacements were effectively presented in a random temporal sequence, LBT displacements were systematically delivered at a fixed time delay after HBT displacements. However, LBT displacements could not have been anticipated because, on the one hand, subjects were highly unlikely to be able to distinguish triggered displacements from spontaneous displacements in the feedback signal as steps in the visual feedback

signal were of a similar order of magnitude to the spontaneous variation in horizontal position of the finger, and, on the other hand, no difference in the latency of the response onset was found between the two conditions. Anticipation of LBT displacements would have been expected to have shortened the latency of corrections to these stimuli.

It could be argued that the increase in cortico-muscular coherence at the time of triggering might be due to an increase in EMG activity coincident with the small corrective movements induced by the perturbations. Indeed, it is true that the small corrective movements were associated with a tiny increase in EMG (Fig 3.2.1, Fig 3.2.4C). However, the triggering burst of beta activity in the EEG (Fig 3.2.1 and 3.2.2B) and the accompanying burst of corticomuscular coherence (Fig 3.2.4) occurred simultaneously with the beta-triggered step perturbation. EMG activity began to increase, albeit very slightly, at about 200 ms after the event (Fig 3.2.4C) and reached its peak at ~1 s after the event (Fig 3.2.1).

A very interesting result was the timing of the effects of beta bursts on subjects' performance, as the latency of the corrective responses to HBT displacements was reported to be on average around 700ms in both experiments. However, even estimates of the maximum duration of beta bursts suggest that these last less than 200 ms beyond the point of triggering (Gilbertson et al., 2005). It seems that the effects of bursts of beta activity outlasted the duration of the actual beta burst, although they had disappeared by the time of presentation of the LBT displacement. Previous studies have demonstrated a temporal difference between the duration of beta bursts and their effects on motor performance (Gilbertson et al., 2005) and on central sensorimotor processing (Lalo et al., 2007). Specifically, these results extend those of Gilbertson et al., 2005 and Lalo et al., 2007 to argue that a cortically driven beta oscillation occurring as far as 700 ms prior to the corrective response to HBT displacement can promote the accuracy of the response. These data imply that beta bursts may be associated with short-lasting plastic effects, whereby changed sensorimotor transformations outlast beta bursts. Consistent with that, it was further demonstrated that beta bursts "bunch", i.e. are more likely to occur for 2-3 s after the last beta burst (Fig 3.2.5). Together these observations suggest that a triggering beta burst may index a temporarily increased likelihood of similar bursts resulting in the alteration of processing for a period longer than the duration of a single beta burst.

Converging evidence suggests that the net effect of elevations in beta synchrony at the level of the motor cortex is the maintenance of a steady state force output (Schoffelen *et al.*, 2005), at least in part through the modulation of the motor response to afferent inputs (Gilbertson *et al.*, 2005; Lalo *et al.*, 2007). This may have significance for Parkinson's disease, where beta synchrony is increased at multiple levels of the motor system (Brown and Williams, 2005; Silberstein *et al.*, 2005) and tonic muscle activity is increased in the setting of increased motor responses to afferent, including visual, inputs (Martin, 1967; Tatton and Lee, 1975).

3.3 Summary

- Spontaneous physiological fluctuations in the degree of beta band synchronization within the corticospinal system may be of behavioural advantage during fine postural tasks involving the hand by temporarily reinforcing the effects of visual input regarding position.

- There was a mismatch between the duration of the actual beta burst (200ms) and the timing of the associated corrective responses to triggered displacements (~700ms). Beta bursts might be associated with short-lasting plasticity or the delayed behavioural effect might reflect the tendency for beta bursts to "bunch" (i.e. are more likely to occur for 2-3 s after the last beta burst).

CHAPTER 4

Anticipatory changes in beta activity in the human corticospinal system and associated improvements in task performance.

Synchronization of cortical neurons in the beta frequency band has been suggested to have some inverse relationship with the processing of new movements given that beta synchrony is particularly marked during holding contractions and is attenuated by voluntary movements (Pfurtscheller, 1981; Sanes and Donoghue 1993; Baker et al., 1997; Kilner et al., 1999; Schoffelen et al., 2005), while actively promoting processing related to postural activity, including tonic holding contractions (Gilbertson et al., 2005). The theory that beta activity may just be a passive characteristic of cortical networks when they are not engaged in active processing has been undermined by demonstrations of the positive attributes of beta band synchrony. Recently, there have been a number of these. Thus the transcortical component of the muscle stretch reflex is potentiated (Gilbertson et al., 2005), somatosensory inputs are up-regulated (Lalo et al., 2007) and corrective postural responses to visual feedback are improved (see Chapter 3) following bursts of physiological beta activity in the cortico-spinal system.

Nevertheless, beta activity and associated changes in sensorimotor reactivity could still be epiphenomenal. In other words, the behavioural associations of the beta state may just be spurious as far as the physiological organisation of postural and motor responses is concerned. Against this would be unequivocal evidence that the beta state is systematically increased and decreased in a task relevant way, so that the functional associations of the beta state are exploited. Kilner et al. (2000) demonstrated a temporary rebound in beta synchrony following movement that scaled with the level of compliance experienced in the succeeding holding contraction (see Chapter 1). The latter result is important in suggesting that beta activity might have a physiological role in tonic contraction, but the parametric relationship between beta synchrony and load compliance was demonstrated in the presence of confounding changes in peripheral feedback. In the following experiment it is shown that there is a systematic and prospective increase in beta synchrony prior to an expected postural challenge, and that such an up-regulation is associated with improved behavioural performance. The material presented here has been previously published (Androulidakis, A.G.,

Doyle, L.M.F., Yarrow, K., Gilbertson, P.T., Brown, P. (2007). Anticipatory changes in beta activity in the human corticospinal system and associated improvements in task performance. European Journal of Neuroscience. 25: 3758-3765).

4.1 Materials and Methods

Subjects

The participants were nine right-handed healthy volunteers (2 females; mean age 29 yrs, range 26 - 35 yrs).

Recordings

Surface EMG was recorded from the FDI of the right hand using bipolar 9-mm silver – silver chloride electrodes referenced to an electrode over the first MCP joint. The position of the right index finger was recorded by an electric goniometer attached to the medial aspect of the first MCP joint. Finger microtremor was detected by a miniature accelerometer taped to the distal phalanx of the right index finger. TMS was used to locate the motor cortex hand area and a Laplacian EEG configuration was recorded. We used five silver – silver chloride electrodes, one over the motor hot spot and four adjacent ones placed 4 cm anterior, posterior, inferior and superior to the hot spot. EEG signals were recorded with respect to a common ear reference and amplified and filtered as described in chapter 2.

Behavioural Task

The subjects were asked to hold their dominant forefinger tonically extended and slightly abducted with a 3mm elastic band (Guilbert Niceday Limited, Andover, Hants, UK) connecting the distal interphalangeal joint of their forefinger to the lever of a servo-controlled torque motor. The elastic band served so that the microtremor of the finger was not damped by inertial load (McAuley et al., 1997). Subjects were asked either to resist adducting pulls of the motor on their index finger (sudden 1N-increases in tangential force delivered over 200ms), so as to keep their finger in the same position, or to make reaction time abducting movements of the finger according to the form taken by a red imperative cue delivered on a PC screen. These imperative cues were preceded by black warning cues and delivered in blocks of 50 trials. Blocks consisted of a pseudo-random mix of four pairs of cues:

A) 20 stretch-stretch trials consisting of a stretch warning cue (black S) followed 2.3 s later by a stretch cue (red S) delivered simultaneously with a finger stretch provided by the torque motor (Fig. 4.1A).

B) 5 go-stretch trials consisting of a warning go cue (black G) followed 2.3 s later by a stretch cue (red S) delivered simultaneously with a finger stretch (Fig. 4.1B),

C) 20 go-go trials consisting of a warning go cue (black G) followed 2.3 s later by an imperative go cue (red G) which indicated that the subjects had to make an abducting movement with their finger $\geq 10^{\circ}$ as quickly as possible (Fig. 4.1C),

D) 5 stretch-go trials consisting of a warning stretch cue (black S) followed 2.3 s later by an imperative go cue (red G) soliciting finger adduction (Fig. 4.1D).

Trials (paired cues) were delivered at pseudo-randomised intervals of 7-10 s. Four blocks of 50 trials were repeated and each block lasted about 10 minutes. Cues would appear on screen for 500 ms. A control period of 4 minutes was also recorded during which subjects were requested to hold their finger still while connected to the torque motor, although this time no cues nor stretches were given.

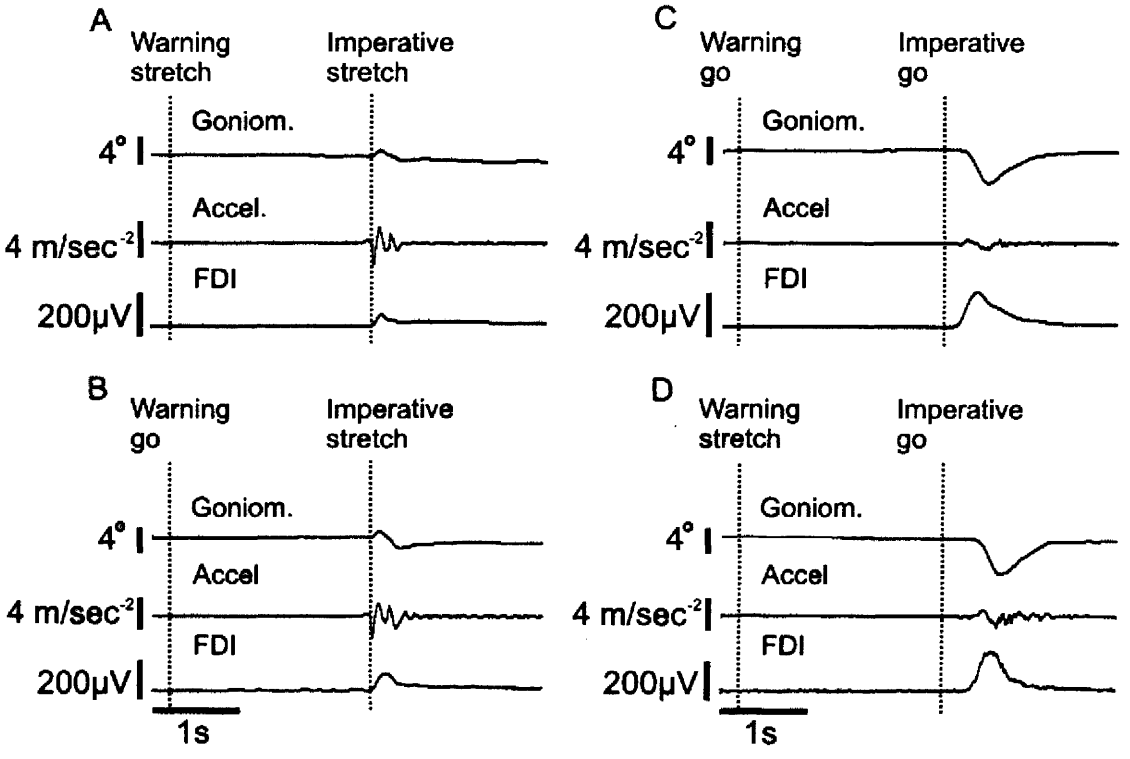

Figure 4.1. Warning and imperative cues and group mean responses. Group average position, acceleration and EMG signals for (A) stretch-stretch, (B) go-stretch, (C) go-go and (D) stretch-go trials. Vertical interrupted lines define cue onsets. FDI EMG (lower most trace in each) was rectified

before averaging.

Analysis

The first step was to reject all trials with inappropriate responses and artifacts. An average of 76 ± 1 stretch-stretch, 19 ± 0.3 go-stretch, 77 ± 0.5 go-go, and 19 ± 0.2 stretch-go trials per subject were analysed.

The first prediction to be tested was whether beta band synchronization between pyramidal neurones in the motor cortex was modulated in a task specific manner. EEG alone does not provide an adequate measure of synchronization within this neuronal population, as it also contains power related to synchronised activity in other ensembles of neurones, at least some of which may not be focal. One way to relatively selectively extract the component of EEG activity which is due to synchronization between pyramidal neurones is to estimate the coherence between EEG and muscle activity, as pyramidal neurones project to the spinal cord and hence drive muscle activity. Finger microtremor was used as an index of muscular activity. This is a sensitive index of the synchronization between motor units, and where this is coupled to EEG it seems reasonable to consider such peripheral synchronization to be driven by synchronization between pyramidal neurones (McAuley et al., 1997; Halliday et al., 1999; Gilbertson et al., 2005). The alternative, that finger microtremor drives an afferent response in the cortex, seems unlikely to be a major consideration in the beta band as cortical activity originates in the motor cortex and leads muscle activity (Mima et al., 2000; Brown, 2000; Schoffelen et al., 2005). Thus coherence between EEG and microtremor in the index finger may relate to the activity of only those pyramidal neurones in the cortical representation of the finger (Gilbertson et al., 2005). Accordingly, the time-evolving coherence between the EEG and finger microtremor (accelerometer signal) was calculated. To improve the estimates of corticomuscular coherence EEG signals were first transformed using the Hjorth scalp current density estimator (Hjorth, 1975; Mima and Hallett, 1999). Thus the difference between potentials recorded at the electrode overlying the motor hot spot and the averaged potential of the four neighbouring electrodes was derived. Event-related coherence between EEG and microtremor was calculated using the Morlet wavelet function $\psi_0(\eta)$, which has previously been used for EEG, EMG, and microtremor analysis (Samar et al., 1999; Strambi et al., 2004; Gilbertson et al., 2005; Li et al.,

2007; see Chapter 1).

Matrices of wavelet power, wavelet coherence and phase at a time resolution of 1ms and at scales corresponding to frequencies between 9 and 40 Hz with a resolution of 0.4Hz were extracted for the period between 0.5s before to 2.5s after the stretch warnings (condition A) and go warnings (condition C) for each subject. The distribution of coherence estimates was made to approximate a normal distribution by applying Fisher's transform to the coherence estimates. Time-evolving percentage event-related power and coherence changes were estimated for the period between the warning and the cue in relation to a 0.5s pre-warning baseline. As coherence was concentrated between 13-19Hz (see results), the wavelet values were averaged across this frequency range for the same time period of interest for each subject. Values that fell within the 95% confidence limits (CL) of background power and coherence were set to zero to avoid spurious fluctuations before averaging the respective spectra. Power and coherence values so treated were normally distributed as determined by the one sample Kolmogorov Smirnov test. Using these data series, serial two-tailed paired t-tests were performed between stretch-stretch and go-go trials, in order to acquire time-evolving p-values for coherence and power. Also, the wavelet values were averaged as a percentage of the baseline period across the whole inter-cue period in the 13-19 Hz band for each subject and the mean level of percentage coherence was compared for stretch-stretch and go-go conditions to the value of 100 (i.e. the mean coherence value of the baseline period defined as no change).

Coherence is a measure of both phase locking and amplitude proportionality over time. To specifically confirm that the phase of the EEG and accelerometer signals became locked / uniform following warning cues, we tested the distribution of the phase across trials both as a function of time and frequency using the Rayleigh statistic of uniformity (see chapter 2). Matrices of phase uniformity were extracted and then averaged across subjects. Finally, the phase synchrony between the EEG and finger microtremor was estimated using the method described by Lachaux et al (1999), with the exception that the signals were not first narrow band-pass filtered prior to convolution with the wavelet.

Goniometer and accelerometer signals were averaged over a period of 4.5s, beginning 0.5s before onset of the warning cue, so that both warning and imperative cues and

motor effects were captured within the same average (Fig 4.1). The magnitude of the adducting finger movement caused by the stretches was measured by subtracting the mean baseline goniometer signal over the 0.5 s period before the stretch onset from the first peak after the stretch onset. The size of the following abducting corrective movement was measured by subtracting the magnitude of the first peak after stretch onset from the subsequent trough. The peak acceleration of the stretched finger was defined as the maximal acceleration within 100 ms of stretch onset. In go trials reaction time was defined as the time between onset of the imperative go cue and the start of the acceleration accompanying movement. The peak acceleration of the voluntarily moved finger was defined as the maximal acceleration within 100 ms after response onset. Behavioural measures were compared between conditions using two-tailed paired t-tests.

Finally, in order to confirm that finger microtremor coherent with EEG is due to an efferent drive from motor cortex rather than peripheral afferance, the phase difference between the two signals from the control (stretch and movement free) recordings was estimated. This allowed greater averaging and thereby more consistent phase estimates than afforded by the time-evolving spectral analysis of intercue intervals. Phase was assessed only when coherence was significant and extended over at least three data points ($\geq$ 3Hz). The time lag between EEG and microtremor was calculated from the slope of the phase estimate after a line had been fitted by linear regression (see Chapter 2), but only if $r^2 > 0.75$ and the linear model was significant.

4.2 Results

Group mean finger position, acceleration and EMG signals in stretch-stretch, go-stretch, go-go and stretch-go trials are illustrated in Figure 4.1. EEG was coherent with finger microtremor in the beta band in all control (stretch and movement free) recordings (mean coherence 0.04 $\pm$ 0.007). In seven subjects EEG (data in two subjects did not meet phase criteria described in the methods) systematically led microtremor, by 23 $\pm$ 5 ms, in line with a cortico-muscular drive in the beta band.

Event-related coherence

Figure 4.2 demonstrates the time-evolving percentage change of the mean event-related coherence between EEG and microtremor in stretch-stretch and go-go trials

(Fig. 4.2A and 4.2B). There are coherence increases over 13-19 Hz after the warning stretch cue but not after the warning go cue. The coherence increases, after the warning stretch cue, are concentrated in the first half of the inter-cue period. Time evolving t-tests confirmed that coherence over this frequency band was episodically significantly higher after the warning stretch cue when compared to the period after the warning go cue (Fig. 4.2C). The increase after the warning stretch cue was also seen when coherence changes over 13-19 Hz were averaged across the whole intercue period (mean change in coherence 174 ± 31% after the warning stretch cue vs. 86 ± 11% after the warning go cue; two-tailed paired t-test; $t = 3.2$, $p = 0.01$; Fig. 4.2D). The coherence change averaged across the whole intercue period after the warning stretch cue was also significantly increased compared to baseline (two-tailed one-sample t-test $t = 2.37$, $p = 0.045$), although the mean decrease after the warning go cue was not significant (two-tailed one-sample t-test; $t = -1.2$, $p = 0.26$).

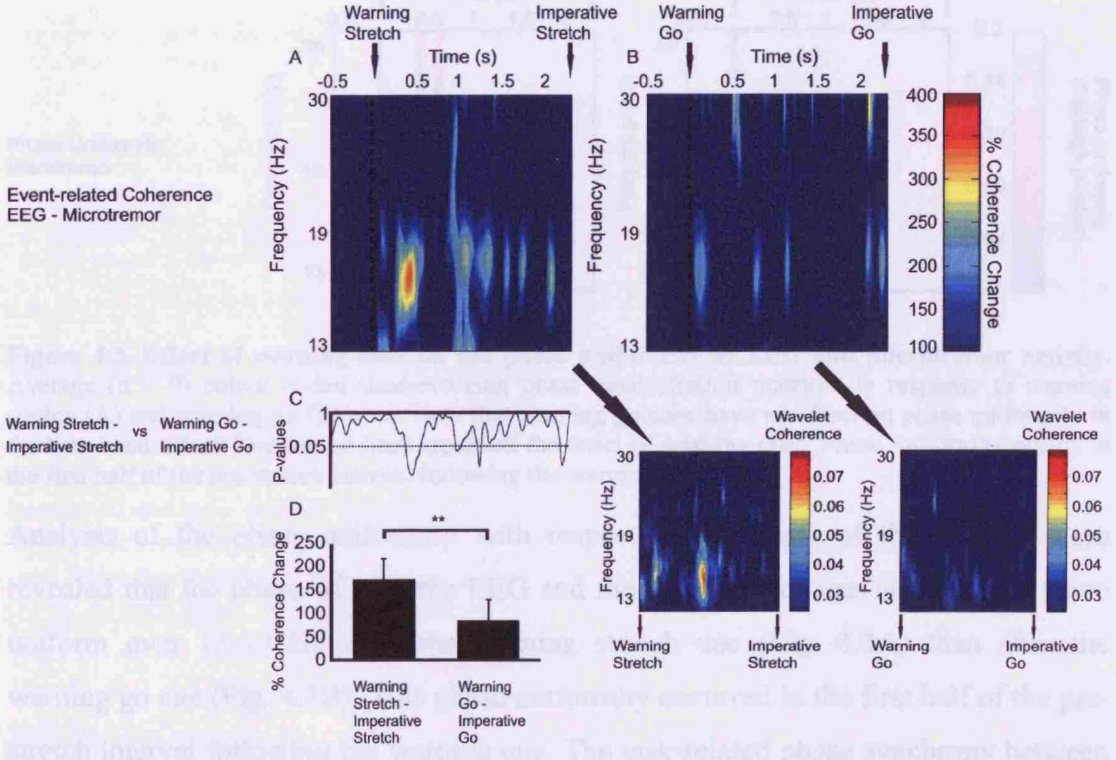

Figure 4.2. Effect of warning cues on coherence between EEG and finger microtremor in the beta band. (A) Average event-related percentage change in EEG – microtremor coherence from 0.5s before stretch warning cue up to the onset of stretch (stretch-stretch trials). Changes are relative to the baseline period from 0.5s before warning onset to warning onset. For visualization purposes, matrices of event-related percentage coherence changes were thresholded so that coherence values within the 99% confidence limits of the averaged baseline coherence were set to 100 % (i.e. defined as no change). Vertical interrupted line indicates warning cue onset. Note the non-linear frequency scale. Diagonal

arrow leads to a colour plot of averaged Fisher-transformed 95% CL thresholded coherence in stretch-stretch trials. (B) Same as (A) but for the period between 0.5s before go warning cue up to the onset of go cue (go-go trials). (C) Time-evolving significance of the difference in EEG-microtremor coherence between stretch-stretch and go-go trials. Horizontal interrupted line is p = 0.05 and y-axis is logged. Coherence is episodically significantly higher in stretch-stretch than go-go trials, principally in the first half of the pre-stretch interval following the warning cue. (D) Event-related coherence averaged across the whole inter-cue period in 9 healthy subjects for stretch-stretch and go-go trials. Mean ± SEM, **p < 0.01.

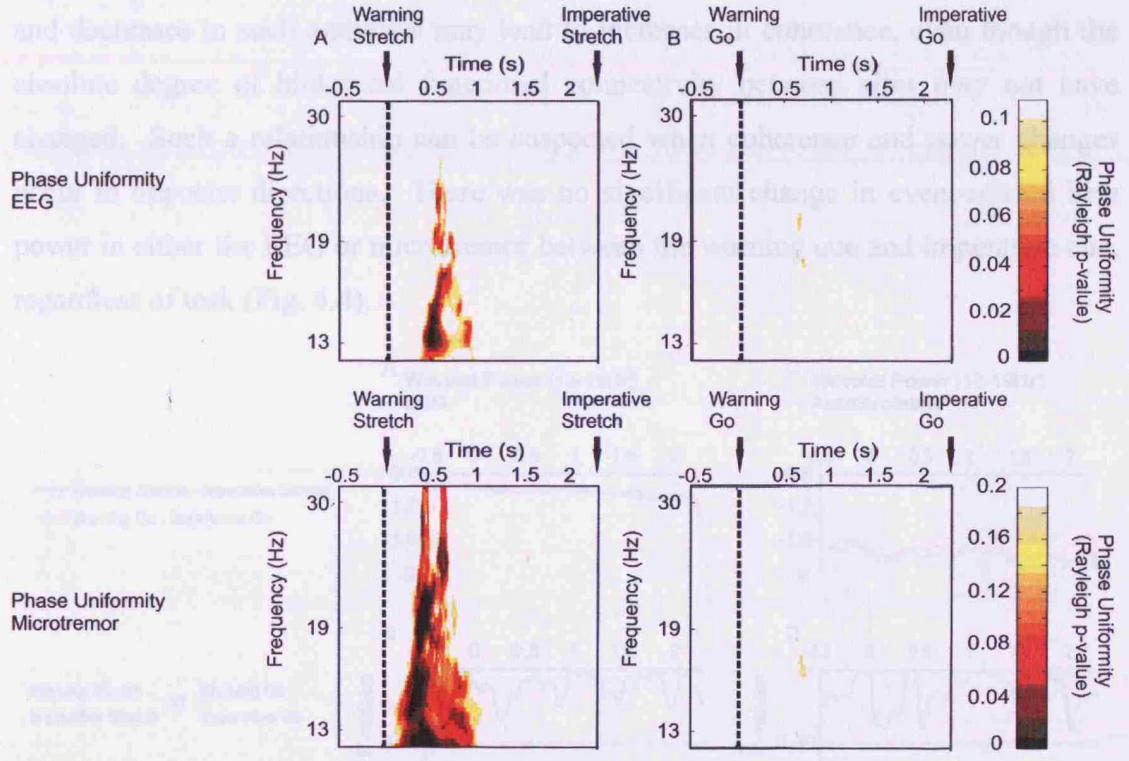

Figure 4.3. Effect of warning cues on the phase uniformity of EEG and microtremor activity. Average (n = 9) colour coded time-evolving phase concentration matrices in response to warning stretch (A) and warning go (B) cues. Note that warning go cues have no effect on phase uniformity in the beta band. Black interrupted lines represent the onset of warning cues. Phase uniformity occurs in the first half of the pre-stretch interval following the warning cue.

Analysis of the phase uniformity with respect to the onset of the warning cues revealed that the phase of both the EEG and the microtremor was significantly more uniform over 13-19 Hz after the warning stretch cue (Fig. 4.3A) than after the warning go cue (Fig. 4.3B). This phase uniformity occurred in the first half of the pre-stretch interval following the warning cue. The task-related phase synchrony between EEG and finger microtremor was also estimated. This was consistent with the above measures in so far as there was an increase in phase synchrony in the first half of the pre-stretch interval following the warning-stretch cue at a time when there was a decrease in phase synchrony following warning-go cues. This difference was

significant 0.3s and 0.9s after the warning cues.

Spectral power was also calculated to test whether changes in coherence were the result of modulations of non-linearly related frequency components (Fein et al., 1988; Florian et al., 1998). Coherence denotes the proportion of a pair of signals that linearly co-varies with respect to phase and amplitude at a given frequency. Thus, increases in activities that do not linearly co-vary may lead to reductions in coherence and decreases in such activities may lead to increases in coherence, even though the absolute degree of biological functional connectivity between sites may not have changed. Such a relationship can be suspected when coherence and power changes occur in opposite directions. There was no significant change in event-related beta power in either the EEG or microtremor between the warning cue and imperative cue, regardless of task (Fig. 4.4).

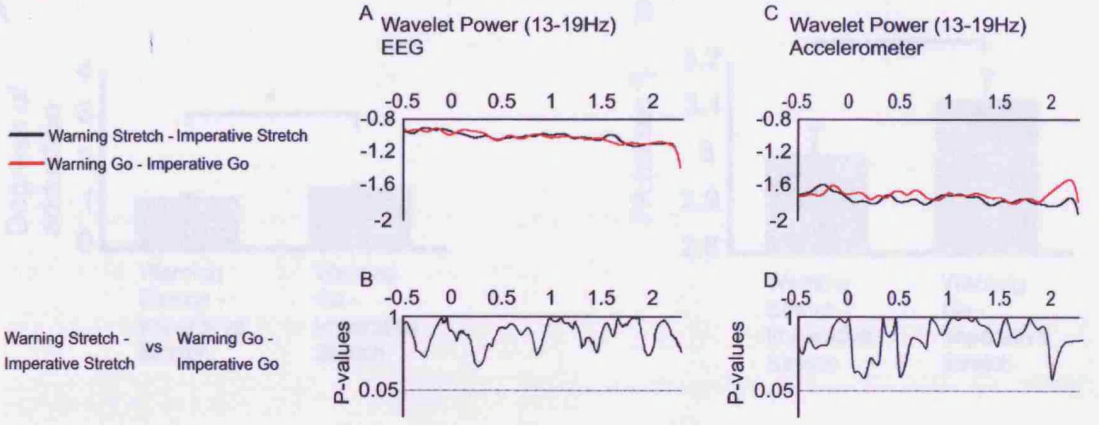

Figure 4.4 Effect of warning cues on event-related power in EEG and finger microtremor in the beta band. (A) Average event-related power in EEG over 13-19 Hz from 0.5s before stretch or go warning cues up to the onset of stretch (stretch-stretch trials) or imperative go cues. (B) Time-evolving significance of the difference in EEG power between stretch-stretch and go-go trials. Horizontal interrupted line is p = 0.05. (C) Average event-related finger microtremor power over 13-19 Hz from 0.5s before stretch or go warning cues up to the onset of stretch (stretch-stretch trials) or imperative go cues. (D) Time-evolving significance of the difference in microtremor power between stretch-stretch and go-go trials. In all plots y-axes are logged.

Behavioural data

There were no positional changes or alterations in mean rectified EMG during the period between cues (Fig. 4.1). Adducting movements caused by the stretch were found to be bigger when preceded by an incongruent warning go cue (1.12 ± 0.18 degrees of MCP joint adduction) than when preceded by a congruent warning stretch

cue (0.93 ± 0.16 degrees of MCP joint adduction; two-tailed paired t-test; t = 2.97, p = 0.017; Fig. 4.5A). Similarly, peak acceleration during stretch was greater when preceded by an incongruent warning go cue (3.11 ± 0.35 m/sec^2) than when preceded by a congruent warning stretch cue (2.90 ± 0.33 m/sec^2; two-tailed paired t-test; t = 2.33, p = 0.048; Fig. 4.5B). Moreover, the amplitude of the subsequent corrective movement was less appropriately scaled leading to further deflection from the target position following incongruous (3.00 ± 0.5 degrees of MCP joint abduction) as opposed to congruous (1.65 ± 0.21 degrees of MCP joint abduction; two-tailed paired t-tests; t = 3.31, p = 0.01; Fig. 4.5C) warning cues in stretch trials. Thus, the elevation in beta band phase stability and in coherence between EEG and microtremor prior to stretch trials was associated with better maintenance of the target postural contraction.

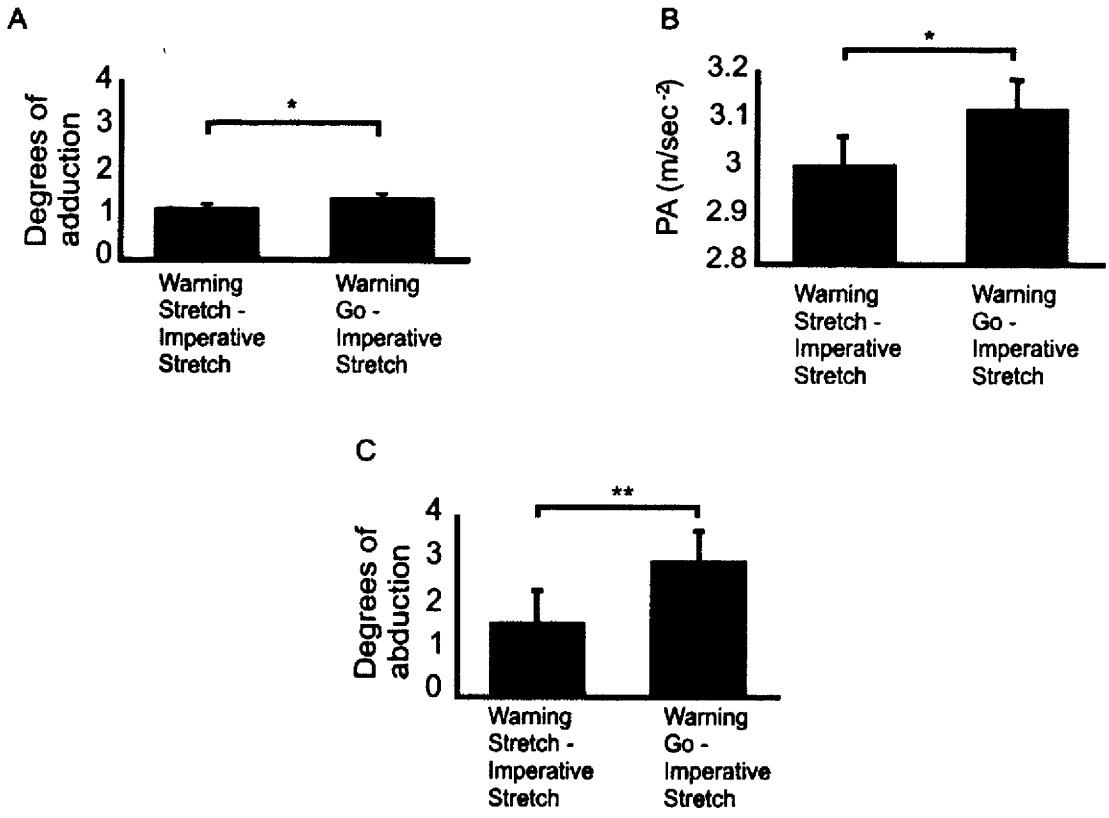

Figure 4.5. Average behavioural data in nine healthy subjects for stretch-stretch and go-stretch trials. (A) Mean ± SEM amplitude of finger adduction following stretch. (B) Mean ± SEM peak acceleration of stretched finger. (C) Mean ± SEM amplitude of abducting corrective finger movement following stretch. *p < 0.05, **p < 0.01.

On the other hand, reaction times in stretch-go trials (0.44 ± 0.04 s) were longer than in go-go trials (0.29 ± 0.03 s; two-tailed paired t-test; t = 5.12, p < 0.001; Fig. 4.6).

This confirmed that subjects attended to warning cues. No difference was found between the two trial types with respect to the peak acceleration of the voluntary responses (go-go trials, 1.22 ± 0.3 m/sec^2; stretch-go trials, 1.5 ± 0.42 m/sec^2; two-tailed paired t-tests; t = 0.7, p = 0.5).

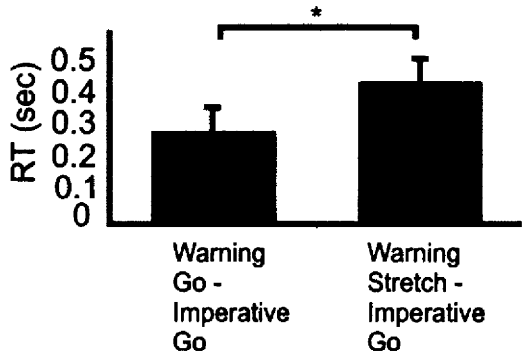

Figure 4.6. Average behavioural data in nine healthy subjects for go–go and stretch–go trials. Mean + SEM reaction time; *P < 0.001.

4.3 Discussion

It was demonstrated that the coherence between EEG and finger microtremor, the phase stability of the respective signals was increased in the beta frequency band when healthy subjects were warned of an upcoming stretch and tended to decrease when they were warned of a forthcoming cue to move. Consistent with this, the phase synchrony was transiently higher in the first half of the period following warning-stretch cues than at the same time after warning-go cues. These fluctuations in beta band phase stability and EEG-microtremor coherence preceded, and were therefore independent of, peripheral feedback related to the task, but were still associated with changes in behavioural performance. The results are in line with the suggestion that elevated beta synchronization in the motor cortex promotes processing relevant to the control of positional tasks (Kilner et al., 1999; Gilbertson et al., 2005; Lalo et al., 2007), and that, moreover, this state can be modulated according to circumstances without change in concurrent peripheral feedback.

EEG-microtremor coherence was not only greater following warning stretch than warning go cues, but was also greater than the preceding baseline activity. The latter confirms that coherence was up-regulated according to baseline, thereby

substantiating the finding of an event-related increase in EEG-microtremor coherence in anticipation of a stretch. In contrast, we did not find significant changes in either cortical or finger microtremor power in the beta frequency band. The absence of a significant reduction in beta band EEG activity following the warning cue is in contrast to the results of Doyle et al (2005b), where they observed decreases in the amplitude of the most reactive frequencies in the EEG expressed as a percentage change compared to a pre-cue baseline of 2s, and it is possible that the current study was under powered in this regard. However, the current study involved fewer subjects and trials which were interleaved rather than presented in blocks and, unlike in the study of Doyle et al (2005), we did not pre-select the most reactive frequencies in each individual.

Elevations in EEG-microtremor coherence were not sustained over the post-warning stretch period, but rather delayed and relatively short-lived throughout the intercue period. Similar phasic short-lived bursts of beta activity have been reported in previous studies (Gilbertson et al., 2005; Lalo et al., 2007) and were also found in the two previous experiments in chapter 3. These observations reinforce the argument that the influence of beta synchrony on sensorimotor integration is plastic, so that input-output relationships in the cortex are strengthened during and for a short period after each beta burst (chapter 3).

The major increase in EEG-microtremor coherence was around 0.5 s after the warning stretch cue (Fig. 4.2). The appearance of this feature in averaged data indicates that it was of relatively consistent timing across trials and subjects. In line with this feature, a concurrent increase in phase stability was observed in cortical and microtremor signals and phase synchrony between the two signals, given the close relationships between these measures (Friston et al., 1997). Similar phase stability has been noted in the motor cortex following visual cues related to movement in the monkey (Rubino et al., 2006). Nevertheless, the timing of differences in coherence, phase stability and phase synchrony were not exactly the same in our study, reflecting among other factors the additional importance of amplitude covariation in coherence measures.

The most striking finding in this study was that the increase in EEG-microtremor coherence due to the expectancy of a forthcoming postural "challenge" occurred without any change in peripheral feedback and was associated with a more efficient

maintenance of posture in response to the imposed perturbation. The lengthening of the reaction time in stretch-go trials suggests that subjects did take into account the nature of the warning cue in these trials and therefore were likely to have increased EEG-microtremor coherence following stretch warnings just as in the more numerous stretch-stretch trials. In contrast to the study of Gilbertson et al. (2005), this experiment failed to show that increases in beta activity have an effect on finger acceleration as no difference in the peak acceleration of voluntary finger adductions were observed between go-go and stretch-go trials. In the aforementioned study, however, reaction time cues were triggered by spontaneous bursts in beta band microtremor and hence microtremor power preceding voluntary movements was especially high. If finger microtremor in the beta frequency band can be considered a surrogate marker of cortical synchrony then this implies that a lower degree of synchronization effects improvements in postural control than penalises processing related to movement.

It is shown here that beta activity is associated with behavioural advantages with respect to holding contractions and can increase or decrease without afferent feedback depending on the expectancy of a forthcoming event. This points to beta synchrony being intimately related to postural set within the motor system, and increases the likelihood that beta synchrony actually helps underpin this motor state. It may be relevant therefore, that beta activity at subcortical and cortical levels is pathologically increased in Parkinson's disease (Brown et al., 2001; Silberstein et al., 2003; Silberstein et al., 2005) and in non-human models of Parkinsonism (Sharrot et al., 2005), -states dominated by excessive postural activity and impaired movement.

4.4 Summary

- There was a systematic and prospective increase in beta synchrony prior to an expected postural challenge. This up-regulation of beta synchrony was associated with improved behavioural performance in postural hold tasks.
- Increase in beta synchrony was not evident prior to an expected reaction time movement.
- Synchronization in the beta band was modulated in a task-relevant way with accompanying behavioural consequences.

CHAPTER 5

Dopaminergic therapy promotes lateralized motor activity in the subthalamic area in Parkinson's disease

In the previous chapters, the experiments with healthy volunteers have shown that regional and coupled changes in oscillatory activity in the motor system are likely to be of functional significance. Beta synchrony is seen in healthy humans, where it seems to favor processing related to postural or tonic modes of contraction (Gilbertson et al., 2005) by in part up-regulating the motor reinforcing effects of relevant sensory input (Lalo et al., 2007; see chapters 3 and 4). It is therefore possible that abnormal alterations in oscillatory activity in the motor system may contribute to the symptomatology seen in movement disorders, such as Parkinson's disease.

One of the most significant findings in depth recordings to date in PD has probably been the tendency for neuronal synchronization in the STN and GP at frequencies between 8 and 30 Hz in patients withdrawn from antiparkinsonian medication (see Chapter 1). This activity, evident as oscillation in the LFP over these frequencies, has been related to the bradykinetic state, which it may serve to promote (Brown, 2003; Dostrovsky and Bergman, 2004; Brown and Williams, 2005). Treatment of PD patients with levodopa has profound effects on both movement and the pattern of movement-related reactivity in the STN. Levodopa, which ameliorates bradykinesia, reduces the level of synchronization over 8-30 Hz at rest (Brown et al., 2001; Levy et al., 2002; Priori et al., 2002, 2004; Kühn et al., 2006b; Alonso-Frech et al., 2006) and may increase the event-related desynchronization that occurs prior to and during voluntary movement (Doyle et al., 2005; Devos et al., 2006). At the same time L-dopa treatment has been associated with synchronization in the gamma band particularly during voluntary movement (Cassidy et al., 2002; Williams et al., 2002; Alegre et al., 2005; Obeso et al., 2004; Foffani et al., 2005b; Fogelson et al., 2005; Alonso-Frech et al., 2006; Devos et al., 2006). The implication has been that dopaminergic therapy is making the pattern of population activity in the STN more physiological (Brown, 2003; Brown and Williams, 2005) in line with its effects on oscillatory activity in the cortex (Devos et al., 2003; 2004). However, there has been little support for this argument, and aspects such as the increased reactivity of subcortical beta activity following levodopa remain contentious (Priori et al., 2002; Alegre et al., 2005). Nor is

it intuitively obvious that treatment with levodopa, itself associated with involuntary movements in those patients in whom recordings are available, necessarily normalises population activity in the basal ganglia.

One approach to this issue is to look for similarities between the pattern of LFP activity in the STN following treatment with levodopa in patients with PD and that found in the cerebral motor cortex of patients without obvious movement disorders, as the motor cortex is both related in function and shows coherent activity with basal ganglia sites (Cassidy et al., 2002; Williams et al., 2002; Fogelson et al., 2006). The electrocorticographic activity (ECoG) in the motor cortex of patients with epilepsy but no extrapyramidal syndrome, shows activity in the gamma band that increases with movement (Crone et al., 1998a; Pfurtscheller et al., 2003). One striking feature of this physiological cortical gamma activity, which distinguishes it from oscillatory activities at lower frequencies, is that it occurs strictly contralateral to the side of movement (see Chapter 1). If the subcortical gamma activity following treatment with levodopa were a feature of physiological activity in basal ganglia-cortical loops then one would predict similar lateralisation of movement-induced increases in gamma activity in the STN. So far studies with small patient numbers (5-6 patients on therapy) have had conflicting results in this regard (Alegre et al., 2005; Devos et al., 2006). The aim of the study was, on the one hand, to elucidate the nature of gamma activity in the basal ganglia and, on the other hand, to replicate previous findings concerning the effect of levodopa on movement-related beta ERD in the STN. The material presented here has previously been published (Androulidakis, A.G., Kühn, A.A., Chen, C.C., Blomstedt, P., Kempf, F., Kupsch, A., Schneider, G.-H., Doyle, L.M.F., Dowsey-Limousin, P., Hariz, M., Brown, P. (2007). Dopaminergic therapy promotes lateralized motor activity in the subthalamic area in Parkinson's disease. Brain.130:457-68).

5.1 Materials and Methods

PD Patients

Eleven patients (age 59 ± 2.7 years, three females) were studied who underwent bilateral implantation of DBS electrodes in the STN for the treatment of severe PD (Table 1). Patients were studied 1-6 days post-operatively, in the interval between DBS electrode implantation and subsequent connection to a subcutaneous stimulator.

Adjustments to the intended surgical coordinates (see chapter 2) were made according to the direct visualization of STN on individual pre-operative stereotactic T2-weighted MRI (Hariz et al., 2003) and, in cases 4-7 and 10 from Berlin, ventriculography and intra-operative microelectrode recordings. Post-operative scanning confirmed that at least one contact was within the STN (Table 1). Correct placement of the DBS electrode in the STN was also supported by significant improvement in UPDRS motor score during DBS OFF levodopa ON stimulation compared to UPDRS OFF levodopa OFF stimulation (mean improvement 48.36% ± 6, two-tailed paired t-test: $t = 5.5$, $p = 0.0003$; table 1).

Tremor patients

Recordings were also made from two patients who had undergone functional neurosurgery for treatment of essential tremor and dystonic right upper limb tremor in cases 1 and 2, respectively. For case 1, the first DBS electrode was implanted in the Vim with the caudal contact within Zi and the second one in the STN. Case 2 was implanted with an electrode bridging posterior STN (rostral contact 3) and the preleminiscal radiation on the left. Neither patient was receiving pharmacological treatment for their tremor at the time of surgery or post-operative recording.

Case 1 was a 57-year-old male with a 5-year history of action and postural tremor of the left > right upper limb and head. Tremor was alcohol responsive. There was a family history of tremor affecting the patient's three siblings and his father. The patient didn't take any medication. On examination there were no abnormal neurological signs, other than severe tremor. The Essential Tremor Rating Scale score was 20. No evidence of a dopaminergic lesion was found on a pre-operative DAT scan.

Case 2 was a 64-year-old male with a 17-year history of dystonic left upper limb and head tremor. His father also suffered from tremor. On examination there were no abnormal neurological signs, other than severe postural and action tremor. MRI of brain showed a few scattered hyper-intensities consistent with small vessel disease and copper studies were normal. The patient did not respond to a sustained trial of levodopa. He did not have a DAT scan.

Table 5.1: Clinical details in PD patients.

Case	Age and sex	Disease duration (years)	Predominant symptoms	Motor UPDRS pre-op (ON/OFF levodopa)	Motor UPDRS post-op (OFF levodopa) ON/OFF DBS	Contacts most likely within STN based on MRI	Medication (daily dose) pre-op	Contacts used (R/L hand)
1*	46/M	11	Dyskinesias, motor fluctuations	8/64	21/61	R STN: 0,1 L STN: 1,2	Levodopa 800mg Entacapone 800mg Pergolide 4mg Amantadine 200mg Apomorphine 6mg	Off: R01 Off: L01/L12 On: R23/R12 On: L12
2	66/F	11	Dyskinesias, tremor rigidity, freezing, motor fluctuations	24/61	17/28	R STN: 0, 1 L STN: 0, 1	Levodopa 1600mg Ropinirole 15mg	Off: R01 Off: L12 On: R23 On: L01/L12
3	58/M	8	Tremor, akinesia, motor fluctuations	8/59	13/43	R STN: 0, 1, 2 L STN: 0, 1, 2	Levodopa 1200mg	Off: R12 Off: L23 On: R12/R23 On: L01/L12
4	52/M	13	Dyskinesias, on-off fluctuations	11/41	16/35	R STN: 1, 2 L STN: 1, 2	Levodopa 650mg Cabergoline 12mg Entacapone 800mg Amantadine 200mg	Off: R23/R12 Off: L23/L12 On: L01 On: R12
5	73/M	16	Freezing, on-off fluctuations	17/36	27/52	R STN: 0, 1 L STN: 0, 1	Levodopa 800mg Amantadine 300mg Entacapone 1200mg Ropinirole 5mg Cabergoline 2mg	Off: R01 Off: L01 On: R01/R12 On: L23/L12
6	67/M	16	Tremor, freezing, on-off fluctuations hallucinations	42/68	14/30	R STN: 1, 2 L STN: 0, 1	Levodopa 800mg Pergolide 6.5mg Entacapone 1200mg Pramipexol 2.1mg Quetiapine 25mg	Off: R01/R23 Off: L12 On: R12 On: L01
7	62/F	12	Dyskinesias, motor fluctuations	13/61	25/34	R STN: 0, 1, 2 L STN: 0, 1, 2	Levodopa 500mg Pramipexol 3.85mg Entacapone 1600mg Amantadine 200mg	Off: R12/R23 Off: L01/L12 On: R12 On: L12/L23

8*	43/F	14	Dyskinesias, motor fluctuations	13/61	14/61	R STN: 0, 1, 2 L STN: 0, 1, 2	Levodopa 500mg Cabergoline 6mg Amantadine 200mg Amytriptilline 10mg Domperidone 30mg Apomorphine 8mg	Off: R23 Off: L12 On: R23 On: L23/L12
9*	62/M	13	Dyskinesias motor fluctuations dopamine overuse	14/86	67/90	R STN: 2, 3 L STN: 2,3 (?)	Levodopa 800mg Apomorphine pump 108mg per day	Off: R01/R23 Off: L01 On: R12/R23 On: L23
10	60/M	15	Dyskinesias, freezing	41/73	missing	R STN: 1, 2 L STN: 1, 2	Levodopa 700mg Ropinirol 15mg Entacapone 1000mg	Off: R12/R01 Off: L01 On: R12/R23 On: L12/L23
11*	64/M	11	Akinesia	18/47	25/33	R STN: 1, 2 L STN: 1, 2	Madopar 700mg Ropinirol 17.5 mg Cabergoline 4mg	Off: R01 Off: L01 On: R12 On: L01

* Left-handed patients

Paradigm and recordings

The subjects were seated comfortably in a chair and recorded while making self-paced movements of a joystick forward and then immediately backward, repeated approximately every 10-20s. This task was performed separately with left and right hands, and, in the case of the PD patients, ON and OFF medication (Fig 5.1). In the latter instance, recordings were made from the STN after patients had been off antiparkinsonian medication overnight and again about 1h after they had taken a minimum of 200 mg levodopa. LFP signal was recorded bipolarly, amplified (x 100,000) and, in the PD patients, pass band filtered at 1-250 Hz. Surface EMG was simultaneously recorded from the FDI of the active hand, amplified (x 10,000), and pass band filtered at 10 Hz - 1 kHz. Joystick movements were also recorded. In the PD patients, amplification was performed using a D150 amplifier (Digitimer Ltd, Welwyn Garden City, UK) or a custom-made battery-operated portable high impedance amplifier (previously described in Kühn et al., 2004).

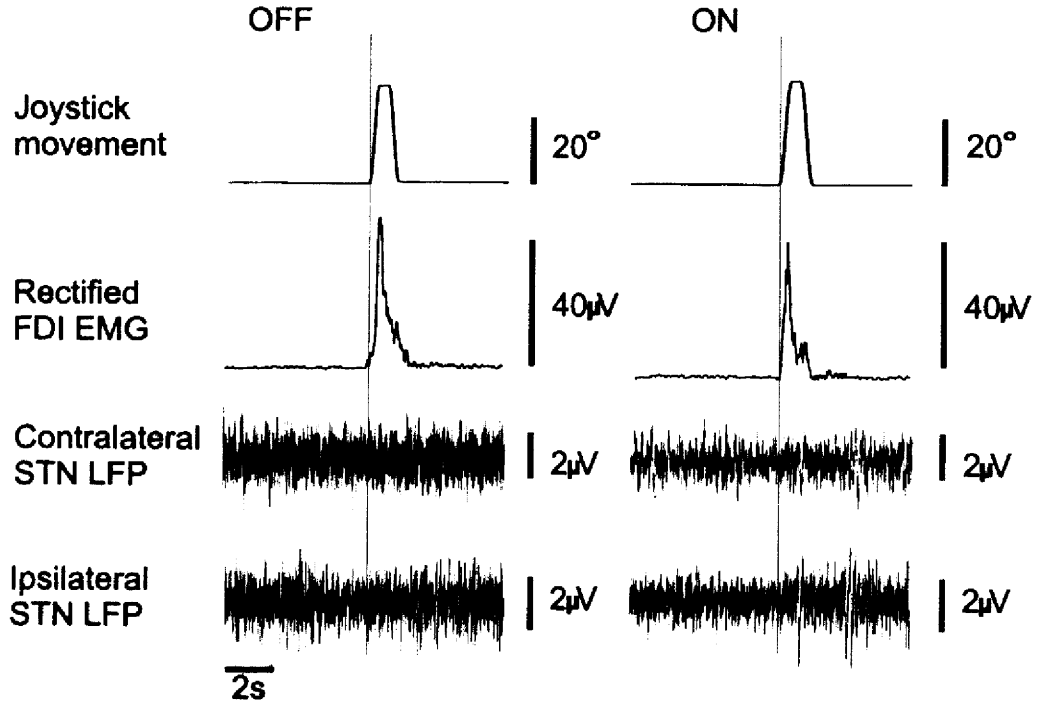

Figure 5.1. Examples of joystick, EMG, and STN LFP recordings in a PD patient. Raw data in case 8. Self-paced joystick movement made with the right hand OFF and ON levodopa and simultaneously recorded right FDI EMG and raw LFP from contralateral (left) and ipsilateral (right) STN.

All signals were sampled at rates of 625 Hz - 2 kHz. For the two tremor patients, signals were amplified and band pass filtered between 1 and 90 Hz (sampling rate 184 Hz) and 1.5 - 200 Hz (sampling rate 1200 Hz) in case 1 and 2, respectively (Biopotential Analyzer Diana, St Petersburg, Russia).

Analysis

Data were interpolated to a common sampling rate of 1 kHz. This was justified as, with one exception, the lowest original sampling rate was 625 Hz, and therefore much higher than either our low pass filter (250 Hz) or our frequency band of interest (<100 Hz). The one exception was one of the tremor patients who was recorded with a sampling rate of 184 Hz, which still remained higher than the low pass filter (90 Hz). Only frequencies up to 90 Hz were analysed in this patient. The onset of movements was visually detected from both joystick position and EMG traces and marked. Movements were only marked when they were not preceded or followed by another movement within a period of 9 s. The mean number of movements was 16 (range, 7-28) and the mean duration of analyzed recordings was 424 s ± 57 s.

The first analysis step was to calculate the event-related spectral power for all contact pairs for a period of 4.5 s before to 4 s after movement onset. Spectral analysis was performed using overlapping blocks of 1024 data points, shifted by 10 ms affording a frequency resolution of 1 Hz (Halliday et al., 1995; Brown et al., 2000). ERD and ERS were defined as the percentage power decrease (ERD) or power increase (ERS) in relation to a pre-movement baseline (-4.5s to -4s) period. The DBS contact pair that afforded the highest mean percentage power change over 40-85 Hz and over 8-30 Hz for a period of 500 ms before and after movement onset on each side was identified (Table 1).

Time-evolving mean percentage event-related power change for each selected contact pair was estimated separately for left and right hand joystick movements in both the ON and OFF states for each implanted side. For quantitative analysis at low frequencies, the frequency with the most pronounced mean ERD between 500 ms before and 500 ms after movement onset over 8-30 Hz was determined, consistent with the frequency distribution

of the ERD in grand averages of event related power change (Fig 5.2) and previous observations (Alegre et al., 2005; Williams et al., 2005; Kühn et al., 2006a). The percentage change in power was measured at this individually defined frequency and over the two (1 Hz) bins on either side of this frequency (i.e over a 5 Hz band). Additionally, the post-movement ERS at the same frequencies was estimated over the period of 2s to 4s after movement onset.

For the quantitative analysis of power change in the gamma band, the whole of the gamma band modulated by movement (40-85 Hz) was analysed for those DBS contact pairs affording the highest mean percentage change in this band for a period of 200 ms before to 500 ms after movement onset on each side (Table 1). This way was preferred as individually defined peaks at high frequencies were not always evident in all matrices of event-related power change.

Percentage values of ERD/ERS were normally distributed as confirmed by the one-sample Kolmogorov-Smirnov test. The principal ANOVA, repeated in both low frequency and gamma bands, was that performed on % power changes with main effects STATE (2 levels: OFF and ON) and LATERALITY (2 levels: ipsilateral and contralateral to hand movement). Further subsidiary ANOVAs, as detailed in the Results, were performed to explore the data and particularly to examine factors previously highlighted in the literature. Mauchly's test confirmed the sphericity of the data entered in the ANOVAs. Post-hoc two-tailed, paired Student's t-tests were used to confirm relevant differences in event-related power. Means ± standard error of the means (SEM) are given in the text.

5.2 Results

Alpha-Beta ERD and ERS in patients with PD

Grand averages of event related power changes in those contact pairs showing the greatest change in the 8-30 Hz band on each side in the OFF state demonstrated a significant alpha-beta ERD which preceded movement in onset and persisted for about 1 s thereafter (Fig 5.2). This was followed by a significant ERS, as previously reported (Cassidy et al., 2002; Doyle et al., 2005).

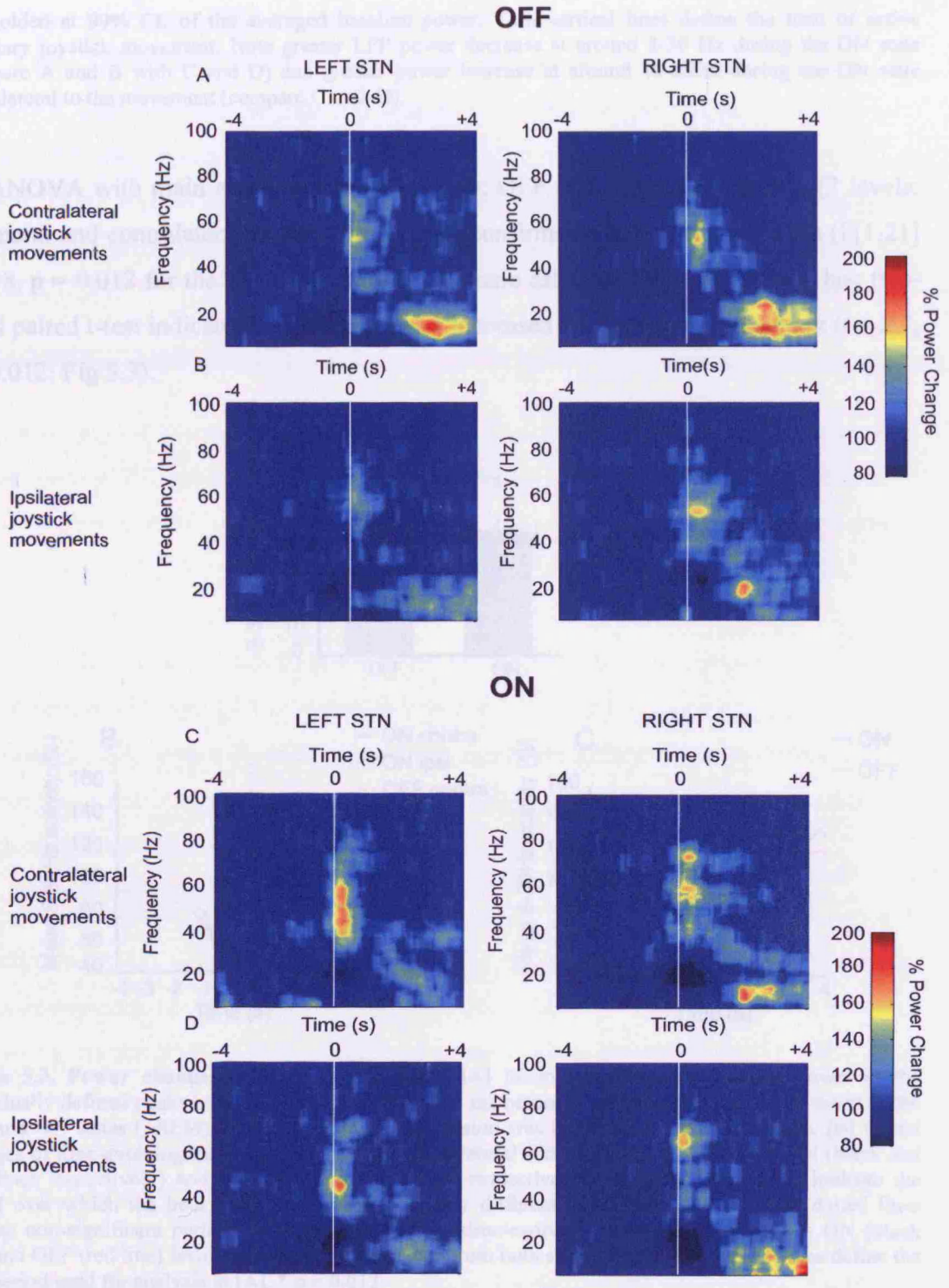

Figure 5.2. Movement-related spectral power in STN LFP before and after levodopa treatment. Relative spectral power change in STN LFP in the OFF state contralateral [A] and ipsilateral [B] to limb movement and in the ON state contralateral [C] and ipsilateral [D] to limb movement. Averaged color coded time-evolving power relative to baseline period (4.5 to 4.0 s prior to movement). The matrices are

thresholded at 99% CL of the averaged baseline power. Thin vertical lines define the time of active voluntary joystick movement. Note greater LFP power decrease at around 8-30 Hz during the ON state (compare A and B with C and D) and greater power increase at around 40-85Hz during the ON state contralateral to the movement (compare C with D).

An ANOVA with main effects of state (2 levels: OFF and ON) and laterality (2 levels: ipsilateral and contralateral to hand movement) confirmed a main effect of state ($F[1,21] = 7.48$, $p = 0.012$ for the 8-30 Hz band) but no main effect of laterality. A post hoc two-tailed paired t-test indicated that the ERD was increased after levodopa treatment ($t = 2.7$, $p = 0.012$; Fig 5.3).

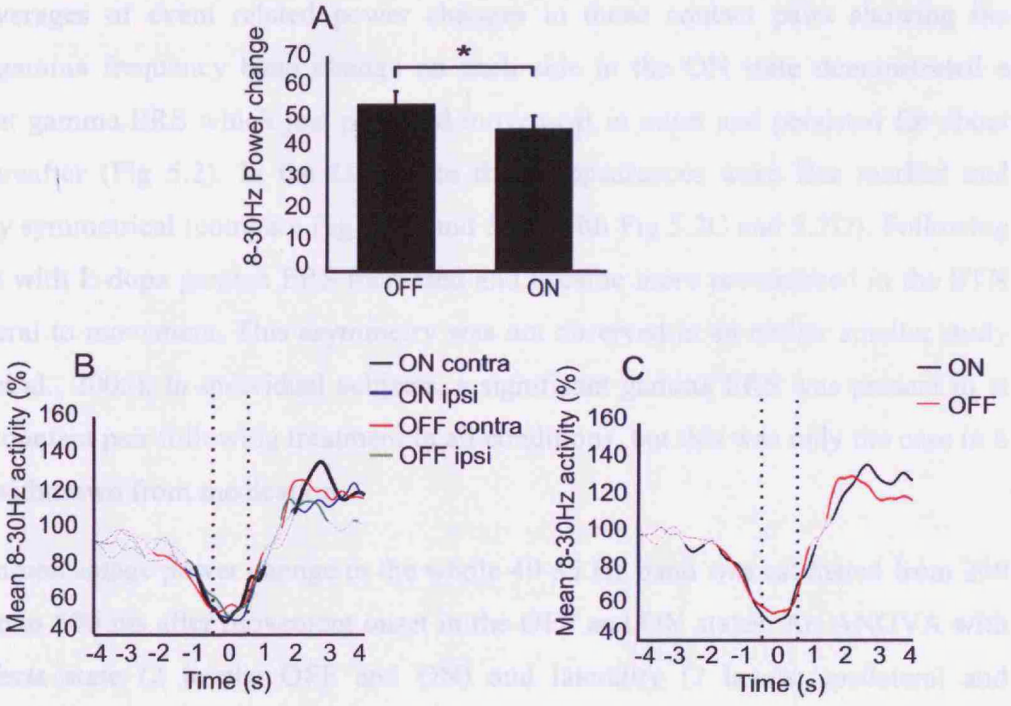

Figure 5.3. Power changes in the 8-30 Hz band. [A] Mean percentage of baseline power in the individually defined peaks in the 8-30 Hz band from 500 ms before to 500 ms after movement onset in the OFF and ON states (+SEM). Percentage power suppression was higher in the ON drug state. [B] Grand averages of time-evolving mean 8-30 Hz changes contralateral and ipsilateral to movement ON (black and gray lines respectively) and OFF (red and green lines respectively) levodopa. Thick lines indicate the period over which the beta ERD becomes significantly different to baseline and thin and dotted lines indicate non-significant periods. [C] Grand average of time-evolving mean 8-30 Hz changes ON (black line) and OFF (red line) levodopa after combining data from both sides. The dotted vertical lines define the time period used for analysis in [A]. * $p = 0.012$.

Another ANOVA was performed with main effects state and worse affected side (two

levels: lesser and worse affected sides). No effect of worse affected side or interaction between main effects was shown. A main effect of laterality was, however, found when an ANOVA with main effects state and laterality was repeated for the percentage power change in the post-movement ERS from 2 s – 4 s after movement onset ($F[1,21] = 5.1$, $p = 0.035$). There was no main effect of state or interaction between main effects. A post-hoc two-tailed paired t-test verified that the beta ERS was increased contralaterally to the movement side.

Gamma ERS in patients with PD

Grand averages of event related power changes in those contact pairs showing the greatest gamma frequency band change on each side in the ON state demonstrated a significant gamma ERS which just preceded movement in onset and persisted for about 0.5 s thereafter (Fig 5.2). In the OFF state these appearances were less marked and bilaterally symmetrical (compare Fig 5.2A and 5.2B with Fig 5.2C and 5.2D). Following treatment with L-dopa gamma ERS increased and became more pronounced in the STN contralateral to movement. This asymmetry was not observed in an earlier smaller study (Alegre et al., 2005). In individual subjects, a significant gamma ERS was present in at least one contact pair following treatment in all conditions, but this was only the case in 6 patients withdrawn from medication.

The mean percentage power change in the whole 40-85 Hz band was estimated from 200 ms before to 500 ms after movement onset in the OFF and ON states. An ANOVA with main effects state (2 levels: OFF and ON) and laterality (2 levels: ipsilateral and contralateral to hand movement) confirmed a main effect of state ($F[1,21] = 4.4$, $p = 0.04$) and laterality ($F[1,21] = 7.2$, $p = 0.014$) and a significant interaction between state and laterality ($F[1,21] = 4.4$, $p = 0.04$). It was also confirmed that an interaction between state and laterality for data from 200 ms before to 500 ms after movement remained when only the subjects that exhibited a percentage improvement of more than 30% (i.e. all cases except 7, 9, 11; see table 1) were included in the analysis ($F[1,15] = 4.54$, $p = 0.05$). Post hoc two-tailed paired t-tests indicated that the gamma ERS was significantly larger during contralateral hand movements ($t = -3.6$, $p = 0.02$ for 11 subjects; $t = 2.9$, $p = 0.011$ for 8 subjects) but only after levodopa medication and not during the OFF state (Fig

5A,B).

To explore this result further, an ANOVA was performed with main effects state and laterality for only the pre-movement gamma ERS (from 200 ms before to movement onset). This confirmed only a main effect of STATE ($F[1,21] = 4.5$, $p = 0.046$) and no interaction between main effects. Post hoc t-tests verified that the pre-movement onset gamma ERS was significantly larger after levodopa medication ($t = 2.1$, $p = 0.048$). Thus the effect of levodopa on the gamma ERS could not have been due to altered re-afferance following changes in motor performance. An ANOVA with main effects of worse affected side and state showed no effect of worse affected side or interaction between state and affected side on the gamma ERS.

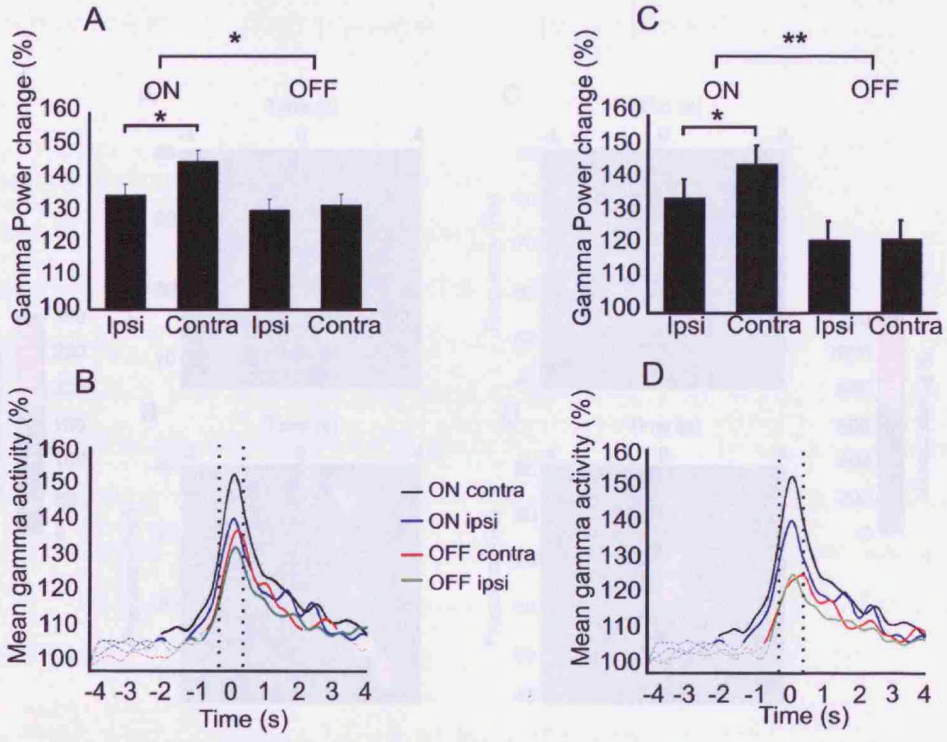

Figure 5.4. Power changes in the gamma frequency band. [A] Mean percentage of baseline power in the 40-85Hz band from 200ms before to 500ms after movement onset in the OFF and ON drug states. [B] Grand averages of time-evolving mean gamma ERS contralateral and ipsilateral to movement ON (black and blue lines, respectively) and OFF (red and green lines, respectively) levodopa. [C, D] Same as for A and B, but power changes here are derived from the contact pairs showing the greatest beta power change in the OFF state rather than the biggest gamma power change in the ON state as in A and B. * $p < 0.05$, ** $p < 0.01$.

The most important finding here was the lateralization of gamma ERS after treatment with levodopa. To check that this feature did not arise through differences in analysis the ANOVA was repeated using mean percentage power changes in the 40-85 Hz band derived from the contact pairs showing the greatest beta power change in the OFF state rather than the biggest gamma power change in the ON state. The interaction between state and laterality remained ($F[1,21] = 7.9$, $p = 0.01$) and post-hoc tests still confirmed that the gamma ERS was significantly larger during contralateral hand movements ($t = -3.6$, $p = 0.02$) after levodopa medication and not during the off state ($t = -0.1$, $p > 0.05$; Fig. 5C,D).

Gamma ERS in patients without PD

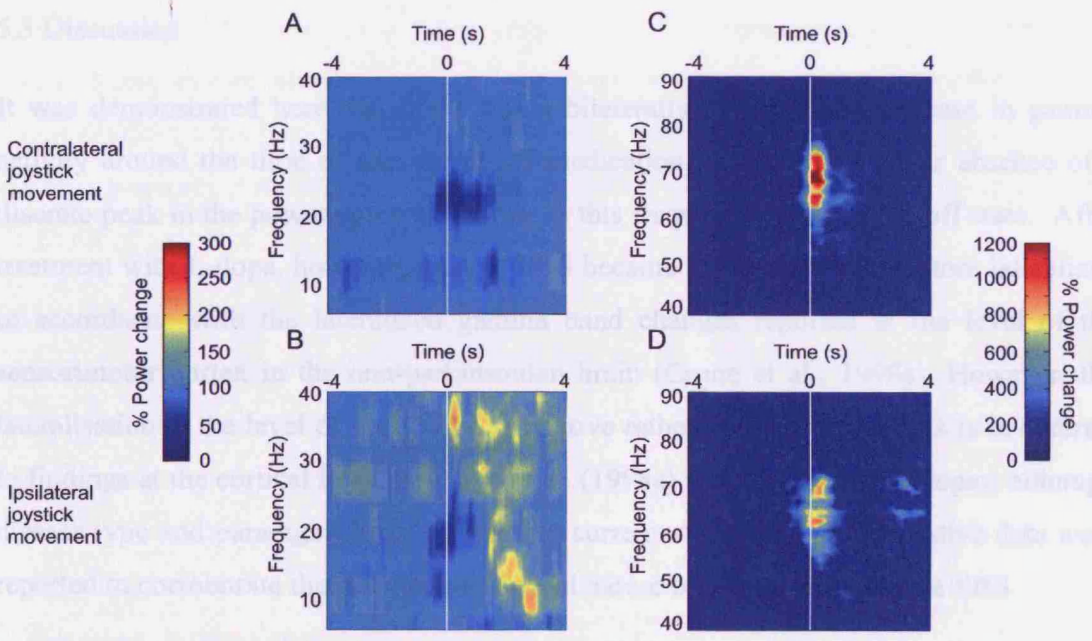

Figure 5.5. Movement-related spectral power in STN LFP in a tremor patient. Relative spectral power change in STN LFP in a patient without PD (case 1) contralateral [A,B] and ipsilateral [C,D] to voluntary limb movement. Averaged color coded time-evolving power relative to baseline period (4.5 to 4.0 s prior to movement). The matrices are thresholded at 99% CL of the averaged baseline power. Thin vertical lines define the time of joystick movement. Note ERD within 8-30 Hz band (A and C: contact 23) and ERS in the gamma band (B and D: contact 12). The latter is clearly bigger contralateral to the movement. The contact pair with the biggest event related change in each band is presented in each case. Only the lateralized gamma ERS was evident in case 2 (data not shown), but here only one contact (contact 3) was in STN on post-operative MRI.

The above data from patients with PD suggested that levodopa promoted the peri-movement increase in LFP power in the gamma band, particularly contralateral to the side of voluntary movement. Thus, the lateralised gamma ERS was interpreted as a physiological feature that returned with improvement in dopaminergic function. This hypothesis was further supported by the recordings of two tremor patients without PD who were implanted in STN. These too showed a relatively lateralised gamma ERS during movement. In contact pairs that were considered to include STN on post-operative MRI, the mean percentage gamma (40-85Hz) ERS from 200 ms before to 500 ms after movement was 369% and 300% in case 1 and 207% and 133% in case 2, contralateral and ipsilateral to the movement. The time-evolving % power changes are illustrated for case 1 in Fig 5.5, which also shows a movement-related ERD within the 8-30 Hz band in this patient (48% and 40%, ipsilateral and contralateral to movement).

5.3 Discussion

It was demonstrated here that there was a bilaterally symmetrical increase in gamma activity around the time of movement off medication, despite the regular absence of a discrete peak in the power spectrum at rest in this frequency range in the off state. After treatment with L-dopa, however, gamma ERS became more marked and more lateralized in accordance with the lateralized gamma band changes reported at the level of the sensorimotor cortex in the non-parkinsonian brain (Crone et al., 1998a). However, the lateralisation at the level of the STN was relative rather than absolute. This is in contrast to findings at the cortical level by Crone et al. (1998a) in patients with epilepsy, although disease type and paradigm differed from the current study, and no quantative data were reported to corroborate the purely contralateral nature of the cortical gamma ERS.

On the other hand, the magnitude of the 8-30 Hz band suppression around movement onset was increased after treatment with levodopa. This finding was in line with results from previous LFP studies (Doyle et al., 2005; Alegre et al., 2005; Devos et al., 2006) and confirmed a parallel function of similar frequencies at the level of the cortex following treatment (Devos et al., 2004). Movement-related suppression of 8-30 Hz band activity in the STN could be regarded as a physiological feature, as suggested by striatal recordings in healthy monkeys (Courtemanche et al., 2003) and in a non-parkinsonian

patient (Sochurkova and Rektor, 2003). This suggestion was further supported by the finding of an ERD in this frequency band in the subthalamic nucleus of case 1. However, whether the increased level of 8-30 Hz ERD in STN after levodopa approximates in degree to that under physiological situations remains a presumption. It is also noteworthy that the movement related suppression of 8-30 Hz activity remained symmetrical after levodopa treatment, as previously reported in PD (Alegre et al., 2005) although a study by Devos and colleagues (2006) found that the power suppression within this band began earlier contralateral to voluntary movement both on (five patients recorded) and off medication (ten patients recorded).

In sum, the data are broadly in keeping with the hypothesis that dopaminergic input helps normalise patterns of population activity in the STN. Consistent with this, Alegre et al. (2005) have reported that both the beta ERD and the gamma ERS tend to occur earlier ipsilateral to the more affected limbs, although in the current study no difference was found in the degree of power change with respect to the more or less affected side. Another relevant finding may be the tendency for mirror movements in PD to be reduced following treatment with levodopa, consistent with a more lateralised and physiologically functioning motor circuit (Cincotta et al., 2006a; Cincotta et al., 2006b).

Given the general similarity between subcortical and cortical patterns of reactivity it is important to consider whether the power changes picked up at the bipolar contacts of the DBS electrode were really focally generated in the region of the subthalamic nucleus. Many arguments have been put forward in support of this contention (reviewed in Brown and Williams, 2005; see Chapter 1), but the most convincing is the recent demonstration that the discharge of neurons in the STN tend to be locked to the beta activity in the LFP (Levy et al., 2002; Kuhn et al., 2005) and that the firing of neurones in both the upper STN and bordering zona incerta tend to be locked to gamma activity in the LFP (Trottenberg et al., 2006).

As mentioned above, there are some inconsistencies with results from previous studies. Devos et al. (2006) reported that power suppression within the 8-30Hz band began earlier contralateral to voluntary movement both ON (five patients recorded) and OFF medication (10 patients recorded), while Alegre et al. (2005) reported that both the beta

ERD and the gamma ERS tend to occur earlier ipsilateral to the more affected limbs. The number of patients could have been an important factor that contributed to these disparities. The current experiment was benefited by the relatively large number of patients compared to the other studies. On the other hand, it must be acknowledged that about half as many trials as in these earlier reports were analysed here, although this may not have necessarily been a major source of variance as the signal to noise ratio in the subthalamic region is generally good. In addition, there are methodological differences in the analysis of the results. The latter involved either the filtering and squaring of activities in pre-defined bands (Devos et al., 2006) or spectra estimated from autoregressive models (Alegre et al., 2005). These studies also concentrated on the latency to onset of power suppression and increase, whereas the present study concentrated on depth of change. Finally, it should be mentioned that the patients studied here suffered from fairly advanced PD. It is possible that lateralisation in terms of latency and depth of low frequency power suppression is seen in patients with less advanced disease, and lost in more advanced disease. However, if this were true then one might have expected lateralisation of the low frequency ERD following treatment with levodopa, but no evidence was found to support this.

Another issue that should be considered is the extent to which the levodopa-induced increase in reactivity could be due to changes in sensory re-afferance related to altered movement patterns following therapy. This possibility could be discounted as it cannot explain the improved reactivity seen in both frequency bands that starts before movement. Thus, at least some of the change in reactivity must have been a primarily central effect of levodopa. However, whether dopaminergic effects on subthalamic oscillations were directly executed at the level of this nucleus, given the evidence for some dopaminergic innervation of the STN, or, as is more likely, were exerted indirectly through the striatum, remains to be established (Parent and Hazrati, 1995).

A suppression of beta band activity occurs in the contralateral sensorimotor cortex prior to movement but becomes bilateral during movement, while a contralateral rebound in beta activity occurs after movement (Crone et al., 1998b; Pfurtscheller et al., 2003). In PD patients, levodopa treatment promotes this lateralization of cortical oscillatory activity

in the beta band (Devos et al., 2003, 2004). This was not the case for the subthalmic 8-30 Hz ERD here or in the study of Alegre et al. (2005), although it was reported by Devos et al (2006). Similarly, levodopa appears to have no effect on the size of the 8-30 Hz power increase in the STN following movement (Doyle et al., 2005; Alegre et al., 2005; but see Devos et al., 2006), despite the clear potentiation of this feature present in the cerebral cortex of patients with PD (Devos et al., 2003; Pfurtscheller et al., 2003). It is possible hence that the cortical and subcortical beta activities may not be homologus but may have partly independent characters (Doyle et al., 2005a). A similar observation was recently supported by Brücke and colleagues (2008) who reported symmetry in the movement-related suppression of beta band activity in the basal ganglia in dystonic patients, pointing to this symmetry of subcortical reactivity being primarily physiological. The possible differences in significance of beta band synchrony in the cortex versus that detected in the basal ganglia both in physiological and pathological states is further discussed in Chapter 8.

Although it is very likely that the oscillatory activity in the STN LFP was locally generated, this by no means implies that it is autonomous. Previous studies have underscored the loop character of these oscillations, demonstrating coherence between activities at various nodes in the basal ganglia-cortical loop (Brown et al., 2001; Cassidy et al., 2002; Williams et al., 2002; Fogelson et al., 2006). As a general rule, these studies point to a net drive to the STN from the cortex in the beta band, but a reversal of net information flow in the gamma band, where activity tends to have a temporal lead over that in the cortex. However, it should be stressed that these conclusions are derived from analyses of spectral phase, which do not allow for bidirectional flow (Cassidy and Brown, 2003; see Chapter 2), and have only considered resting patterns of functional connectivity. The predominant direction of information flow may of course change during movement. Such changes have been demonstrated in the rat where the phase relationships between cortex and STN were mixed with clear examples of STN leading the cortex after cortical stimulation (Magill et al., 2006). The above differential effects of levodopa treatment on oscillatory activities at the cortical and subcortical levels argues that at some level specific aspects of processing may be grafted onto the general looping architecture.

Given that oscillatory activity in the subthalamic LFP likely reflects the synchronisation of local neurons (Levy et al., 2002; Kühn et al., 2005; Trottenberg et al., 2006) the improved reactivity of these oscillations following therapy with levodopa suggests that dopaminergic mechanisms accentuate task-related changes in neuronal synchronization in the subthalamic region. Elsewhere it has been speculated that dopaminergic inputs may effectively work to high pass filter synchronised activity in the basal ganglia (Magill et al., 2001; Sharott et al., 2005). This may account for the reduction in baseline levels of 8-30 Hz activity and the increase in baseline gamma activity previously reported (Brown et al., 2001), but would only explain the improved task-related reactivity in these bands if movement was preceded and accompanied by release in dopamine and that this release was increased and/or the system became more sensitive to this release following levodopa. There is evidence to support the former (Magarinos-Ascone et al., 1992; Goerendt et al., 2003; Badgaiyan et al., 2003), but the latter remains speculative.

The improvements in reactivity following levodopa treatment are in the direction that should favour motor-related processing. There is increasing evidence that synchronization of local populations of neurons at frequencies of 8-30 Hz antagonizes motor related processing and that suppression of this pattern of activity is necessary to allow voluntary movement (reviewed in Brown and Williams, 2005). Recent recordings in primates confirm an inverse relationship between oscillatory LFP activity in the beta band and local task-related spike activity so that oscillations are preferentially suppressed in the striatum showing task-related increases in discharge rate (Courtemanche et al., 2003). Similar observations have been made in the motor cortex where it has been found that during periods of 20-40 Hz oscillatory synchrony motor cortical single unit firing rates were clamped to a relatively narrow range (Murthy and Fetz, 1996b), while decrease in motor cortical oscillations coincided with the appearance of firing rate modulation (Donoghue et al., 1998). Conversely, increases in LFP activity in the gamma band are associated with increases in local neuronal discharge rates (Trottenberg et al., 2006), so the increased reactivity in neuronal synchrony following levodopa will result to an increase in the potential for rate coding around the time of voluntary movement (Pogosyan et al., 2006). It is possible hence that increased reactivity in neuronal synchrony following levodopa might lead to an increased probability for greater rate and

temporal coding around the time of voluntary movement. The relative lateralization of the movement-related increase in gamma activity following L-dopa would support a more specific role in motor processing than the bilateral change in the beta band. Thus levodopa may help switch the pattern of neuronal synchronisation from one that limits neuronal firing rates to one that increases discharge rates and may form the basis for the dynamic formation of neuronal assemblies suitable for motor processing.

5.4 Summary

- Event-related synchronization in the gamma band is bilaterally symmetrical around the time of the movement in PD patients that are withdrawn from antiparkinsonian medication but becomes more marked and contralaterally predominant after reinstitution with levodopa. Movement-related gamma synchronization was also found lateralized during movement in patients without dopaminergic lesions.
- Levodopa augments reactivity of gamma activity in the STN paralleling the lateralization of increase of similar frequencies noted at the cortical level after treatment and shifts it towards a more physiological pattern.
- Event-related 8-30Hz synchronization is increased in the STN after l-dopa treatment but it is not lateralized. Treatment with levodopa does not promote lateralization of movement-related suppression of low frequencies in the STN. The fact that 8-30Hz synchronization in the STN after levodopa treatment does not follow the pattern of 8-30Hz synchronization seen in the cortex under physiological situations makes it possible that cortical and subcortical beta activities have partly independent characters.

CHAPTER 6

Amplitude modulation of oscillatory activity in the subthalamic nucleus during movement

Depth recordings in patients with PD have demonstrated exaggerated LFP activity at frequencies between 10-30 Hz in the STN which have been hypothesized to be pathophysiologically relevant to bradykinesia (Brown, 2003; Dostrovsky and Bergman, 2004; Brown and Williams, 2005; Hammond et al, 2007). There is evidence that population activity over this band may be modulated as part of the feedforward organisation of incipient voluntary movement and in response to afferent feedback following movement. In the previous chapter it was confirmed that movement-related power suppression of low frequencies was higher after levodopa treatment than when the patients were off medication. Amplitude modulation of the beta band, specifically, amplitude reduction, precedes phasic movements (Cassidy et al., 2002; Levy et al., 2002; Priori et al., 2002; Loukas and Brown, 2004; Kühn et al., 2004; Doyle et al., 2005; Williams et al., 2005; also see Chapter 5) and may be divorced from physical movement if movement is imagined (Kühn et al, 2006), consistent with a role in the feedforward organization of movement. In contrast, amplitude increases in this frequency band follow phasic movements (Cassidy et al, 2002; Priori et al., 2002; Alegre et al., 2005; Devos et al., 2006), and are absent if movement is imagined (Kühn et al, 2006), pointing to an additional involvement in feedback related processing, particularly that necessary for trial-to-trial learning (Brown et al, 2006). However, it remains unclear whether any modulation of activity in the beta band occurs during sustained or repetitive movements and whether this relates to continued feedforward processing of the movement after its initiation, ongoing feedback or to a combination of these activities.

Here neuronal activity was recorded from the STN of PD patients withdrawn from antiparkinsonian medication while they performed repetitive index finger to thumb taps. The involvement of the basal ganglia in processing of self-paced simple upper limb movements, such as tapping, was recently demonstrated (Chen et al., 2006). The aim of this study was to test the hypothesis that modulation of subthalamic activity in the 10-30 Hz band occurs during and correlates with behavioural performance within a movement.

The material presented here has been previously published (Androulidakis, A.G., Brücke, C., Kempf, F., Kupsch, A., Aziz, T., Ashkan, K., Kühn, A.A., Brown, P. (2008) Ampitude modulation of oscillatory activity in the subthalamic nucleus during movement. European Journal of Neuroscience. 27: 1277-1284).

6.1 Materials and Methods

Patients and surgery

Seven patients (age 60.5 ± 2.8 years, three males) were studied who underwent bilateral implantation of DBS electrodes in the STN for the treatment of severe PD. Their clinical details are summarized in Table 6.1. Target coordinates (see chapter 2) were based on direct visualization of the STN in the individual stereotactic T_2-weighted MRI. DBS-electrode location was confirmed by intra-operative direct macrostimulation and immediate post-operative stereotactic MRI or CT, with fusion to the pre-operative MRI (case 6 and 7). Microelectrode recordings were also performed to confirm targeting in all but case 6 and 7.

Paradigm and recordings

Patients were studied 2-6 days post-operatively, in the interval between DBS electrode implantation and subsequent connection to a subcutaneous stimulator. The subjects were seated comfortably in a chair and recorded while making repetitive, self-paced index finger to thumb taps with their dominant hand (see Fig 6.1A). These were predominantly executed by flexion and extension at the MCP joint of the index finger. Patients were asked to make large movements as fast as possible. They were instructed to perform four to five tapping blocks each of which lasted from 25 s to 100 s. Patients were asked to stop tapping after 100s, but more usually (see below) would terminate the run prematurely because of bradykinesia and fatigue. Blocks were separated by 30-40s rest.

Recordings were made from the contralateral STN (e.g. contralateral to the tested dominant hand) after patients had been off antiparkinsonian medication overnight. Deep brain activity was recorded bipolarly from the adjacent four contacts of each DBS electrode (0-1, 1-2, 2-3), amplified and pass-band filtered at 1-250 Hz. Angle of

excursion at the MCP joint of the index finger was also recorded by an electric goniometer fixed over the superior aspect of the relevant joint with tape. In cases 1-6 signals were recorded using a 1401 A/D converter and Spike2 software and in case 7 signals were initially collected with a Biopotential Analyzer Diana (St Petersburg, Russia) and then exported for processing in Spike2. Signals were sampled at a minimum rate of 625 Hz (up to 2.5 kHz) across patients.

Table 6.1: Clinical details in PD patients.

Case	Age and sex	Disease duration (years)	Predominant symptoms	Motor UPDRS pre-op (ON/OFF levodopa)	Motor UPDRS post-op (OFF l-dopa) ON/OFF DBS	Medication (daily dose) pre-op
1	48/F	8	Dyskinesias, tremor On-off fluctuations	9/27	11/24	Levodopa 675mg Entacapone1200mg Pramipexol 2.1mg Citalopram 40mg
2	69/F	14	Tremor	11/18	2/13	Pramipexol 2.1mg Citalopram 10mg
3	60/M	12	Dyskinesia, akinesia	23/40	13/47	Levodopa 500mg Pergolide 2mg
4	69/M	12	Dyskinesias, akinesia	26/56	G	Levodopa 650mg Ropinirole 30mg
5*	57/F	10	Akinesia	12/33	G	Levodopa 200mg Pramipexol 2.1mg
6	57/F	17	Bradykinesia Gait difficulties	14/40	G	Levodopa 300mg Pramipexole 2.1mg
7	63/M	20	Tremor, diskinesias	42/63	G	Levodopa 900mg Pramipexole 0.8mg Apomorphine 7.5mg

* Left-handed patient.

G = good qualitative response but 6 month post-operation off medication DBS ratings not available.

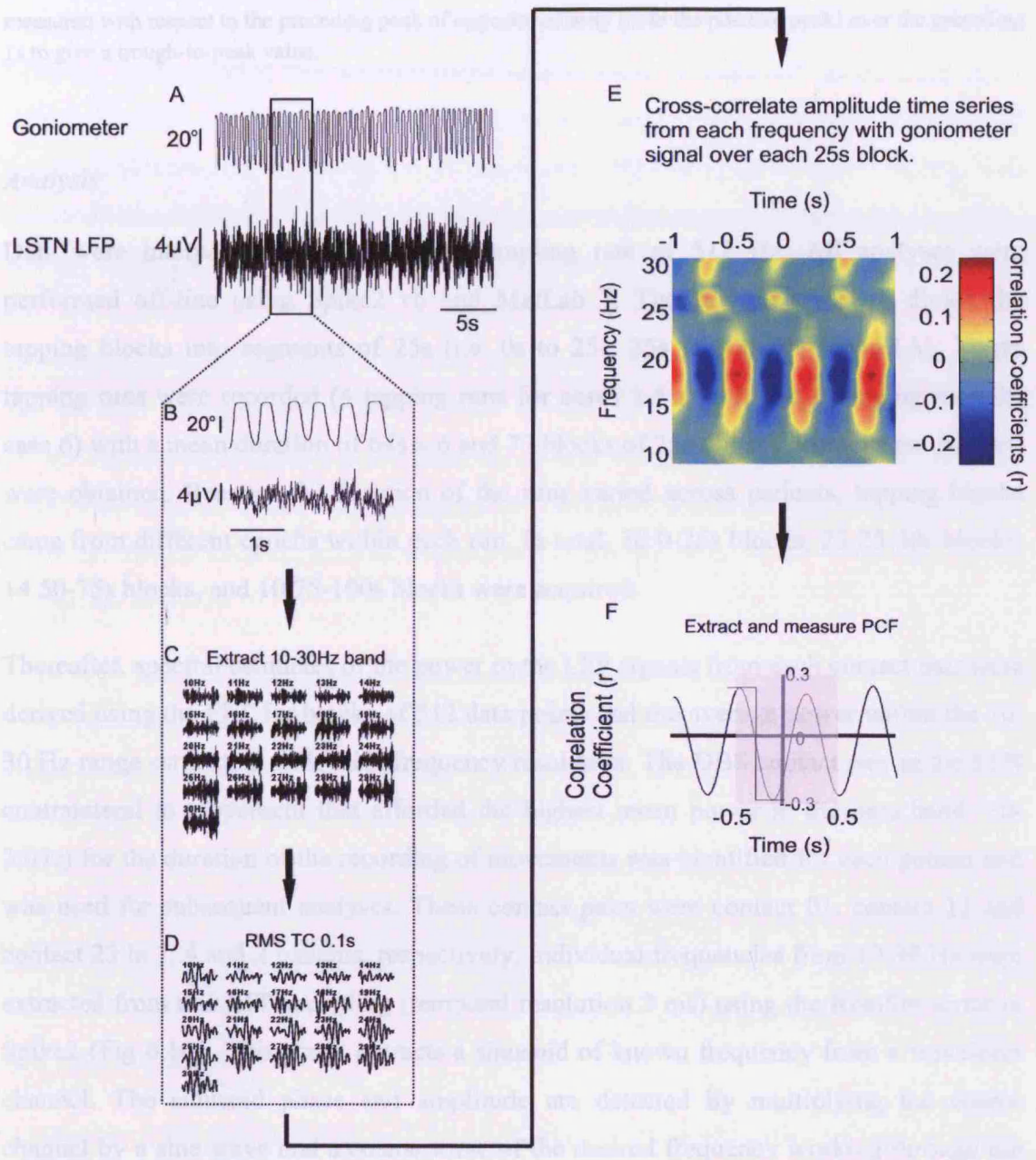

Figure 6.1 Determination of cross-correlation between LFP activities and goniometer signal. Self-paced repetitive index finger to thumb taps made with the right hand after overnight withdrawal of levodopa and simultaneously recorded LFP from left (L) STN over 25s in [A] and illustrated in higher resolution over 3s in [B]. Individual frequencies from 10-30 Hz extracted from this LFP recording [C] and root mean squared [D]. Note that the analysis was done for the whole 25s tapping period, but for presentation purposes it is illustrated in the boxed area in higher resolution for only 3s. [E] Waveform cross-correlations between each one of the RMS pass-band filtered LFP signals and the goniometer signal over a 25s block and selection of PCF (the frequency that correlates best with the goniometer). Here, PCF is 18Hz. [F] To determine the strength of the PCF, the highest cross-correlation value (note the negative trough) was identified within a correlation lag of -0.5s to +0.5s (shaded area) and the magnitude of this was

measured with respect to the preceding peak of opposite polarity (note the positive peak) over the preceding 1s to give a trough-to-peak value.

Analysis

Data were interpolated to a common sampling rate of 512 Hz. All analyses were performed off-line using Spike2 v6 and MatLab 7. The first step was to divide the tapping blocks into segments of 25s (i.e. 0s to 25s, 25s to 50s etc; Fig 6.1A). Thirty tapping runs were recorded (4 tapping runs for cases 1-5 and 7, and 6 tapping runs for case 6) with a mean duration of 64s ± 6 and 77 blocks of 25s (11 ± 1.5 blocks per patient) were obtained. Because the duration of the runs varied across patients, tapping blocks came from different epochs within each run. In total, 30 0-25s blocks, 23 25-50s blocks, 14 50-75s blocks, and 10 75-100s blocks were acquired.

Thereafter, spectral estimates of the power in the LFP signals from each contact pair were derived using the FFT for blocks of 512 data points and the average power within the 10-30 Hz range estimated, with 1 Hz frequency resolution. The DBS contact pair in the STN contralateral to movement that afforded the highest mean power in the beta band (10-30Hz) for the duration of the recording of movements was identified for each patient and was used for subsequent analyses. These contact pairs were contact 01, contact 12 and contact 23 in 1, 4 and 2 patients, respectively. Individual frequencies from 10-30 Hz were extracted from this LFP recording (temporal resolution 2 ms) using the RemSin script in Spike2 (Fig 6.1C). This script extracts a sinusoid of known frequency from a waveform channel. The sinusoid phase and amplitude are detected by multiplying the source channel by a sine wave and a cosine wave of the desired frequency working through the data in steps of one sinusoid cycle time. In order to estimate the amplitude modulation time series of the extracted frequencies, the results were root mean squared and smoothed with a moving average filter. In the latter, output waveforms at time t were the mean RMS value of the extracted frequencies from time t - 0.1s to t + 0.1s (Fig 6.1D). Waveform cross-correlations (Spike2 v6) were performed between each one of the root mean squared pass-band filtered LFP signals and the goniometer signal across all tapping blocks. The correlation covered a lag from -1s to +1s (Fig 6.1E). Cross-correlation

measures the similarity in shape at different times between two signals as a scalar between -1 to 1, and in this instance afforded a measure of amplitude modulation of the LFP coupled to tapping. A total of 77 blocks were analyzed in the seven patients. All cross-correlations had some evidence of oscillations. However, 12 cross-correlations with a period longer than 1s were rejected, so as to concentrate on amplitude modulation of the LFP by tapping, which had a frequency of more than 1 Hz. To determine the strength of the cross-correlation in the remaining 65 blocks (9.3 ± 1.1 blocks per patient) the peak cross-correlation value (whether positive or negative) was identified within a correlation lag of -0.5s to +0.5s and the magnitude of this was measured with respect to the preceding peak of opposite polarity determined over the preceding 1s to give a trough-to-peak value (Fig 6.1F). The LFP frequency that correlated maximally with the goniometer (peak correlation frequency; PCF) within a correlation lag of -0.5 s to +0.5 s was selected for further analysis.

In order to quantify tapping performance, the goniometer signals were DC removed, root mean squared and averaged over the 25 s period of each block. This affords a composite index of the amplitude of each tapping movement and of how often tapping movements were made. Because performance in the tapping task varied both across patients and across blocks within patients, the data were normalized by expressing performance as the percentage of the best performance that each patient achieved. Then, the percentage best performances were correlated with the strength of the corresponding cross-correlation of PCF with tapping both across all patients and separately for each patient using Pearson's correlation coefficient.

It was then evaluated how many of the remaining 65 cross-correlations were significant according to two further empirical criteria, both of which had to be met: [1] In setting the first criterion, the LFP time series was randomly shuffled 20 times and the previously determined PCF was extracted from the shuffled data and root mean squared and smoothed with a moving average filter as described above. Waveform cross-correlations were then performed between the PCF extracted from the shuffled data and the goniometer signal over a correlation lag from -1s to +1s across all tapping blocks, and upper and lower 95% CLs were calculated. Cross-correlations of the original data had to

exceed either the upper or lower or both lower and upper CLs for over 50 contiguous points (i.e. 0.1 seconds) over a correlation lag of -0.5 s to +0.5 s. This lead to the rejection of a further 25 cross-correlations. [2] In order to make sure that the remaining waveform correlations were truly significant, a further set of CLs was also estimated by preserving the original frequency content of the LFPs but degrading the coupling between the signals. To this end, waveform cross-correlations were performed between the PCF time series extracted from the original (non-shuffled) data and the goniometer signal with an offset of 12 s and CLs were determined. The cross-correlation of the original data had to exceed either the upper or lower or both new upper and lower CLs for over 50 contiguous points over lags from -0.5 s to +0.5s as well. This lead to the rejection of a further four cross-correlations leaving 36 (5.1 ± 1.2 blocks per STN) cross-correlations of PCF with goniometer signal that were considered significant.

In order to show whether PCFs from significant cross-correlations were more consistent in individual STN than expected by chance, it was determined how many of the PCFs for a given STN were the same in frequency or fell within ± 3 Hz of this frequency across tapping blocks. Given that the frequency band of interest spanned 20 Hz, it would have been expected only 7/20, i.e. 35 % of PCFs to follow this rule by chance.

The peak latency of the significant cross-correlations was either negative or positive depending on whether LFP activity led or lagged the goniometer signal. In order to show whether or not correlations exhibited more consistent temporal relationships in individual STNs than expected by chance, each STN was scored according to how many of the total number of significant cross-correlations in that subject involved leads and lags, the scores were expressed as percentages, and then it was checked whether they were significantly different from the 50% expected by chance using a one-sample t-test.

As a last step in the analysis it was determined whether significant cross-correlations between LFP activity and goniometer signal were focal. To this end, the selected PCFs were extracted from all the contact pairs, root mean squared and the result was smoothed with a moving average filter as before. Waveform cross-correlation was then performed between this and the goniometer signal and the strength of the correlation was determined. All correlation coefficients were then expressed as a percentage of the peak

coefficient at the contact pair with the best cross-correlation, which in every case was the same as that selected on the basis of maximum beta power (see above).

Statistics

All statistical analyses were conducted using SPSS v12 (SPSS Inc, Chicago, IL, USA). The data were normally distributed as confirmed by the one-sample Kolmogorov - Smirnov test. Differences were considered statistically significant at $p < 0.05$. Results are presented as means ± standard errors of the mean (SEM).

6.2 Results

An example of the raw STN LFP and goniometer signal is shown in Fig 6.1. The analysis began by plotting matrices of the waveform cross-correlation between the extracted frequencies (10 - 30 Hz) of the STN LFP and the goniometer signal in each consecutive 25 s block of tapping. These were suggestive of amplitude modulation of LFP activity within the 10 – 30 Hz band by tapping and the peak correlation frequency (PCF) was determined for each block (Fig 6.2). Weaker cross-correlations tended to be found in those blocks with poorer tapping performance, as shown by a correlation of peak cross-correlation per 25 s block with corresponding tapping performance per block across all patients (Fig 6.3). There was a positive linear correlation between tapping performance and cross-correlation strength ($r = 0.38$ and $p = 0.002$) across patients (Fig 6.3A). A similar relationship could also be seen separately within cases 3 and 2 ($r = 0.61$, $p = 0.04$ and $r = 0.73$, $p = 0.002$, respectively), despite the relatively small number of observations (range 6 to 15) available for correlation in each subject. Cases 7 and 5 showed a trend in the same direction ($r = 0.79$, $p = 0.06$ and $r = 0.68$, $p = 0.09$, respectively).

Impaired tapping and lower cross-correlations developed over time as bradykinesia set in. Thus cross-correlation coefficients were higher at the beginning of each recording when tapping performance was better and degraded over time in tandem with performance (Fig 6.3B, C). This was true whether cross-correlations were expressed as a % of the best cross-correlation in the corresponding STN (Fig 6.3B, C) or if non-normalised cross-correlations were considered. In the latter case, raw cross-correlations were higher during the first 25s of tapping ($r = 0.3 \pm 0.1$) than over 25-50s ($r = 0.2 \pm 0.09$; unpaired t-test t =

3.7, p = 0.001) or over 50-75s (r = 0.2 ± 0.12; unpaired t-test t = 2.27, p = 0.029). Note that there were fewer estimates for 50-75 s and these were necessarily drawn from those patients with less bradykinesia, who were able to perform the test for longer. On the other hand, the average power at PCF did not seem to change over time as no significant differences were found between the first 25s of tapping and the blocks that followed (0-25s: 7 ± 3 a.u.; 25-50s: 6 ± 3 a.u.; 50-75s: 4 ± 3 a.u.).

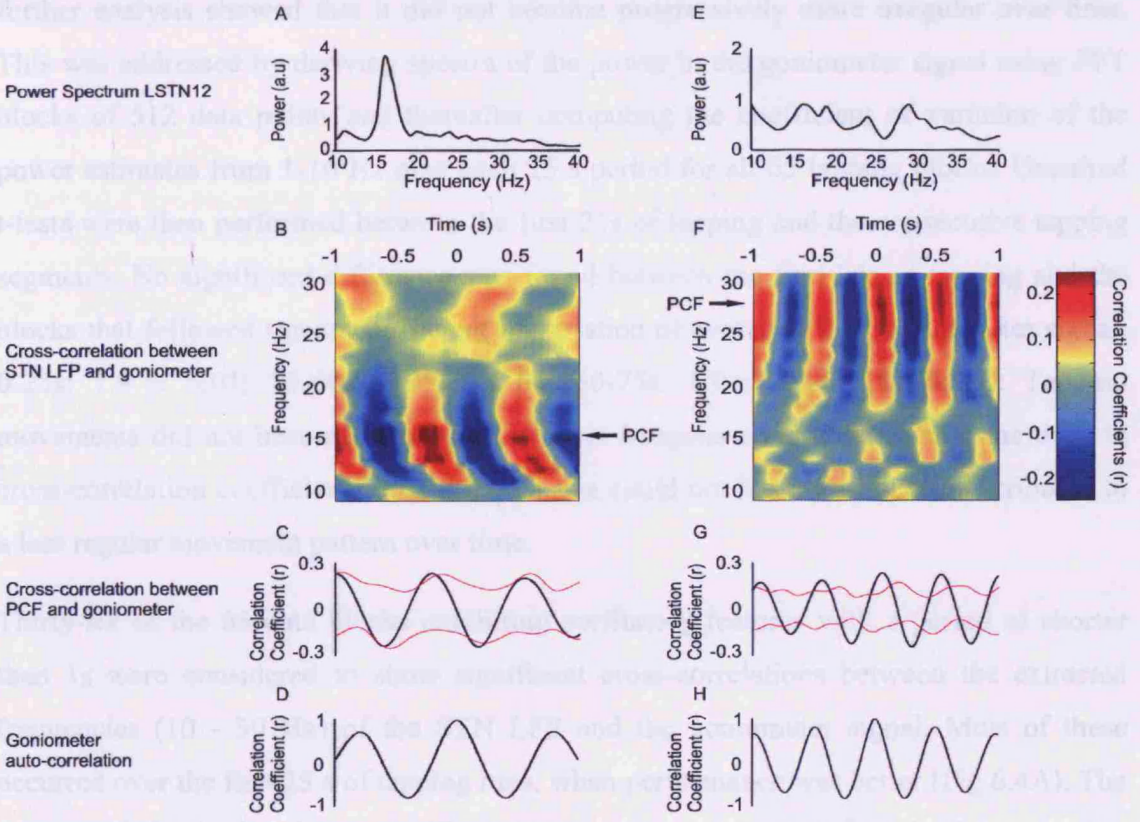

Figure 6.2 Examples of STN LFP – goniometer cross-correlations. [A] Power of STN LFP over 0-25 s of tapping. Peak power is at 16 Hz. [B] Colour-coded cross-correlation matrix between the extracted STN LFP frequencies (10-30 Hz, 1 Hz resolution) and the goniometer signal over 0-25 s of tapping. The PCF is at 16 Hz, in accordance with the power spectral peak, and is maximal before movement onset. [C] Cross-correlation at PCF (16 Hz) illustrated by black line and upper and lower 95% CL derived from shuffled data illustrated by red lines. [D] Goniometer autocorrelation over 0-25 s. Note how the period of the goniometer oscillations matches that of the cross-correlation, although the latter is phase shifted. [E] STN LFP power for tapping block of 50-75 s. The power in this block peaks at 28 Hz. [F] Colour-coded cross-correlation matrix of same block in [E]. PCF is at 28 Hz, in accordance with the power spectral peak, and when maximal lags movement. [G] Cross-correlation at PCF (28 Hz) illustrated by black line and upper

and lower 95% CL derived from shuffled data illustrated by red lines. [H] Goniometer autocorrelation over 50-75s.

An important point that was raised here was whether the weakening of cross-correlations was accounted for by a possible increase in the irregularity of the tapping movement over time. The amplitude and the velocity as well as the irregularity of a repetitive movement might decrease in time in PD. Is it possible that the lack of correlation in later segments could represent one signal remaining regular (LFP) and the other becoming irregular? In the current recordings finger tapping became slower and of lower amplitude over time but further analysis showed that it did not become progressively more irregular over time. This was addressed by deriving spectra of the power in the goniometer signal using FFT blocks of 512 data points and thereafter computing the coefficient of variation of the power estimates from 1-10 Hz over each 25 s period for all 65 tapping blocks. Unpaired t-tests were then performed between the first 25s of tapping and the consecutive tapping segments. No significant difference was found between the first 25s of tapping and the blocks that followed (mean coefficient of variation of averaged RMS goniometer signal: 0-25s: 1.9 ± 0.03; 25-50s: 1.95 ± 0.04; 50-75s: 1.9 ± 0.08; Fig 6.3D). Tapping movements did not become progressively more irregular over time, so that the drop in cross-correlation coefficients with bradykinesia could not have simply been attributed to a less regular movement pattern over time.

Thirty-six of the 65 data blocks exhibiting oscillatory features with a period of shorter than 1s were considered to show significant cross-correlations between the extracted frequencies (10 - 30 Hz) of the STN LFP and the goniometer signal. Most of these occurred over the first 25 s of tapping runs, when performance was better (Fig 6.4A). The average PCF (22 ± 0.8 Hz) in significant blocks was similar to but slightly higher than the frequency of the peak in the corresponding LFP power spectrum (20.5 ± 0.8 Hz). The PCFs from significant blocks tended to be more consistent in individual STN than expected by chance. Thirty-one PCFs occurred at the same frequency ± 3 Hz across 25 s blocks from the same STNs (Fisher's exact test, $p < 0.0001$). In addition, significant cross-correlation coefficients were higher in the contact pair that afforded the highest beta peak in power spectra of LFP activity, confirming the focality of amplitude modulation in the LFP (Fig 6.4B).

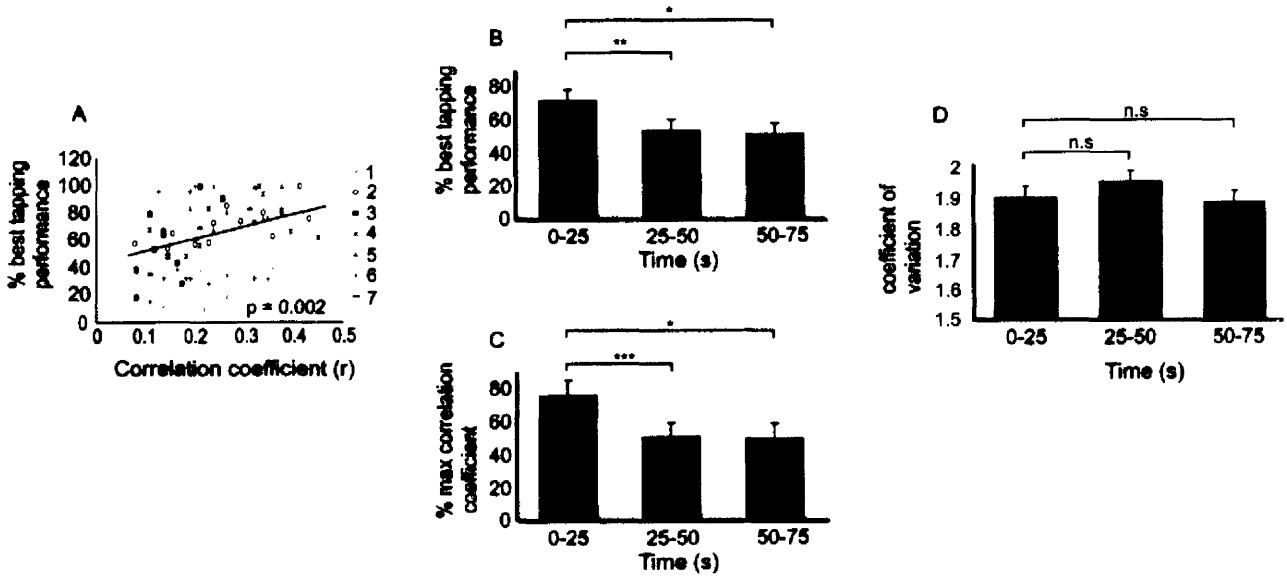

Figure 6.3 Cross-correlation strength and tapping performance estimates in seven PD patients. [A] Correlation between tapping performance and cross-correlation strength for all 65 cross-correlograms with a period ≤ 1 s. Performance is expressed as percentage of the best tapping performance achieved by each patient (numbers on the left correspond to patient cases in Table 1). [B] Mean ± SEM % best tapping performance over time for all patients. Only four patients managed up to 75s of tapping. [C] Mean ± SEM % highest cross-correlation between PCFs and goniometer signal over time for all seven patients. In line with [B], cross-correlations are expressed as percentage of the highest cross-correlation estimated for each patient. Note the parallel decrement in tapping performance and cross-correlation strength with time. [D] Mean coefficient of variation of averaged RMS goniometer signal over time. No difference was found in the regularity of tapping movements across tapping segments. * $p < 0.05$; **$p < 0.01$; *** $p < 0.001$, n.s. = non-significant.

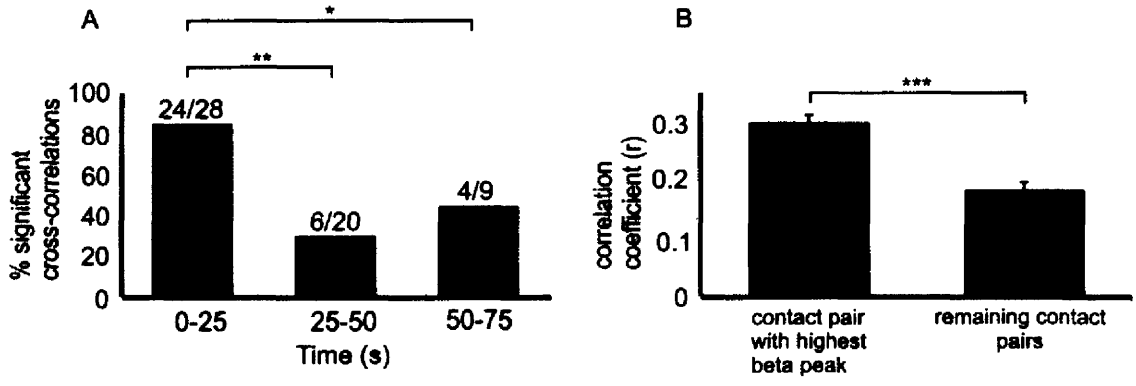

Figure 6.4 **Cross-correlation coefficients across tapping segments and electrode contact pairs.** [A] Percentage (%) significant cross-correlations over time. Note that the total number of the cross-correlations is 34 out of 36 significant cross-correlations. The remaining two came from 75-100 s in one patient. *p = 0.02, ** $p < 0.001$, Fisher's exact tests. [B] Difference between mean ± SEM significant cross-correlation

coefficient at contact pair with the highest beta LFP power and that at remaining contact pairs. *** $p < 0.0001$.

Among the 36 significant cross-correlations peak latencies were negative in 23 and positive in 13. Latencies were normally distributed around a mean latency of -50 ± 58 ms (Kolmogorov-Smirnov test). Despite the relatively wide range of peak latencies, correlations exhibited more consistent temporal relationships in individual STNs than expected by chance (score for LFP leads 65 ± 10 %; one sample t-test $t = 3.5$, $p = 0.013$, and score for LFP lags 35 ± 10 %; one sample t-test $t = 3.5$, $p = 0.013$). There were no significant differences in tapping performance or cross-correlation strength between leading and lagging correlations. Correlation of the percentage best performance with the peak cross-correlation during corresponding tapping blocks, but restricted to those 25 s blocks in which peak cross-correlations were negative (i.e. where peak correlation preceded movement) showed a strong trend for positive linear correlation between tapping performance and cross-correlation strength across subjects ($r = 0.3$, $p = 0.06$).

6.3 Discussion

It has been demonstrated here that the LFP activity in the beta band recorded in the STN is modulated in time with repetitive index finger to thumb taps in patients with PD. A critical consideration in the present study is whether or not the LFP modulation indexed in cross-correlations was significant and represented a biologically relevant amplitude modulation of the beta activity rather than a spurious consequence of the highly rhythmic nature of the tapping time series. The former seems more likely. Cross-correlations exceeded the confidence limits determined from shuffled and also time-shifted data, and for a given STN tended to occur at relatively fixed frequencies within the broad beta band. Moreover, cross-correlations were focal across DBS electrode contact pairs.

The recordings from a given STN more consistently involved peak cross-correlations with leads, or conversely lags, than expected by chance. There could be two explanations for this: either there may be some spatial distribution between feed-forward and feedback related processing in the STN, so that subtle variations in targeting preferentially lead to sampling from one or other functional subpopulation of neurones, or variation arises between rather than within STNs, and the predominance of feedforward over feedback

related processing between STNs is dictated either directly, by disease processes, or indirectly, as a function of secondary compensation.

What is the nature of the amplitude modulation of the beta activity in the STN LFP? LFP oscillations are likely to be the product of synchronized activity across large populations of local neuronal elements and hence index synchronization. This is most directly supported by the coupling of neuronal spiking activity in this frequency band between pairs of neurons (Levy et al., 2000) and between neurons and the LFP (Levy et al., 2002; Kühn et al., 2005; Trottenberg et al., 2006; Weinberger et al, 2006). At the simplest level, therefore, amplitude suppression of beta activity in the LFP may represent the temporary release of neurons from an otherwise pervasive synchronising oscillation that constrains the ability of individual neurones to code in time and space, as adjacent and spatially distributed neurons preferentially fire locked to the beta rhythm. Once temporarily released these neurones can more effectively engage in any dynamic assembly formation and rate coding necessary for the processing of movement (Courtemanche et al, 2003; Amirnovin et al, 2004). Viewed in this light, failure to release neurons from the beta rhythm in a task appropriate manner would be expected to impair the organisation of forthcoming movement and later feedback related processing. Accordingly, we found that the modulation of the beta activity was diminished as tapping became more bradykinetic. The precise aspect of the behavioural performance that was predicted by the amplitude modulation of LFP activity in the case of cross-correlation peaks that lead, or that predicted the amplitude modulation in the case of cross-correlations that lagged, remains unclear. The goniometer signal contained both amplitude and temporal information, so the important features could include amplitude, velocity, force or some combination of these variables. Indeed, perhaps it is more likely that there is no specific relevant behavioural parameter, and that different neurons are temporarily released from the beta synchrony to code for different parameters as they become relevant. In this schema, amplitude modulation of the beta band is not coding for specific parameters of movement, but rather resourcing the subsequent coding of parameters of movement, with the precise nature of these dictated by the instantaneous functional requirements.

In Chapter 5 it was demonstrated that amplitude modulation in the gamma band, specifically amplitude increase, is more marked and contralaterally predominant around the time of self-paced movements after levodopa medication as opposed to a bilateral symmetrical gamma ERS in patients withdrawn from levodopa. Based on those findings it remains to be seen whether any cross-correlations of LFP activity with sustained finger tapping appear in the gamma band in the OFF parkinsonian state and whether similar if not stronger cross-correlations can be found following re-introduction of dopaminergic therapy. It has been proposed that synchronous oscillations at different frequencies do not necessarily serve the same functions, and that tuning of oscillatory activity to distinct frequencies might provide a means of functionally segregating related processing in the motor system (Fogelson et al., 2006; Kempf et al., 2007). For example, the relative lateralization of the movement-related increase in gamma activity in PD patients following L-dopa as well as in tremor patients (Chapter 5) and dystonic patients (Brücke et al., 2008) might support a more specific role in motor processing than the bilateral change in the beta band (Chapter 5). It might be of relevance therefore to also examine whether cross-correlations (if any) of finger tapping with gamma activity are stronger when the behavioural signal entails information about specific parameters of movement (such as velocity or amplitude). In other words, it would be useful to also explore whether amplitude modulation of gamma activity codes for more specific features of movement than amplitude modulation in beta activity.

In conclusion, beta synchrony is modulated during ongoing movement, consistent with both feed-forward and feedback related processing during the movement. Previous studies have shown that beta suppression precedes phasic movements and correlates with reaction time (Kühn et al., 2004; Williams et al., 2005), but did not address the question of whether beta reactivity is sustained when movements are repeated as in sustained finger tapping. The present study suggests that the modulation of beta oscillations may also be important during sustained movement or movements. Thus the modulation of the beta activity was diminished as tapping became more bradykinetic.

6.4 Summary

- STN activity in the beta band is modulated in time with repetitive index finger-thumb taps in patients with PD OFF levodopa. This modulation is higher when tapping performance is good and diminishes when tapping becomes bradykinetic.
- Amplitude modulation of beta activity in the LFP may represent the temporary release of neurons from an "antikinetic" synchronizing oscillation in order for them to engage in processing of movement. Failure to release neurons from the beta rhythm during movement might impair the organization of forthcoming movement and later feedback related processing leading to bradykinesia.

CHAPTER 7

Local field potential recordings from the pedunculopontine nucleus.

In the previous two chapters, recordings from the STN of PD patients showed that neuronal activity in the beta band is a neuronal pattern characteristic of parkinsonism which is linked to patients' motor control deficits in all stages of movement (before, during, and after movement). Levodopa therapy as well as high frequency STN DBS reduce neuronal synchronization in the beta band and at the same time improve motor control (Chapter 1). A number of PD patients however have little or no benefit from STN DBS. These are usually the patients who suffer predominantly from postural instability and freezing of gait. The PPN has been implicated as having a role in these symptoms through several lines of evidence (see Chapter 1).

Therefore the PPN has recently been introduced as a new therapeutic target for DBS in PD patients with this symptomatology (Mazzone et al., 2005; Plaha & Gill, 2005; Florio et al., 2007; Stefani et al., 2007). Effective stimulation is delivered at low frequencies of around 20 - 60 Hz, based on studies in MPTP-treated primates where stimulation of PPN at 10 Hz was most effective (Jenkinson et al., 2004). This is in contrast to the high frequency stimulation required to improve Parkinsonism through stimulation of targets such as the GPi, STN and thalamus. It is argued that high frequency DBS at these sites is effective as it suppresses excessive low frequency synchronised oscillations that are found in the basal ganglia-thalamocortical loop in PD patients. These are thought to contribute to motor impairment and are accordingly, also suppressed by dopaminergic treatment (Gatev et al., 2006; Uhlhaas & Singer, 2006; Hammond et al., 2007). Just how and why this unique stimulation regime should work in the PPN in PD remains unclear.

Low frequency oscillations have been shown to have a physiological function in maintaining the current motor set in healthy volunteers (Gilbertson et al., 2005) and PPN electrical stimulation at low frequencies is likely to activate rather than block local neural elements and might therefore possibly mimic a physiological form of synchronization necessary for normal movement and postural control. Therefore, the first experiment was designed in order to seek evidence for low frequency synchronisation of activity in the

PPN of a patient with PD who was implanted in Bristol. We found that treatment with levodopa in this patient lead to the appearance of alpha band activity in the LFP recorded from PPN. This prompted the suggestion that alpha band synchronisation is a physiological feature of PPN function and that this activity may be mimicked by low frequency stimulation of the PPN. The second experiment confirmed this earlier result in a series of six more PD patients in whom the PPN area was implanted in Rome, and investigated the functional connectivity and reactivity of the subcortical alpha activity with the aim of deducing the possible role of this activity in behavioural performance in PD.

7.1 Experiment 1

The material presented here has previously been published (Androulidakis, A.G., Khan, S., Litvak, V., Pleydell-Pearce, C.W., Brown, P., Gill, S. (2008) Local field potential recordings from the pedunculopontine nucleus. Neuroreport. 19(1): 59-62.)

7.1.1 Methods

Patient Details and Surgery

The patient was a 39-year-old female who met the clinical criteria for Parkinson's disease and had no clinical evidence of other neurological disease (Hughes et al., 1992). Her predominant symptoms prior to surgical intervention consisted of difficulty initiating gait, postural instability and frequent falls in both the ON and OFF medication state. Preoperatively her medication consisted of a dopamine agonist, Pramipexole, and the levodopa preparation Sinemet Plus. Her daily levodopa dose equivalent was 1.5g. Postoperatively she remained on the same antiparkinsonian agents at a reduced dosage, with the daily levodopa dose equivalent at 3 months post DBS insertion being 850mg. Pre- and post-operative motor UPDRS scores are detailed in Table 7.1.1. The patient had undergone implantation of bilateral subthalamic region (STR) and PPN DBS electrodes 4 months prior to the current recordings being taken.

The technique used by the Bristol group for implanting electrodes into the PPN and STR has been described in detail in previous publications (Plaha & Gill, 2005; Plaha et al.,

2006) and in Chapter 2. An intraoperative coronal MRI image demonstrating the position of the plastic guide tubes and indwelling stylettes that represent the final position of the stimulating electrodes in the PPN is shown in Figure 7.1.1. Therapeutic PPN stimulation was delivered at a frequency of 60Hz, pulse width 60μs and amplitude of 2.5v. Four months following implantation the patient experienced a sudden deterioration in her symptom control and interrogation of the system suggested a potential current leak in the leads that would require surgical exploration. Following approval from the local ethics committee and informed consent from the patient at the time of surgical exploration the deep brain stimulating leads were externalized for 5 days in order to enable LFP recording.

Table 7.1.1 Pre -operative UPDRS scores in the ON and OFF medication state and post-operative OFF medication scores in the ON and OFF stimulation states.

Test Conditions	Motor (Part III) UPDRS Score	Motor UPDRS (Part III) Subscores			
		Gait	Posture	Postural Stability	Arising From Chair
Pre Operative OFF medication	55	3	2	3	1
Pre Operative ON medication	23	2	2	2	1
Post Operative OFF Medication/OFF PPN Stimulation	50	3	2	3	2
Post Operative OFF Medication/ON PPN Stimulation	35	1	1	1	1

Test Conditions and Data Recording

Depth electrode recordings were performed in the resting, awake state with the patient in a sitting position. OFF medication recordings were performed following a withdrawal of

all anti-parkinsonian medication in the preceding 12 hours. ON medication recordings were performed following administration of at least three of the patients eight daily doses of anti-parkinsonian medication. LFP recordings were taken from contacts of the stimulating electrodes implanted bilaterally into the PPN. Recordings employed a PsyLab SAM Contact Precision Amplifier. The high pass filter was 0.1Hz and the low pass filter was 200Hz. Data were acquired at 500Hz.

Analysis

LFP signals were digitally converted off-line to contiguous bipolar derivations (eg 01, 12, 23). All data analysis was performed offline in MatLab using the open source toolbox "FieldTrip" developed at the F. C. Donders Centre for Cognitive Neuroimaging (www.ru.nl/fcdonders/fieldtrip). The recordings were resampled at 300 Hz and divided into blocks of 3 s. Blocks containing eye blinks, saccades and muscle artifacts were rejected from further analysis based on visual inspection. In total, 179 blocks were analyzed in the OFF and 180 in the ON state, while 20 were rejected in the former and 19 in the latter state based on the above criteria.

Thereafter, spectral estimates of the power in the LFP signals were derived by Fourier analysis (frequency resolution ~1 Hz) using the "multitaper" method applied to sliding time windows. Spectra of LFPs showed prominent peaks between 7-11 Hz in recordings from all electrode contact pairs in the ON state, so the contact pair (23 on each side) with the highest 7-11 Hz peak was selected and the average power within the 7-11 Hz band was estimated across all blocks in the ON and OFF conditions. We then performed unpaired t-tests between the two conditions. Data were normally distributed as confirmed by the one-sample Kolmogorov - Smirnov test. Differences were considered statistically significant if $p < 0.05$. Results are presented as means ± SEM.

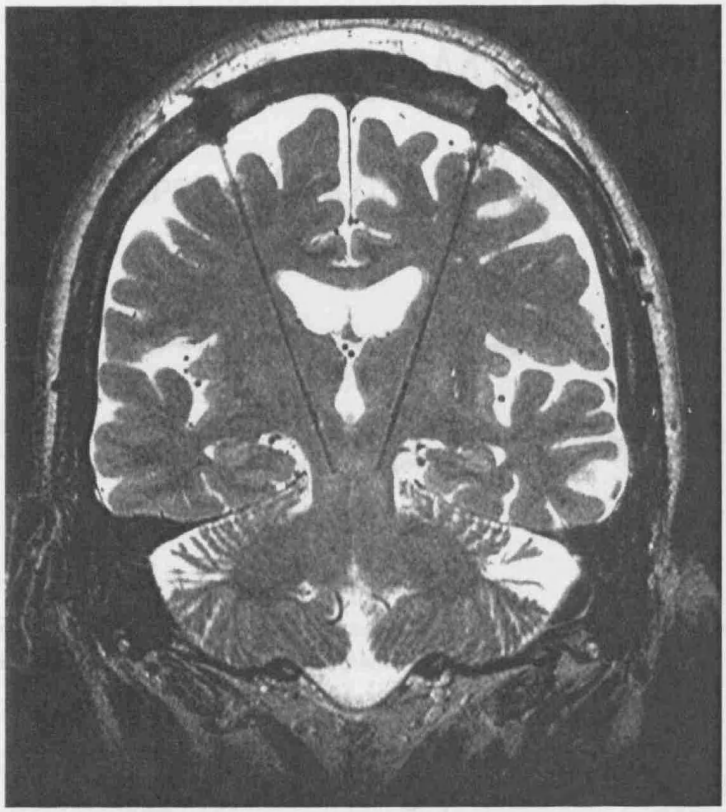

Figure 7.1.1 Intra-operative MRI in a PD patient. An intraoperative coronal MRI image demonstrating the position of the plastic guide tubes and indwelling stylette that represents the final position of the stimulating electrodes in the PPN.

7.1.2 Results

Raw data showed a prominent activity at 7-11 Hz in the PPN bilaterally, but only after treatment with levodopa (Fig 7.1.2). Spectral analysis demonstrated that at contact pair 23, where 7-11 Hz activity was most evident, this increased after treatment with levodopa on both sides (Fig 7.1.3A, B). Thus mean power between 7-11 Hz was higher in the ON (left PPN, 2.20 ± 0.10; right PPN, 1.10 ± 0.06) than in the OFF state (left PPN, 0.10 ± 0.01; $t = 20$, $p < 0.0001$, unpaired t-test; right PPN, 0.28 ± 0.01; $t = 11$, $p < 0.0001$; Fig 7.1.3C).

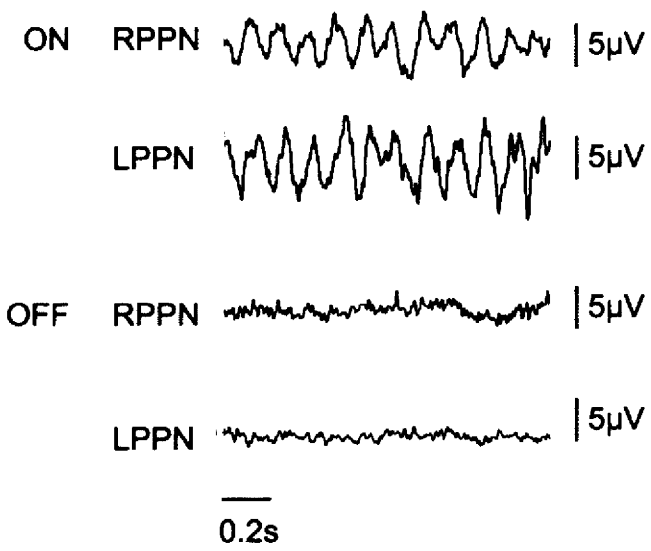

Figure 7.1.2 PPN LFP recordings in a PD patient. Examples of PPN (contact pair 23) LFP data taken from the right and left sides on levodopa and after overnight withdrawal of medication.

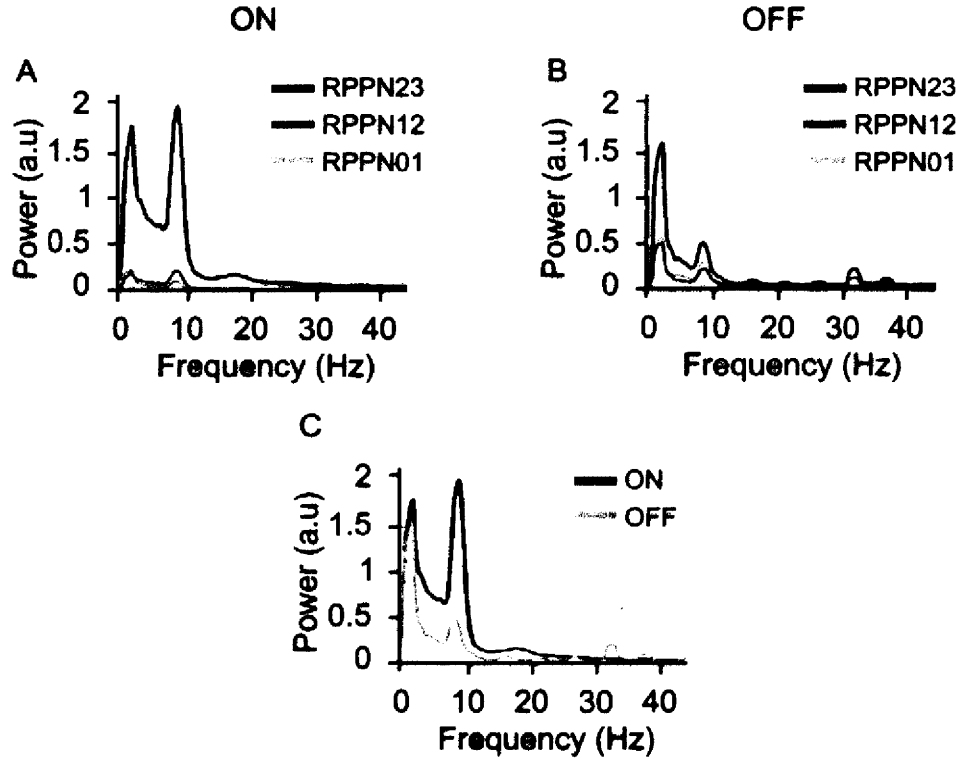

Figure 7.1.3 PPN LFP spectra from the right side. [A] Power spectrum from contact pairs 01, 12, 23 after reinstitution of levodopa therapy. [B] Same as [A], but this time after overnight withdrawal of medication. [C] Power spectra from contact pairs 23 in the ON and OFF states.

7.1.3 Discussion

The striking feature of the current case study is that dopaminergic stimulation promoted low frequency oscillatory synchronization in the region of the PPN as indexed by increased LFP power over 7-11 Hz after treatment with levodopa. The implications of this finding are twofold. First, unlike the STN, prominent synchronization at low frequencies may have a physiological role in PPN as this was increased by levodopa treatment, in tandem with clinical improvement. Second, the effect of dopaminergic activity on spontaneous network activity may be frequency and site specific.

As it was alluded above, the findings in PPN contrast with those in STN, although this requires corroboration in further patients (see section 7.2). In PD excessive synchronization in the beta band in the STN has been considered as a pathophysiological phenomenon associated with akinesia (Gatev et al., 2006; Uhlhaas & Singer, 2006; Chen et al., 2007; Hammond et al., 2007). This is supported by studies that have shown that power over this frequency band is suppressed in the STN of PD patients treated with levodopa and direct stimulation of this nucleus at 20 Hz can exacerbate bradykinesia (Foffani et al., 2005b; Colloca et al., 2006). The role of synchronized neuronal activity in the alpha band in the STN in PD may be broadly similar. LFP power in this band is also decreased following dopaminergic therapy (Priori et al., 2004) and direct stimulation of STN at 10 Hz has been reported to worsen parkinsonism (Moro et al., 2002; Timmermann et al., 2004; Fogelson et al., 2005; Chen et al., 2007).

This case report demonstrates that low frequency oscillations in PPN are augmented by the administration of levodopa in PD. In contrast to STN, stimulation of the PPN at low frequencies results in symptomatic improvement in Parkinsonian symptom (Mazzone et al., 2005; Plaha & Gill, 2005; Stefani et al., 2007), further supporting the hypothesis that alpha frequency oscillations may have a physiological role, at least in the resting state. Moreover, the results suggest that PPN DBS may be effective at even lower frequencies than currently utilized, with consequent prolonging of stimulator battery life.

7.2 Experiment 2

The material presented here has previously been published (Androulidakis, A.G., Mazzone, P., Litvak, V., Penny, W.D., Di Leone, M., Doyle-Gaynor, L.M.F., Tisch, S., Di Lazzaro, V., Brown, P. (2008) Oscillatory activity in the pedunculopontine area of patients with Parkinson's disease. Experimental Neurology. 27(5):1277-84)

7.2.1 Methods

Patients and Surgery

Six patients gave written informed consent to take part in this study which was approved by the local ethics committee. Cases 1 and 2 underwent bilateral implantation of the STN and PPN area, case 3 and 4 unilateral implantation of the STN and PPN area, case 5 unilateral implantation of the GPi and PPN area, and case 6 unilateral implantation of PPN area alone for the treatment of severe Parkinson's disease. Clinical findings in case 6 have been previously reported as case 3 in Stefani et al., 2007. Figure 7.2.1 illustrates the post-operative MRI in case 4.

The targeting of PPN in this series merits some comment. It has been reported in detail in previous publications (Mazzone et al., 2005; Stefani et al., 2007; Mazzone et al., 2007) and in Chapter 2. However, the precise nature of the target has been questioned (Yelnik, 2007; Zrinzo et al., 2007a, b) and because of this, and the uncertainty regarding the definition of the limits of the extent of PPN (Mena-Segovia et al., 2005), the conservative term 'PPN area' will be adopted in describing the current results.

Recordings

Patients were studied 3–6 days postoperatively, in the interval between DBS electrode implantation and subsequent connection to a subcutaneous stimulator. The subjects were seated comfortably in a chair and recorded in the resting, awake state. Recordings were performed after overnight withdrawal of antiparkinsonian medication and again about 1 hour after they had taken a minimum of 200mg levodopa.

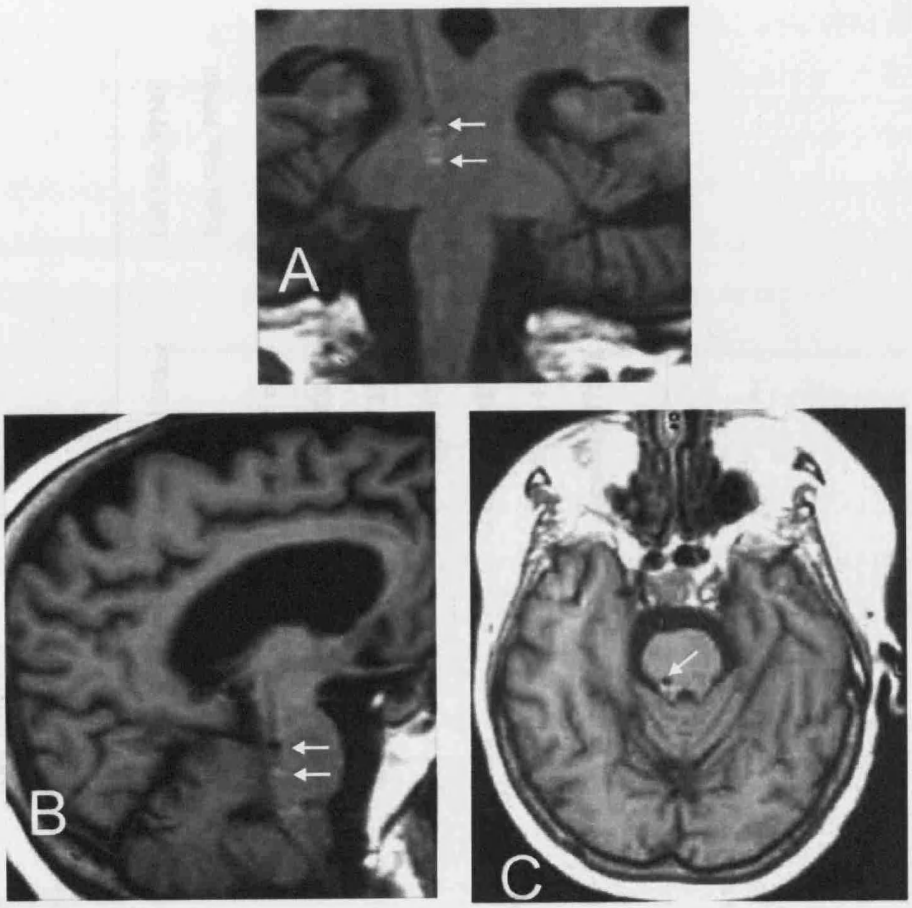

Figure 7.2.1 Post-operative MRI in a PD patient (case 5). (A) Coronal (B) Sagital, (C) Axial slices demonstrating position of DBS electrode in posterolateral pons. Arrows show approximate extent of artifact from electrode contacts.

Table 7.2.1: Clinical details in PD patients.

Case	Age and sex (years)	Disease duration	Predominant symptoms	Motor UPDRS pre-op (ON/OFF levodopa)	Motor UPDRS post-op (OFF levodopa) ON/OFF DBS	Medication (daily dose) pre-op	Contacts used in analysis
1	49/M	13	freezing and rigidity	32/72	25/75	Levodopa 1250mg	Left Side: PPN01 Right Side: PPN01
2	56/M	23	freezing, rigidity, dyskinesia	44/72	30/70	Lisuride 9.6 mg Levodopa 500mg	Left Side: PPN23 Right Side: PPN12
3	48/M	16	freezing, rigidity, dyskinesia	44/72	30/72	Levodopa 1325mg	PPN12
4	66/F	16	freezing, dystonia, gait deficit	62/82	58/75	Levodopa 1325mg	PPN01
5	51/M	8	freezing, rigidity, dyskinesia	60/68	32/68	Levodpoa 825mg Entacapone 125mg	PPN01
6	67M	11	freezing, rigidity, postural deficit	32/75	26/70	Levodopa 875mg	PPN12

The clinical findings in case 6 have been previously reported as case 3 in Stefani et al, 2007.

Deep brain activity was recorded bipolarly from the adjacent four contacts of each DBS electrode (0–1, 1–2, 2–3), amplified (x 100,000) and pass band filtered at 1–500 Hz (amplifier D160; Digitimer Ltd, Welwyn Garden City, Herts, UK). EEG activity was recorded monopolarly from FPz using a needle electrode and an ear reference and amplified and bandpass-filtered as before. For cases 1-3 and 5 (see Table 7.2.1) recorded EEG and LFP activity from the PPN area was recorded (i.e. 6 sides) ON and OFF medication at rest. In case 6 the PPN area LFP activity was recorded in both states (1 side) and EEG activity only in the ON state and for case 4 the PPN area LFP activity was recorded only in the ON state. For cases 1-3 and 5 (i.e. 6 sides), LFP activity from the PPN area was also recorded while they made self-paced movements of a joystick forward and then immediately backward, repeated approximately every 10-15s. This task was performed separately with left and right hands in both drug states. Recordings in the area of the STN were only possible on 5 sides (3 patients) and are not considered further. All signals were recorded using a 1401 analogue-to digital converter (1401, Cambridge Electronic Design, Cambridge, UK) using Spike 2 software (Cambridge Electronic Design) and sampled at rates of 1-2 kHz.

Analysis of rest recordings

All analyses were performed offline in Spike2 v6 and MatLab 7. Data were interpolated to a common sampling rate of 1 kHz. Spectral estimates of the power in the LFP and EEG signals from each contact pair were derived using the FFT for blocks of 1024 data points (frequency resolution ~1 Hz). The first step was to identify the PPN area DBS contact pairs that afforded the highest mean power in the 7-11 Hz band. We then estimated the average power within the 7-11 Hz band across all trials in the ON and OFF conditions for the PPN area and the EEG and compared conditions by means of the Wilcoxon matched-pairs test. Thereafter we calculated the bivariate coherence between the PPN area LFP and EEG for the two drug states. We averaged the Fisher transformed coherence values across the 7-11 Hz band for each subject and performed Wilcoxon matched-pairs tests between the two drug states.

Significant power and coherence between the PPN region and EEG was only recorded in the ON medication state. The functional connectivity between the PPN area and cortex in

this drug state was further investigated using the DTF implemented through the open source toolbox "FieldTrip" developed at the F. C. Donders Centre for Cognitive neuroimaging and the SPM toolbox (http://www.fil.ion.ucl.ac.uk/spm). A detailed description of the methodology and principles of the DTF can be found in Kaminski and Blinowska (1991), Korzeniewska et al. (2003), Cassidy and Brown (2003), and in Chapter 2. To this end, the MAR model that best described the signals coming from the two regions of interest is determined. The MAR methodology is essential for the DTF, as the DTF is built directly from the MAR coefficients.

The DTF has two potential advantages over spectral phase estimates. First, it does not assume unidirectional flow, an assumption that can potentially lead to erroneous physiological conclusions (Cassidy and Brown, 2003). On the other hand the DTF is relatively insensitive when phase/temporal differences between signals are small (Cassidy and Brown, 2003). There is no reason to think this is the case in the coupling between the LFP in the PPN area and EEG, given the indirect connectivity (see section 7.2.3). Second, the estimation of temporal differences from phase spectra is best performed through linear regression analysis of phase over periods of significant coherence (Mima and Hallett, 1999; Grosse et al, 2002). This, in turn, requires peaks in coherence that are reasonably broad, to allow for several phase estimates. This was not the case with the present data set.

For computing the DTF we used the MAR modelling toolbox distributed as a part of SPM (http://www.fil.ion.ucl.ac.uk/spm, in the subdirectory toolbox/spectral). This relies on a Bayesian estimation algorithm described by Penny and Roberts (2002). Before estimating the DTF, recordings were low-pass filtered at 30 Hz (to avoid modelling line noise) and resampled at 60 Hz and divided into trials of 3s. A MAR model of order 5 (the optimal order according to Bayesian model comparison) was fitted to the data. In total, we analyzed 69 ± 10 trials in the ON state. An identical number of shift predictors were generated by analyzing the same dataset with one of the signals shifted by one trial. The DTF and shift predictor values for each direction were averaged across the 7-11 Hz band for each side. We performed Friedman's related sample test to assess the differences

between DTF and shift predictor for each direction and post hoc Wilcoxon matched-pairs tests to confirm relevant differences.

Power was expressed in a.u. All statistical analyses were conducted using SPSS v12. Differences were considered statistically significant at $p < 0.05$. Results are presented as medians, where data were not normally distributed.

Analysis of movement task recordings

Data were interpolated to a common sampling rate of 1 kHz. Using Spike2 software, the onset of movements was detected from joystick position and marked. Movements were only marked when they were not preceded or followed by another movement within a period of 9 s. The mean number of movements marked was 14 (range, 9-18) and the mean duration of analyzed recordings was 330 s ± 19 s.

The first analysis step was to calculate the event-related spectral power for those contact pairs that afforded the highest mean power in the alpha band at rest (Table 7.2.1) for a period of 4 s before to 4 s after movement onset. Spectra were estimated using the discrete Fourier transform as outlined in Halliday et al. (1995) and in Chapter 2. Records were divided into a number of sections of equal duration with a block size of 1024 data points, affording a frequency resolution of ~1 Hz. Spectra were estimated by averaging across sections and a Hanning window filter was used. Blocks were shifted by 10 ms and averaged again until the whole record length had been analysed (using a modified Spike2 script). Movement-related activity was estimated separately for left and right hand joystick movements in both the ON and OFF states for each implanted side (2 movement sides x 6 implanted sides) and defined as the percentage power change in relation to a pre-movement baseline (-4s to -3.5s) period. For visualization purposes, matrices of event-related percentage power changes were thresholded so that power values within the 99% confidence limits of the averaged baseline power were set to 100 % (i.e. defined as no change). For quantitative analysis, we determined the frequency with the most pronounced mean ERS between 3.5s before to 4s after movement onset over 6–12 Hz for each side from each patient, in accordance with the frequency distribution of the ERS in matrices of event-related power change of each patient.

7.2.2 Results

PPN area alpha band power and reactivity

Raw data showed a prominent 7-11 Hz activity in the LFP from the PPN area but only after treatment with levodopa (8 and 7 sides studied ON and OFF, respectively; Fig 7.2.2 and Fig 7.2.3A). Power between 7-11 Hz was significantly higher in the ON (median = 0.14 a.u.) than in the OFF state (median = 0.078 a.u.; $z = 2.36$, $p = 0.018$, Wilcoxon test; Fig 7.2.3B). For each DBS electrode, alpha power showed a well-defined peak at one contact pair in the ON state. This peak was arbitrarily distributed between contact pairs (see Table 7.2.1) with a mean gradient of alpha power at the remaining contact pairs of 45 ± 16 %. This is consistent with a fairly local origin, and similar to the decrement previously reported across contacts in the STN (Kühn et al., 2006). However, no evidence of polarity reversal was found in the alpha band across the contact pairs. There was no difference in power in the 7-11Hz band in the EEG between the two drug states.

Grand averages of event-related power changes demonstrated a significant alpha ERS which started about 3s prior to movement and persisted for more than 2 s thereafter in the ON but not in the OFF state (Fig 7.2.4A, B). Time-evolving grand averages of the most reactive frequencies over the 6-12 Hz band (mean most reactive frequencies: ON state, 8.4 ± 0.7 Hz; OFF state, 8.2 ± 0.6 Hz) showed that the alpha ERS in the ON state was higher compared to the reactivity over the same band in the OFF state (Fig 7.2.4C). Time-evolving Wilcoxon tests confirmed that this difference was significant prior to movement ($p < 0.05$, Fig 7.2.4D).

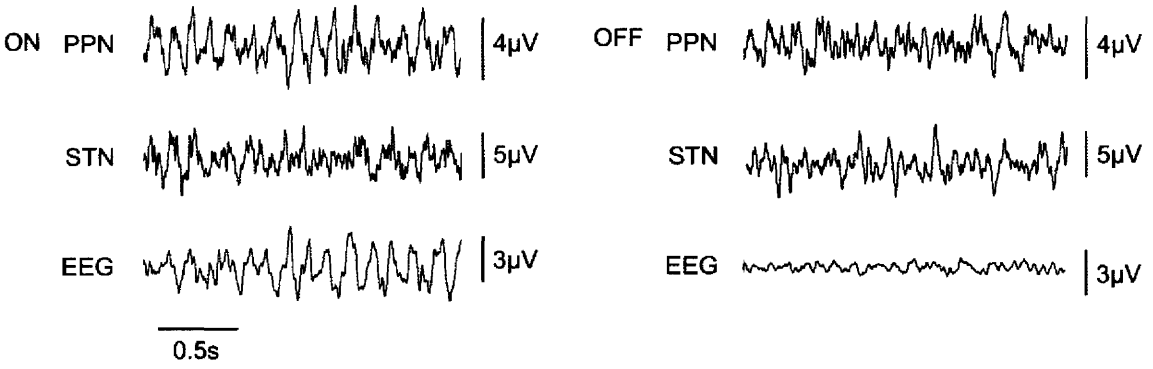

Figure 7.2.2 PPN area, STN LFP, and EEG recordings in a PD patient. Examples of the PPN area and STN LFP and EEG data taken from the right side of case 2 ON levodopa and after overnight withdrawal of medication.

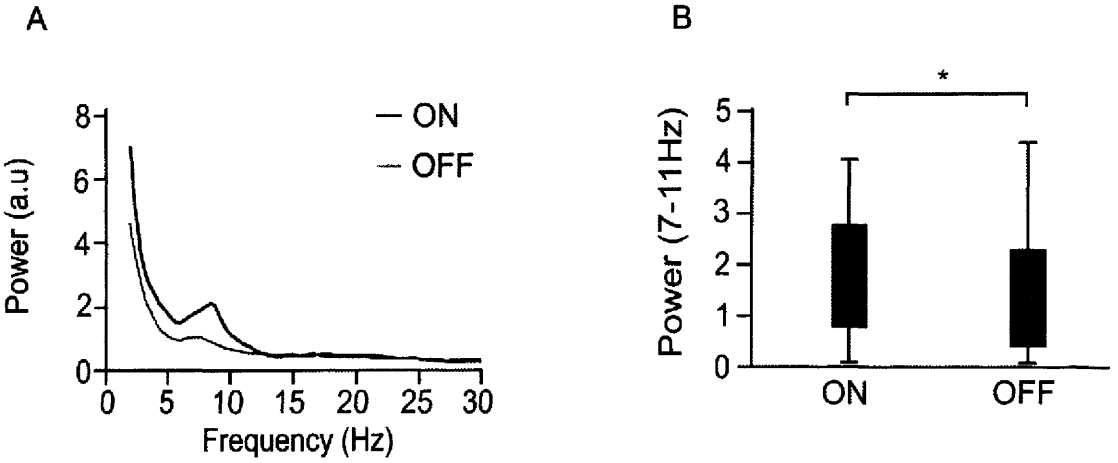

Figure 7.2.3 PPN area LFP power. Group medians of PPN area LFP spectral power ON (black lines) and OFF (grey lines) medication and [B] corresponding boxes of 7-11Hz power of PPN area LFP (n = 7 sides). The boxes show the median (marked by a horizontal line), the inter-quartile range, and the extreme values of power in both drug states. * p = 0.018.

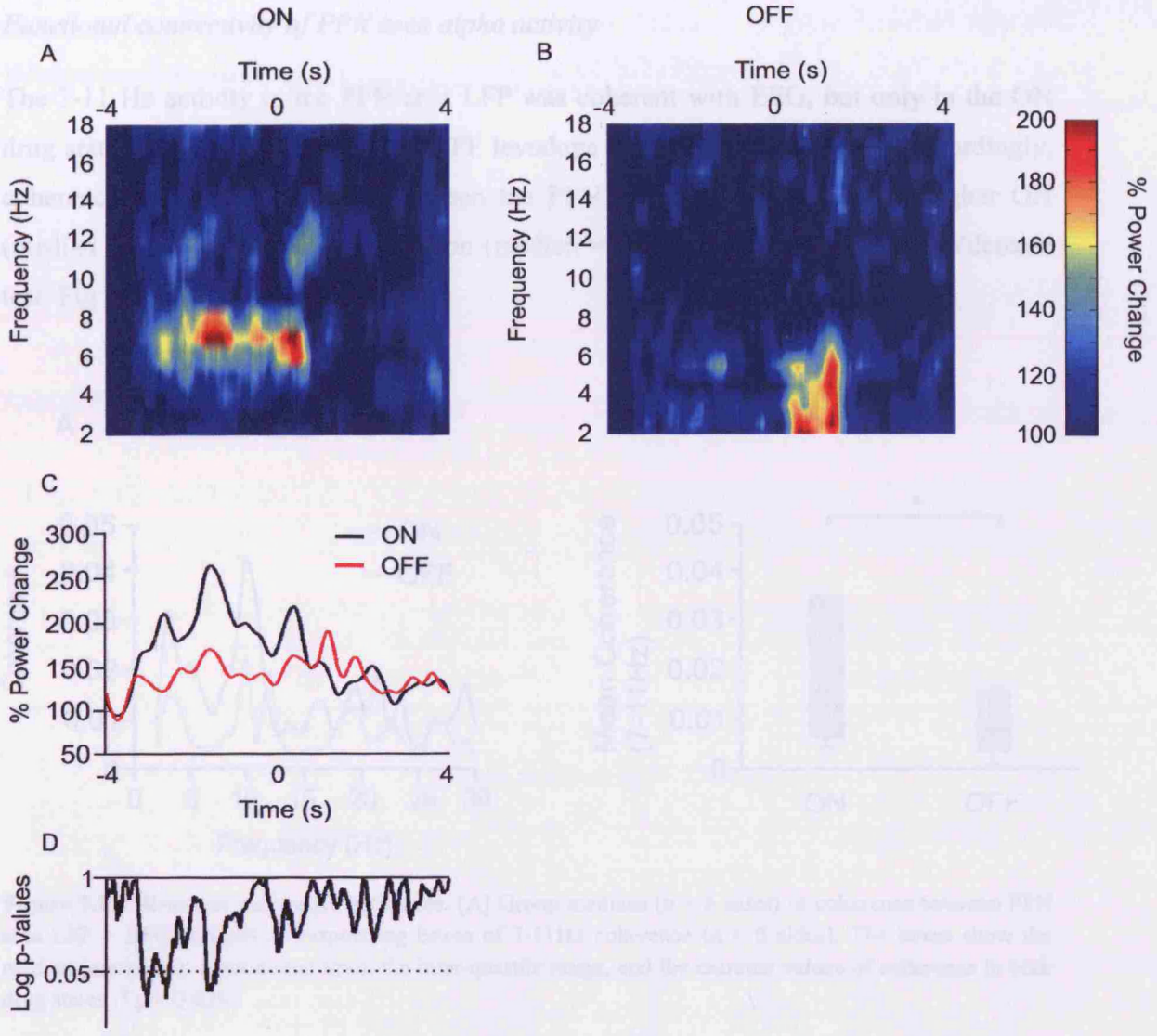

Figure 7.2.4 Movement-related spectral power in PPN area LFP before and after levodopa treatment. Movement-related spectral power change in the ON (A) and OFF (B) state. Averaged color coded time-evolving power relative to baseline period (4 to 3.5 s prior to movement). For visualization purposes, the matrices were thresholded at 99% CL of the averaged baseline power. (C) Grand averages of time-evolving mean most reactive frequencies 6–12 Hz movement-related changes ON (black line) and OFF (red line) levodopa. (D) Time-evolving significance of the difference in percentage power change in the most reactive frequencies over the 6-12Hz band between ON state and OFF states. Horizontal interrupted line is p = 0.05 and y-axis is logged. Alpha reactivity is episodically significantly higher in the ON than in the OFF state.

Functional connectivity of PPN area alpha activity

The 7-11 Hz activity in the PPN area LFP was coherent with EEG, but only in the ON drug state (6 sides studied ON and OFF levodopa with EEG; Fig 7.2.5A). Accordingly, coherence in the 7-11Hz band between the PPN area LFP and EEG was higher ON (median = 0.022) than OFF medication (median = 0.008; z = 2.2, p = 0.028, Wilcoxon test; Fig 7.2.5B).

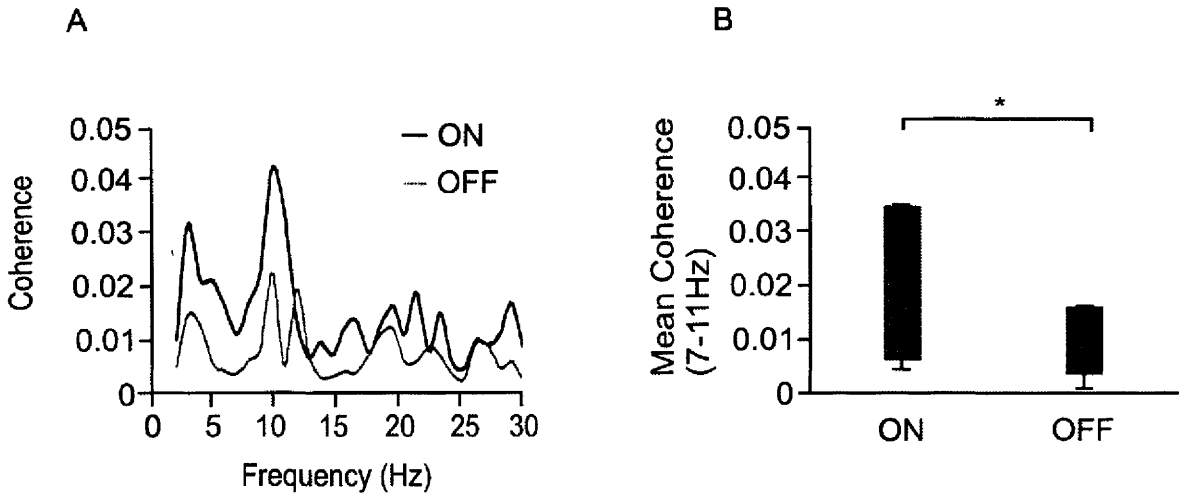

Figure 7.2.5 Bivariate coherence estimates. [A] Group medians (n = 6 sides) of coherence between PPN area LFP – EEG and [B] corresponding boxes of 7-11Hz coherence (n = 6 sides). The boxes show the median (marked by a horizontal line), the inter-quartile range, and the extreme values of coherence in both drug states. * p = 0.028.

The directed coherence between cortex and the PPN area was estimated to characterize bidirectional interactions between these levels. Friedman tests demonstrated significant differences between DTF and shift predictors from the PPN area to cortex and vice versa (7 sides studied ON levodopa with EEG; $\chi^2 = 8.65$, p = 0.034). Post hoc Wilcoxon tests confirmed that interactions between activities in the PPN area and cortex were significant in the ON medication state both from the PPN area to cortex (medians: 0.15 vs. 0.13; z = 2.2, p = 0.028; Fig 7.2.6A) and from cortex to the PPN area (medians: 0.21 vs. 0.16; z = 2.37, p = 0.018; Fig 7.2.6B). An example of the DTF between these sites is shown for

case 1 in figure 7.2.6C, D. These findings suggest that there is a bidirectional flow of information between the PPN area and cortex in the 7-11 Hz range.

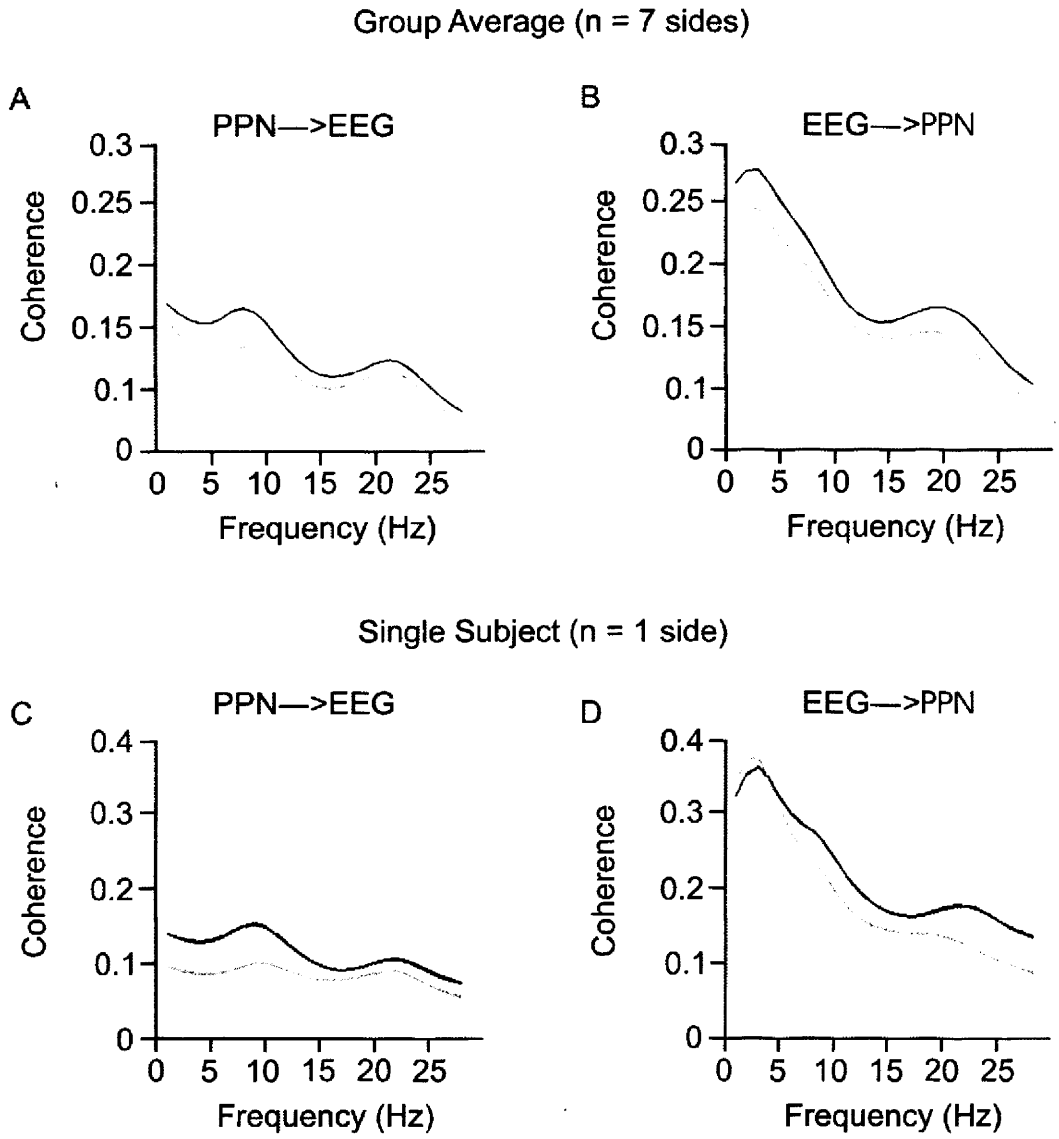

Figure 7.2.6 DTF analysis of PPN area LFP and cortex at rest. [A-B] Group averages (n = 7 sides) of directed coherence in the ON drug state. Plots demonstrate the mean directed coherence of all subjects (black line) and the corresponding shift predictor (grey line) in each direction. [C-D] Examples of directed coherence from the left hemisphere of case 1.

7.2.3 Discussion

In this series of patients with Parkinson's disease it was demonstrated that levodopa promoted 7-11 Hz oscillatory synchronization in the region of PPN, in accordance with the previous case report (section 7.1). Moreover, it was shown that this oscillatory activity in the PPN area was coherent with similar activity in the cortical EEG, but only after treatment with levodopa. Estimation of the directed coherence revealed that this coupling between the PPN area and cortex was bidirectional, perhaps involving connections with the basal ganglia and thalamus (Pahapill and Lozano, 2000; Mena-Segovia et al., 2004; Mena-Segovia et al., 2005). The data are broadly in keeping with the hypothesis that prominent synchronization at low frequencies may have a physiological role in PPN (section 7.1) and in the communication between PPN and cortex.

However, before considering the significance of these findings in greater detail it would be circumspect to describe the limitations of the current data set. First, there is, without post-mortem histology, no way of currently confirming the precise structure or structures targeted in this series. Accordingly, the conservative term PPN area has been used to describe the target, thereby acknowledging the debate about the precise targeting of PPN (Mazzone et al., 2005; Stefani et al., 2007; Mazzone et al., 2007; Yelnik, 2007; Zrinzo et al., 2007a, b) and the difficulty in transcribing the anatomical details of this region to the human when, even in animal studies, the extent of the PPN remains unclear (Mena-Segovia et al., 2005). Nevertheless, we would stress that the therapeutic effects of stimulation of the target selected here are so far indistinguishable from those of other reports of PPN stimulation in Parkinson's disease (Plaha and Gill, 2005; Lim et al., 2007), and the central finding of increased spectral 7-11 Hz power in the PPN region upon treatment with levodopa has been previously reported in a single patient implanted in PPN, where surgery was performed by another group in Bristol (section 7.1). A second consideration is the extent to which the present findings might be representative of Parkinson's disease. Patients were selected for DBS in the PPN area on the basis of gait freezing that was unresponsive to medication and/or postural instability (Stefani et al., 2007), -symptoms that tend to mark advanced PD and are not indications for more conventional STN DBS in isolation. Accordingly, the present findings may be

representative of only a subset of parkinsonian patients. A further limitation of the present data is the limited sampling of the EEG, dictated by surgical constraints. Recording was only possible over Fpz. As such a monopolar signal was elected to be used so that the EEG signal was as representative of distributed cortical activity as possible. Finally, the small number of patients (n = 6) reported in this study should be stressed.

With the above provisos in mind, what might be the relevance of the findings presented here? The appearance of oscillatory electric fields over 7-11 Hz after levodopa may predominantly reflect synchronized oscillatory input to the PPN area, as LFPs tend to be dominated by such inputs (Boraud et al., 2005). This synchronized oscillatory input following dopaminergic stimulation may potentially be exerted via the major afferents to the PPN from the basal ganglia output nuclei, GPi and SNr (Mena-Segovia and Giordano, 2003; Mena-Segovia et al., 2005). In PD this would mean a reduction in the inhibitory input to PPN from the latter nuclei. In accordance with this, it was recently shown in the rat that high frequency stimulation of the STN can induce disinhibition of the PPN (Florio et al., 2007).

There is reasonable evidence to suggest that oscillatory electric fields, such as the LFP in the PPN area following treatment with levodopa, may influence the emergent properties of neuronal networks both locally (Deans et al., 2007) and at subsequent projection targets. This seems to be the case with respect to pathological beta oscillations in the STN area which are locked to population activities at projection targets (Brown et al., 2001) and may even shape the firing probability of local neurons (Kühn et al., 2005; Weinberger et al., 2006). Indeed, experiments in brain slices suggest that the influence of oscillatory fields increases as their frequency drops so that the lower frequency oscillations in the PPN area after dopaminergic therapy may potentially have even greater effects (Deans et al., 2007). The notion that the 7-11 Hz oscillations in the PPN area after dopaminergic therapy may be both physiological and influential is further supported by the effects of local DBS. In contrast to STN, where DBS is performed at high frequencies, stimulation of the PPN area at low frequencies results in symptomatic improvement in parkinsonian symptoms (Jenkinson et al., 2004; Mazzone et al., 2005;

Plaha and Gill, 2005; Stefani et al., 2007). The increase in 7-11 Hz activity in the PPN region upon treatment with levodopa suggests that DBS at low frequency may be partly mimicking this spontaneous activity by direct driving of neural elements in the region of stimulation (section 7.1). This, however, remains to be established.

In PD excessive synchronization in the beta band in the STN has been considered as a pathophysiological phenomenon associated with the akinetic-rigid symptoms. No oscillatory activity in the beta band in either pharmacological state was reported in the PPN LFP in the patients here or the patient in section 7.1. Considering, however, that exaggerated beta synchrony in the basal ganglia and hence the akinetic-rigid state is probably a consequence of or at least linked to pharmacological dopaminergic upset, lack of beta oscillations in a non-dopaminergic structure such as the PPN is not a surprise. This is in agreement with the fact that dopamine and STN DBS do not help significantly PD patients with axial symptoms (Chapter 1). As mentioned above, dopaminergic stimulation and STN DBS may induce PPN disinhibition indirectly through the basal ganglia output nuclei.

The present data also provide clues as to the function of the subcortical oscillatory activity over 7-11 Hz. This activity was only significant after treatment with levodopa, and may therefore represent a more physiological type of activity. Moreover, it increased prior to self-paced movements. This increase was sustained for several seconds suggesting that it was more likely to be related to attentional processes than any parameterization of movement. Furthermore, the activity was coherent with oscillatory activity at the cerebral cortical level in the alpha band. Alpha oscillations are thought to play an important role in attentional processes, particularly when these tend to occur over the lower frequencies in the alpha range, as here (Klimesch, 1999; Palva, 2007). In particular, it has been suggested that alpha activity may indicate that attention is actively suppressing cortical activity related to distracters as a part of the process of focusing attention on important targets (Ward, 2003). For example, alpha power increases with memory load in the Sternberg memory-scanning task, reflecting an increase in the need to suppress distraction (Jensen et al., 2002). Moreover, when attention is directed internally towards mental imagery, alpha power at attention-relevant scalp sites is greater than

during externally directed, information-intake tasks, reflecting suppression of external input during the imagery task (Cooper et al., 2003). In the same study, alpha power increased with increasing external task load, reflecting the need to suppress competing information sources. Extrapolation of these data lead to the speculation that the PPN area may have a function in supporting the network subserving internal attention and characterized and perhaps underpinned by alpha oscillatory activity. The posited role of PPN in internal attention might also help explain why PPN DBS can ameliorate freezing, by improving the focusing of internal attention on the motor task (Okuma, 2006; Giladi and Hausdorff, 2006). The above schema would be consistent with the position of the PPN area as part of the reticular activating system (Pahapill and Lozano, 2000; Mena-Segovia et al., 2004; Mena-Segovia et al., 2005).

In conclusion, levodopa strongly promotes 7-11 Hz oscillatory synchronization in the region of PPN and coupling of this activity with similar activity in the cortical EEG in patients with PD. The 7-11 Hz activity is further increased prior to self-paced movement and the coupling between the PPN area and cortex in the same band is bidirectional. These findings suggest that alpha oscillations in the PPN area may represent a physiological pattern of activity. The subcortical oscillations are coupled to cortical alpha activity and may possibly be allied to attentional- and/or alertness-related processes.

7.3 Summary

- Levodopa promoted 7-11 Hz oscillatory synchronization in the region of PPN. Similarly, oscillatory activity over 7-11 Hz in the PPN area was coherent with similar activity in the cortical EEG but only after levodopa administration. It seems that prominent synchronization at low frequencies may have a physiological role in PPN and in the communication between PPN and cortex.

- Alpha band activity was increased in the PPN prior to self-paced movements ON levodopa and it remained increased for several seconds. This increase seems unlikely to be related to any parameterization of movement but rather allied to motor-related attentional processes.

CHAPTER 8

Conclusions

The first aim of this thesis was to investigate the behavioural correlate of beta-range coherence in healthy people. In chapter 3 it was demonstrated that bursts of beta band synchrony in the corticospinal motor system were associated with larger and more appropriately scaled responses to displacements in visual feedback in a visually controlled positional hold task showing that the influence of visual feedback on performance is increased during these bursts. Spontaneous physiological fluctuations in the degree of beta band synchronization in the motor cortex and the corticospinal system may be of behavioural advantage during fine postural tasks involving the hand by temporarily up-regulating the effects of visual inputs. In chapter 4 it was evidenced that the behavioural advantage of beta-range corticomuscular coherence on postural tasks was maintained even in the absence of relevant peripheral inputs when subjects were just warned of an upcoming postural challenge. Specifically, it was shown that increases in corticomuscular coherence preceded peripheral feedback related to the task and that such an up-regulation was associated with improved behavioural performance. The results from these two chapters constitute substantial evidence for task specificity of oscillatory activity in the beta band suggesting a role of beta synchrony in the promotion of postural/tonic contraction (Gilbertson et al., 2005; Lalo et al., 2007).

The second aim of the thesis was to examine the role of population oscillations in the parkinsonian basal ganglia and their relation to motor symptoms that accompany the disease. In chapter 5, it was demonstrated that treatment with levodopa favours motor processing by making the pattern of activity in the STN more normal. The STN of PD patients exhibited deeper movement-related power suppression over the beta band and higher power increase in the gamma band around the time of the movement after treatment with levodopa than when patients were off medication. In fact, the movement-related gamma band synchronization was higher contralateral to the movement side following the same pattern as in the non dopamine-depleted cortex (Crone et al., 1998a; Pfurtscheller et al., 2003) and STN (Brücke et al., 2008). In chapter 6, it was shown that beta synchrony in the dopamine-depleted parkinsonian STN is not only modulated before

and after movement but also during repetitive movements possibly reflecting a role in ongoing motor performance and in the occurrence of bradykinesia. Together these two chapters confirm that oscillatory activity in the STN is associated with the feedforward- and feedback-related processing before, during, and after voluntary movement. Finally, in chapter 7 it is demonstrated that treatment with levodopa promoted alpha band oscillatory activity in the PPN which was found to be coupled with alpha activity in the cortex. It seems that alpha band oscillations are a physiological feature in the PPN and they are probably associated with motor-related attentional parameters as they were found to be increased for some time prior to self-paced movements. In this chapter, the implications of these findings will be discussed as well as the role of population oscillations in both the healthy and dopamine-depleted basal ganglia.

8.1 Beta oscillations and their role in plasticity

It has been shown that beta bursts promote postural/tonic contraction by temporarily reinforcing the effects of sensory inputs such as stretches (Gilbertson et al., 2005), median nerve shocks (Lalo et al., 2007) or visual information regarding positional status (chapter 3). In all these experiments an interesting and recurring feature has been reported: a mismatch between the duration of spontaneous beta bursts and the timing of associated changes in peak acceleration during triggered reaction time movements (Gilbertson et al., 2005), the timing of altered central processing of triggered sensory inputs (Lalo et al., 2007), and the timing of improved responses to visual feedback of postural control (chapter 3). This raises the possibility that beta bursts represent a cortical state in which sensorimotor transformation necessary to achieve the intended contraction is strengthened by plastic effects that outlast the duration of the beta burst.

Support for a role of beta activity in altered plasticity has also come from in vitro studies where oscillations over this band were shown to participate in synaptic plasticity and memory processes that last for about 50 minutes (Bibbig et al., 2001). In the experiment described in chapter 3, the time-course of this plastic effect maybe party accounted for by the repetition frequency of spontaneous bursts that bunch in time (Fig. 3.2.6). One triggering beta burst may herald a temporarily increased probability of similar bursts to occur resulting in the alteration of processing for a period longer than the duration of a

single beta burst. Similarly phasic, short-lived increases in beta coherence were observed in the expectancy of a forthcoming postural challenge (chapter 4). It needs to be noted however that there is still no direct proof for plasticity being induced by oscillations in the motor system.

These hypothesised plastic changes seem to last around 2s. The manner in which they take place is not known. It is possible that sensorimotor inputs related to the aim of the task are strengthened temporarily when they coincide with beta bursts. For example it is likely that during a postural contraction beta bursts that might occur reinforce inputs that are necessary for the successful performance of the task and take place at this time point. The fact that beta oscillations show preference to task-relevant stimuli has also been demonstrated in LFP recordings from PD patients (Williams et al., 2003). Such a proposal, of course, needs further investigations.

Another explanation for the effects of beta bursts could be the one proposed by Riddle and Baker (2006). These authors suggested that beta coherence represents a mixture of online feedforward (cortical) and feedback (peripheral somaesthetic) mechanisms, a process whose aim is to reassess the preceding experience and return the system to previous accuracy levels by preparing it for the next step. This theory, however, does not explain the phasic increases in beta coherence and their effect on motor behaviour in the absence of any change in somaesthetic feedback, as demonstrated in chapter 4.

On the other hand, excessive synchrony in the beta band in the basal ganglia as well as increased coupling between cortex and basal ganglia in this band have been linked to motor impairments in patients with PD (Brown & Williams, 2005; Gatev et al., 2006; Hammond et al., 2007; Brown, 2008; see Chapter 1). If beta oscillatory activity seen in association with motor processing paradigms in healthy humans participates in plastic changes in the motor system, then the question that arises is whether the excessive beta seen in PD represents abnormal short-term plasticity. The causes underlying the pathological oscillatory synchrony in PD are also unclear. The inappropriate processing of rhythmic cortical input in the STN-GPi network due to lack of dopamine (Magill et al., 2001) as well as further aberrant processing within the basal ganglia circuitry (Terman et al., 2002) have been proposed as possible mechanisms that contribute to oscillatory

synchrony. Leblois et al. (2006) have also suggested that these oscillations may also be driven by the imbalance between direct and hyperdirect pathways caused by dopamine depletion.

The next question therefore is one of significance. Does beta in the basal ganglia in PD signify an exaggerated version of the corticomuscular "posture-promoting" beta seen in healthy humans? Can these behavioural correlates be seen as mechanisms of bradykinesia? First of all, it needs to be stressed that beta activity has been linked to posture-related tasks only in the healthy and not in the parkinsonian brain. Coherence over this band is not higher in the corticomuscular system in PD patients making the scenario that corticomuscular beta and cortico-basal ganglia beta are managed by different processes a likely candidate (Brown 2008). In PD corticomuscular coherence is evident at tremor frequencies (Salenius et al., 2002) and this pattern of activity has been proposed to have little connection with the increased beta in the basal ganglia or the increased cortico-basal ganglia beta coherence (Brown 2008) but rather be related to the pathophysiology of tremor which maybe distinct from that of bradykinesia and rigidity (Pavese et al., 2006; Weinberger et al., 2006; Hammond et al., 2007).

Secondly, there is no evidence of increase in beta band power in the cortical activity in PD, despite the clear potentiation of coherence in the same band between cortex and basal ganglia (Fogelson et al., 2006) and between different cortical areas (Silberstein et al., 2005). The former could be due to the fact that beta oscillatory activity is amplified on the way from the cortex to the basal ganglia or even within the basal ganglia nuclei possibly due to dopaminergic deficiency. The latter could be seen as a clear increase in the proportion of distinct cortical areas that are phase and amplitude locked in the beta band. At this point, a distinction should be made between cortical beta activity and event-related cortical beta reactivity which has indeed been found abnormal in PD (Labyt et al., 2005). Even though results of non-human primate studies and of pharmacological studies in patients suggest that increased subcortical beta in PD is, at the very least, a pathological exaggeration of physiological activity (Fogelson et al., 2006; Hammond et al., 2008), this still remains to be established.

8.2 Oscillations in the basal ganglia and motor deficits in PD

A recent study demonstrated that beta activity may lead to bradykinesia since stimulation of the STN at 20Hz exacerbated patients' bradykinesia (Chen et al., 2007) proving for the first time that synchronization of STN output at this frequency may slow movement in PD. Is beta oscillatory activity in the basal ganglia the cause or the effect of bradykinesia? Leblois et al. (2007) found that oscillations at low frequencies 2-30Hz in the pallidum of non-human primates emerged after the onset of major motor signs, while changes in task-related activity occurred early and paralleled the onset of bradykinesia. They showed that the emergence of synchronized oscillatory activity in the GPi occurs late in progressive parkinsonism and may thus not be a prerequisite for the onset of bradykinesia or akinesia. The pathological disruption of movement-related activity in the basal ganglia is a better correlate to bradykinesia and stands as the best candidate to explain this motor symptom (Leblois et al., 2007). However, these authors only considered relatively insensitive measures of oscillatory synchronization and did not record the LFP which is a very sensitive measure (Zeitler et al., 2006).

Treatment of PD patients with levodopa has profound effects on both movement and the pattern of movement-related reactivity in the STN, as reflected in the LFP. In chapter 5 it was proposed that levodopa is promoting a more physiological pattern of motor processing that facilitates information coding and processing (Pogosyan et al., 2006). The most striking finding in this chapter was the promotion of reactivity in the gamma frequency band slightly before and after movement onset. Whether gamma activity in the STN is itself a pathological feature, possibly associated with levodopa-induced dyskinesias (Fogelson et al., 2005), or is primarily physiological remains unclear. Movement-related activity over this band has been found to increase before double movements (Kempf et al., 2007) and contralaterally to single self-paced movements in the STN of patients with PD (chapter 5) suggesting that gamma oscillations might have a more direct role in the parameterisation of movement. This gamma ERS presented in these two studies is not strictly contralateral as in the non-PD cortex (Crone et al., 1998b) but rather asymmetric. Similarly, Brücke et al. (2008) reported an increase in gamma band LFP activity in the GP during and strictly contralateral to voluntary movement in a series of dystonic patients supporting thus the idea that movement-related lateralized

gamma band synchronization is a feature of basal ganglia activity that parallels the activity at the cortical level (Crone et al., 1998b).

In chapter 5 it was mentioned that movement-related gamma activity changes occurred in the STN of PD patients that had no obvious gamma peak in their rest data. This was also reported in a study by Kempf et al. (2007) but not in other studies where PD patients were reported to have a finely tuned and prominent gamma peak in LFP spectra at rest following treatment (Brown et al., 2001; Silberstein et al., 2003). One reason that could explain this inconsistency is – as mentioned earlier (Fogelson et al., 2005) – the fact that baseline gamma activity might be related to levodopa-induced dyskinesias, which are not present in the same degree in all patients. It needs to be stressed however that Fogelson and colleagues in this study excluded patients that did not show a prominent gamma peak in the power spectra of the STN LFPs at rest. Another reason could be the fact that high frequency activities tend to be more focal than lower ones and the localization of the electrode is very critical in that case. Alternatively, this discrepancy could also be related to the firing rates of neurons and how they are affected by the level of dopamine deficiency. It was mentioned earlier that background beta increases only in late PD stages as opposed to movement-related beta which changes earlier in the MPTP-treated primate and that disruption of the movement-related activity is the best candidate to explain bradykinesia (Leblois et al., 2007). Consistent with this proposal, it could also be argued that the increase and lateralization of gamma ERS after treatment with levodopa is one of the first features that is restored irrespective of the background gamma power levels and is probably the best candidate to explain the changes in motor control after treatment.

So, how can synchronized oscillatory activity in the basal ganglia affect movement? Abnormally increased synchronization in the beta band constrains the ability of neurons to code information in time and space, as both adjacent and spatially distributed neurons preferentially fire locked to the beta rhythm (Hammond et al., 2007). Once temporarily released these neurones can more effectively engage in any dynamic assembly formation and rate coding necessary for the processing of movement (Courtemanche et al, 2003; Amirnovin et al, 2004). Consistent with this, in chapter 6 it was demonstrated that LFP activity in the beta band recorded in the STN is modulated in time with repetitive finger

tapping in patients with PD and that this modulation decreases as tapping becomes more bradykinetic suggesting that failure to release neurons from the beta rhythm in a task appropriate manner may impair the organisation of forthcoming movement and later feedback related processing. Dopamine has been shown to suppress pathological synchrony in the beta band and increase synchrony in the gamma band prior to and during movement (chapter 5). Dopamine affects directly the pattern of basal ganglia activity and reduces parkinsonian motor symptoms by promoting the formation of dynamic temporal binding between neuronal assemblies through gamma synchronization (Engel & Singer, 2001; Engel et al., 2001) and also by further increasing the potential for rate coding during motor processing around the time of voluntary movement (Pogosyan et al., 2006).

It has been proposed that there might be a reciprocal relationship between beta and gamma band oscillatory activity during contralateral limb dyskinesias (Fogelson et al., 2005). As short-lived reciprocal effects on these oscillations are seen just before and during voluntary movement (chapter 5), it is possible that spontaneous fluctuations in the balance between these activities contribute to the development of motor symptoms seen in PD (Fogelson et al., 2005). In agreement with this, it has been shown that the loss of dopamine in PD alters this equilibrium causing the appearance of non-linear correlations between STN LFP rhythms thereby leading to loss of functional segregation between these rhythms. After dopaminergic treatment these non-linear correlations decrease and segregation is restored (Marceglia et al., 2006). This study actually concluded that the pathophysiology of information processing in the human basal ganglia involves not only activities of individual rhythms but also interactions between rhythms and that a breakdown of the independent processing of the functional subcircuits in the basal ganglia is a hallmark of PD (Marceglia et al., 2006). It is thus implied that different frequency bands and their interactions may be associated with different functions and probably different functional deficits in PD and that frequency of synchronization may provide a means of functionally segregating related processing in the motor system (Fogelson et al., 2006).

Studies in rodents have demonstrated that low frequency rhythmic theta oscillations (defined as rhythms over the 7-11Hz band in the rodent, but alpha in the human) may also have a physiological role in the basal ganglia (DeCoteau et al., 2007b). Consistent with this, in chapter 7 it was proposed that low frequencies in the alpha range (~8Hz) may have a physiological role in the PPN as it tends to increase after levodopa medication for several seconds prior to voluntary movements indicating that this might be related to attention- and/or alertness-related processes. Previous studies have suggested that oscillations in the alpha band in the cortex suppress activity related to distracters, i.e. external input unrelated to the task. It is possible that in PD the increased inhibitory basal ganglia flow to PPN causes overinhibition of this nucleus (Strafella et al., 2008) which as a result may also disrupt the effect of alpha activity on aberrant, "distracting" external input that probably comes from the cortex or other basal ganglia structures. Direct stimulation of PPN may remove this disruptive influence on physiological alpha activity promoting attention-related processes and hence improving behavioural performance and aiding a restoration of normal activation of the PPN-cortical network. Interestingly, Strafella and colleagues recently reported that disinhibition of the PPN due to low-frequency DBS stimulation may cause an increase in the regional cerebral blood flow in different subcortical structures most notably the thalamus (Strafella et al., 2008).

8.3 Future perspectives

The field of oscillatory phenomena is only in its infancy. The realization, however, that abnormal patterns of oscillatory events prevail in disabling disorders such as PD, dystonia, myoclonous, epilepsy, schizophrenia, and Alzheimer's necessitate the furthering of research on the nature of these phenomena in both health and disease.

In chapters 3 and 4 it was demonstrated that the improvement in the accuracy of postural tasks after bursts of beta synchrony lasts for several hundreds of milliseconds supporting a role of oscillations in plasticity. However, it still remains unclear whether bursts of oscillatory activity in this band are in fact associated with short-term plastic effects. Therefore, techniques that manipulate cortical plasticity on this time course could answer that question. The effects of pharmacological agents or the effects of repetitive TMS to

the motor cortex on beta bursts might be able to reduce beta synchrony during a positional hold task thereby leading to a deterioration in performance.

Finally, it is still unknown whether beta oscillations in the basal ganglia of PD patients have the same "posture-promoting" properties as in the healthy corticospinal motor system. Rigidity, one of the major disabling symptoms in PD, is characterized by stiffness – a heightened resistance to perturbations and an exaggerated postural set – and does in fact correlate with the degree of synchronization in the beta band in the STN and cortex. However, such a behavioural association has never been shown in PD patients. Positional hold tasks could be used in order to investigate whether bursts of beta activity detected in STN in PD patients are correlated with phasic increases in the gain of sensory re-afferance and increases in rigidity in postural hold tasks. In this case the imposed task could be triggered by beta bursts that are detected in the LFP recorded from the STN.

The data presented about the physiology of PPN in PD only come from a limited number of patients and surely more studies are needed in order to shed light on this nucleus and its possible role in motor control in health and disease. Creating animal models of PD that can mimic the progression and extent of the symptoms seen in this specific group of patients that match the criteria for PPN surgery will be a valuable tool not only in order to investigate the electrophysiological properties of this nucleus and its connectivity with other structures in disease but also use it as a screening tool for possible therapies. Additionally, given the extensive cholinergic neurotransmission of the PPN, it would be useful to assess the effect of cholinergic treatment on the electrophysiological properties of the nucleus during various motor tasks. Elucidating the characteristics of PPN will provide neurophysiological landmarks that may aid the proper placement of DBS electrodes in the nucleus.

Further understanding of the properties of neuronal synchronization in the motor system seems of principal importance to allow in-depth knowledge and manipulation of the system. Similarly, ongoing work examining the mechanisms of action of DBS will likely lead to refinement and development of such therapies.

REFERENCE LIST

Alderson H, Winn P (2005) The Pedunculopontine and Reinforcement. In: Bolam JP, Ingham CA, Magill PJ (Editors), The Basal Ganglia VIII. Springer Science and Business Media, New York, pp 523-532.

Alegre M, onso-Frech F, Rodriguez-Oroz MC, Guridi J, Zamarbide I, Valencia M, Manrique M, Obeso JA, Artieda J (2005) Movement-related changes in oscillatory activity in the human subthalamic nucleus: ipsilateral vs. contralateral movements. Eur J Neurosci 22:2315-2324.

Alexander GE, DeLong MR, Strick PL (1986) Parallel organization of functionally segregated circuits linking basal ganglia and cortex. Annu Rev Neurosci 9:357-381.

Alexander GÈ, Crutcher MD (1990) Functional architecture of basal ganglia circuits: neural substrates of parallel processing. Trends Neurosci 13:266-271.

Alonso-Frech F, Zamarbide I, Alegre M, Rodriguez-Oroz MC, Guridi J, Manrique M, Valencia M, Artieda J, Obeso JA (2006) Slow oscillatory activity and levodopa-induced dyskinesias in Parkinson's disease. Brain 129:1748-1757.

Amirnovin R, Williams ZM, Cosgrove GR, Eskandar EN (2004) Visually guided movements suppress subthalamic oscillations in Parkinson's disease patients. J Neurosci 24:11302-11306.

Aravamuthan BR, Muthusamy KA, Stein JF, Aziz TZ, Johansen-Berg H (2007) Topography of cortical and subcortical connections of the human pedunculopontine and subthalamic nuclei. Neuroimage 37:694-705.

Astolfi L, Cincotti F, Mattia D, de Vico FF, Lai M, Baccala L, Salinari S, Ursino M, Zavaglia M, Babiloni F (2005) Comparison of different multivariate methods for the estimation of cortical connectivity: simulations and applications to EEG data. Conf Proc IEEE Eng Med Biol Soc 5:4484-4487.

Aziz TZ, Davies L, Stein J, France S (1998) The role of descending basal ganglia connections to the brain stem in parkinsonian akinesia. Br J Neurosurg 12:245-249.

Baccala LA, Sameshima K (2001) Partial directed coherence: a new concept in neural structure determination. Biol Cybern 84:463-474.

Badgaiyan RD, Fischman AJ, Alpert NM (2003) Striatal dopamine release during unrewarded motor task in human volunteers. Neuroreport 14:1421-1424.

Baker SN, Olivier E, Lemon RN (1997) Coherent oscillations in monkey motor cortex and hand muscle EMG show task-dependent modulation. J Physiol 501 (Pt 1):225-241.

Baker SN, Spinks R, Jackson A, Lemon RN (2001) Synchronization in monkey motor cortex during a precision grip task. I. Task-dependent modulation in single-unit synchrony. J Neurophysiol 85:869-885.

Baker SN, Chiu M, Fetz EE (2006) Afferent encoding of central oscillations in the monkey arm. J Neurophysiol 95:3904-3910.

Bar-Gad I, Morris G, Bergman H (2003) Information processing, dimensionality reduction and reinforcement learning in the basal ganglia. Prog Neurobiol 71:439-473.

Behrens TE, Johansen-Berg H, Woolrich MW, Smith SM, Wheeler-Kingshott CA, Boulby PA, Barker GJ, Sillery EL, Sheehan K, Ciccarelli O, Thompson AJ, Brady JM, Matthews PM (2003) Non-invasive mapping of connections between human thalamus and cortex using diffusion imaging. Nat Neurosci 6:750-757

Bergman H, Wichmann T, Karmon B, DeLong MR (1994) The primate subthalamic nucleus. II. Neuronal activity in the MPTP model of parkinsonism. J Neurophysiol 72:507-520.

Bergman H, Feingold A, Nini A, Raz A, Slovin H, Abeles M, Vaadia E (1998) Physiological aspects of information processing in the basal ganglia of normal and parkinsonian primates. Trends Neurosci 21:32-38.

Berke JD, Okatan M, Skurski J, Eichenbaum HB (2004) Oscillatory entrainment of striatal neurons in freely moving rats. Neuron 43:883-896.

Bibbig A, Faulkner HJ, Whittington MA, Traub RD (2001) Self-organized synaptic plasticity contributes to the shaping of gamma and beta oscillations in vitro. J Neurosci 21:9053-9067.

Boecker H, Jankowski J, Ditter P, Scheef L (2008) A role of the basal ganglia and midbrain nuclei for initiation of motor sequences. Neuroimage 39:1356-1369

Boraud T, Bezard E, Bioulac B, Gross CE (2001) Dopamine agonist-induced dyskinesias are correlated to both firing pattern and frequency alterations of pallidal neurones in the MPTP-treated monkey. Brain 124:546-557.

Boraud T, Bezard E, Bioulac B, Gross CE (2002) From single extracellular unit recording in experimental and human Parkinsonism to the development of a functional concept of the role played by the basal ganglia in motor control. Prog Neurobiol 66:265-283.

Boraud T, Brown P, Goldberg J, Graybiel A, Magill P (2005) Oscillations in the Basal Ganglia: The good, the bad, and the unexpected. In: Bolam, J.P., Ingham, C.A., Magill, P.J. (Editors), The Basal Ganglia VIII. Springer Science and Business Media, New York, pp 1-24.

Breit S, Bouali-Benazzouz R, Benabid AL, Benazzouz A (2001) Unilateral lesion of the nigrostriatal pathway induces an increase of neuronal activity of the pedunculopontine nucleus, which is reversed by the lesion of the subthalamic nucleus in the rat. Eur J Neurosci 14:1833-1842.

Brillinger DR (1981) Some aspects of modern population mathematics. Can J Stat 9:173-194.

Brovelli A, Ding M, Ledberg A, Chen Y, Nakamura R, Bressler SL (2004) Beta oscillations in a large-scale sensorimotor cortical network: directional influences revealed by Granger causality. Proc Natl Acad Sci U S A 101:9849-9854.

Brown P, Salenius S, Rothwell JC, Hari R (1998) Cortical correlate of the Piper rhythm in humans. J Neurophysiol 80:2911-2917.

Brown P (2000) Cortical drives to human muscle: the Piper and related rhythms. Prog Neurobiol 60:97-108.

Brown P, Oliviero A, Mazzone P, Insola A, Tonali P, Di L, V (2001) Dopamine dependency of oscillations between subthalamic nucleus and pallidum in Parkinson's disease. J Neurosci 21:1033-1038.

Brown P (2003) Oscillatory nature of human basal ganglia activity: relationship to the pathophysiology of Parkinson's disease. Mov Disord 18:357-363.

Brown P, Williams D (2005) Basal ganglia local field potential activity: character and functional significance in the human. Clin Neurophysiol 116:2510-2519.

Brown P (2006) Bad oscillations in Parkinson's disease. J Neural Transm Suppl27-30.

Brown P (2007) Abnormal oscillatory synchronisation in the motor system leads to impaired movement. Curr Opin Neurobiol 17:656-664.

Brown P, Eusebio A (2008) Paradoxes of functional neurosurgery: clues from basal ganglia recordings. Mov Disord 23:12-20.

Brucke C, Kempf F, Kupsch A, Schneider GH, Krauss JK, Aziz T, Yarrow K, Pogosyan A, Brown P, Kuhn AA (2008) Movement-related synchronization of gamma activity is lateralized in patients with dystonia. Eur J Neurosci 27:2322-2329.

Buzsaki G, Draguhn A (2004) Neuronal oscillations in cortical networks. Science 304:1926-1929.

Canedo A (1997) Primary motor cortex influences on the descending and ascending systems. Prog Neurobiol 51:287-335.

Cassidy M, Mazzone P, Oliviero A, Insola A, Tonali P, Di L, V, Brown P (2002) Movement-related changes in synchronization in the human basal ganglia. Brain 125:1235-1246.

Cassidy M, Brown P (2003) Spectral phase estimates in the setting of multidirectional coupling. J Neurosci Methods 127:95-103.

Cassidy MJ, Brown P (2002) Hidden Markov based autoregressive analysis of stationary and non-stationary electrophysiological signals for functional coupling studies. J Neurosci Methods 116:35-53.

Challis RE, Kitney RI (1991) Biomedical signal processing (in four parts). Part 3. The power spectrum and coherence function. Med Biol Eng Comput 29:225-241.

Chen CC, Brucke C, Kempf F, Kupsch A, Lu CS, Lee ST, Tisch S, Limousin P, Hariz M, Brown P (2006) Deep brain stimulation of the subthalamic nucleus: a two-edged sword. Curr Biol 16:R952-R953.

Chen CC, Pogosyan A, Zrinzo LU, Tisch S, Limousin P, Ashkan K, Yousry T, Hariz MI, Brown P (2006) Intra-operative recordings of local field potentials can help localize the subthalamic nucleus in Parkinson's disease surgery. Exp Neurol 198:214-221.

Chen CC, Litvak V, Gilbertson T, Kuhn A, Lu CS, Lee ST, Tsai CH, Tisch S, Limousin P, Hariz M, Brown P (2007) Excessive synchronization of basal ganglia neurons at 20 Hz slows movement in Parkinson's disease. Exp Neurol 205:214-221.

Chouinard PA, Paus T (2006) The primary motor and premotor areas of the human cerebral cortex. Neuroscientist 12:143-152.

Christou EA, Rudroff T, Enoka JA, Meyer F, Enoka RM (2006) Discharge rate during low-force isometric contractions influences motor unit coherence below 15 Hz but not motor unit synchronization. Exp Brain Res 178(3):285-95.

Cincotta M, Giovannelli F, Borgheresi A, Balestrieri F, Vanni P, Ragazzoni A, Zaccara G, Ziemann U (2006) Surface electromyography shows increased mirroring in Parkinson's disease patients without overt mirror movements. Mov Disord 21(9):1461-5.

Cincotta M, Borgheresi A, Balestrieri F, Giovannelli F, Ragazzoni A, Vanni P, Benvenuti F, Zaccara G, Ziemann U (2006) Mechanisms underlying mirror movements in Parkinson's disease: a transcranial magnetic stimulation study. Mov Disord 21:1019-1025.

Colloca L, Benedetti F, Bergamasco B, Vighetti S, Zibetti M, Ducati A, Lanotte M, Lopiano M (2006) Electroencephalographic responses to intraoperative subthalamic stimulation. Neuroreport 17: 1465–1468.

Connors BW, Amitai Y (1997) Making waves in the neocortex. Neuron 18:347-349.

Conway BA, Halliday DM, Farmer SF, Shahani U, Maas P, Weir AI, Rosenberg JR (1995) Synchronization between motor cortex and spinal motoneuronal pool during the performance of a maintained motor task in man. J Physiol 489 (Pt 3):917-924.

Cooper NR, Croft RJ, Dominey SJ, Burgess AP, Gruzelier JH (2003) Paradox lost? Exploring the role of alpha oscillations during externally vs. internally directed attention and the implications for idling and inhibition hypotheses. Int J Psychophysiol 47:65-74.

Courtemanche R, Fujii N, Graybiel AM (2003) Synchronous, focally modulated beta-band oscillations characterize local field potential activity in the striatum of awake behaving monkeys. J Neurosci 23:11741-11752.

Crone NE, Miglioretti DL, Gordon B, Lesser RP (1998) Functional mapping of human sensorimotor cortex with electrocorticographic spectral analysis. II. Event-related synchronization in the gamma band. Brain 121 (Pt 12):2301-2315.

Crone NE, Miglioretti DL, Gordon B, Sieracki JM, Wilson MT, Uematsu S, Lesser RP (1998) Functional mapping of human sensorimotor cortex with electrocorticographic spectral analysis. I. Alpha and beta event-related desynchronization. Brain 121 (Pt 12):2271-2299.

Deans JK, Powell AD, Jefferys JG (2007) Sensitivity of coherent oscillations in rat hippocampus to AC electric fields. J Physiol 583:555-565.

DeCoteau WE, Thorn C, Gibson DJ, Courtemanche R, Mitra P, Kubota Y, Graybiel AM (2007) Oscillations of local field potentials in the rat dorsal striatum during spontaneous and instructed behaviors. J Neurophysiol 97:3800-3805.

DeCoteau WE, Thorn C, Gibson DJ, Courtemanche R, Mitra P, Kubota Y, Graybiel AM (2007) Learning-related coordination of striatal and hippocampal theta rhythms during acquisition of a procedural maze task. Proc Natl Acad Sci U S A 104:5644-5649.

Devos D, Labyt E, Cassim F, Bourriez JL, Reyns N, Touzet G, Blond S, Guieu JD, Derambure P, Destee A, Defebvre L (2003) Subthalamic stimulation influences postmovement cortical somatosensory processing in Parkinson's disease. Eur J Neurosci 18:1884-1888.

Devos D, Labyt E, Derambure P, Bourriez JL, Cassim F, Reyns N, Blond S, Guieu JD, Destee A, Defebvre L (2004) Subthalamic nucleus stimulation modulates motor cortex oscillatory activity in Parkinson's disease. Brain 127:408-419.

Devos D, Szurhaj W, Reyns N, Labyt E, Houdayer E, Bourriez JL, Cassim F, Krystkowiak P, Blond S, Destee A, Derambure P, Defebvre L (2006) Predominance of the contralateral movement-related activity in the subthalamo-cortical loop. Clin Neurophysiol 117:2315-2327.

Donoghue JP, Sanes JN, Hatsopoulos NG, Gaal G (1998) Neural discharge and local field potential oscillations in primate motor cortex during voluntary movements. J Neurophysiol 79:159-173.

Dostrovsky J, Bergman H (2004) Oscillatory activity in the basal ganglia--relationship to normal physiology and pathophysiology. Brain 127:721-722.

Doyle LM, Kuhn AA, Hariz M, Kupsch A, Schneider GH, Brown P (2005a) Levodopa-induced modulation of subthalamic beta oscillations during self-paced movements in patients with Parkinson's disease. Eur J Neurosci 21:1403-1412.

Doyle LM, Yarrow K, Brown P (2005b) Lateralization of event-related beta desynchronization in the EEG during pre-cued reaction time tasks. Clin Neurophys 116: 1879-1888.

Draganski B, Kherif F, Kloppel S, Cook PA, Alexander DC, Parker GJ, Deichmann R, Ashburner J, Frackowiak RS (2008) Evidence for segregated and integrative connectivity patterns in the human Basal Ganglia. J Neurosci 28:7143-7152

Dum RP, Strick PL (2002) Motor areas in the frontal lobe of the primate. Physiol Behav 77:677-682.

Eeckman FH, Freeman WJ (1990) Correlations between unit firing and EEG in the rat olfactory system. Brain Res 528:238-244.

Engel AK, Fries P, Singer W (2001) Dynamic predictions: oscillations and synchrony in top-down processing. Nat Rev Neurosci 2:704-716.

Engel AK, Singer W (2001) Temporal binding and the neural correlates of sensory awareness. Trends Cogn Sci 5:16-25.

Eusebio A, Chen CC, Lu CS, Lee ST, Tsai CH, Limousin P, Hariz M, Brown P (2008) Effects of low-frequency stimulation of the subthalamic nucleus on movement in Parkinson's disease. Exp Neurol 209:125-130.

Evarts EV (1965) Relation of discharge frequency to conduction velocity in pyramidal tract neurons. J Neurophysiol 28:216-228.

Evarts EV (1966) Pyramidal tract activity associated with a conditioned hand movement in the monkey. J Neurophysiol 29:1011-1027.

Farge, M. Wavelet Transforms and Their Applications to Turbulence. Annu Rev Fluid Mech 24, 395-457. 1992.

Farmer SF, Bremner FD, Halliday DM, Rosenberg JR, Stephens JA (1993) The frequency content of common synaptic inputs to motoneurones studied during voluntary isometric contraction in man. J Physiol 470:127-155.

Fein G, Raz J, Brown FF, Merrin EL (1988) Common reference coherence data are confounded by power and phase effects. Electroencephalogr Clin Neurophysiol 69:581-584.

Fetz EE, Chen D, Murthy VN, Matsumura M (2000) Synaptic interactions mediating synchrony and oscillations in primate sensorimotor cortex. J Physiol Paris 94:323-331.

Florian G, Andrew C, Pfurtscheller G (1998) Do changes in coherence always reflect changes in functional coupling? Electroencephalogr Clin Neurophysiol 106:87-91.

Foffani G, Priori A, Egidi M, Rampini P, Tamma F, Caputo E, Moxon KA, Cerutti S, Barbieri S (2003) 300-Hz subthalamic oscillations in Parkinson's disease. Brain 126:2153-2163.

Foffani G, Ardolino G, Rampini P, Tamma F, Caputo E, Egidi M, Cerutti S, Barbieri S, Priori A (2005) Physiological recordings from electrodes implanted in the basal ganglia for deep brain stimulation in Parkinson's disease. the relevance of fast subthalamic rhythms. Acta Neurochir Suppl 93:97-99.

Foffani G, Bianchi AM, Baselli G, Priori A (2005) Movement-related frequency modulation of beta oscillatory activity in the human subthalamic nucleus. J Physiol 568:699-711.

Foffani G, Ardolino G, Meda B, Egidi M, Rampini P, Caputo E, Baselli G, Priori A (2005) Altered subthalamo-pallidal synchronisation in parkinsonian dyskinesias. J Neurol Neurosurg Psychiatry 76:426-428.

Fogelson N, Pogosyan A, Kuhn AA, Kupsch A, Van BG, Speelman H, Tijssen M, Quartarone A, Insola A, Mazzone P, Di L, V, Limousin P, Brown P (2005) Reciprocal interactions between oscillatory activities of different frequencies in the subthalamic region of patients with Parkinson's disease. Eur J Neurosci 22:257-266.

Fogelson N, Williams D, Tijssen M, Van BG, Speelman H, Brown P (2006) Different functional loops between cerebral cortex and the subthalmic area in Parkinson's disease. Cereb Cortex 16:64-75.

Freiwald WA, Kreiter AK, Singer W (2001) Synchronization and assembly formation in the visual cortex. Prog Brain Res 130:111-140.

Freund HJ (1983) Motor unit and muscle activity in voluntary motor control. Physiol Rev 63:387-436.

Fries P (2005) A mechanism for cognitive dynamics: neuronal communication through neuronal coherence. Trends Cogn Sci 9:474-480.

Friston, K. J., Stephan, K. M., and Frackowiak, R. S. J. (1997) Transient phase-locking and dynamic correlations: are they the same thing? Hum Brain Map 5, 48-57.

Fukae J, Mizuno Y, Hattori N (2007) Mitochondrial dysfunction in Parkinson's disease. Mitochondrion 7:58-62.

Garcia-Rill E, Skinner RD (1988) Modulation of rhythmic function in the posterior midbrain. Neuroscience 27:639-654.

Gatev P, Darbin O, Wichmann T (2006) Oscillations in the basal ganglia under normal conditions and in movement disorders. Mov Disord 21:1566-1577.

Gatev P, Darbin O, Wichmann T (2006) Oscillations in the basal ganglia under normal conditions and in movement disorders. Mov Disord 21:1566-1577.

Gibbs J, Harrison LM, Stephens JA (1995) Organization of inputs to motoneurone pools in man. J Physiol 485 (Pt 1):245-256.

Giladi N, Hausdorff JM (2006) The role of mental function in the pathogenesis of freezing of gait in Parkinson's disease. J Neurol Sci 248:173-176.

Gilbertson T, Lalo E, Doyle L, Di L, V, Cioni B, Brown P (2005) Existing motor state is favored at the expense of new movement during 13-35 Hz oscillatory synchrony in the human corticospinal system. J Neurosci 25:7771-7779.

Goerendt IK, Messa C, Lawrence AD, Grasby PM, Piccini P, Brooks DJ (2003) Dopamine release during sequential finger movements in health and Parkinson's disease: a PET study. Brain 126:312-325.

Granger J (1969) Investigating causal relations by econometric models and cross-spectral methods. Econometrica 37:424-438.

Gray CM, McCormick DA (1996) Chattering cells: superficial pyramidal neurons contributing to the generation of synchronous oscillations in the visual cortex. Science 274:109-113.

Grosse P, Cassidy MJ, Brown P (2002) EEG-EMG, MEG-EMG and EMG-EMG frequency analysis: physiological principles and clinical applications. Clin Neurophysiol 113:1523-1531.

Gutfreund Y, Yarom Y, Segev I (1995) Subthreshold oscillations and resonant frequency in guinea-pig cortical neurons: physiology and modelling. J Physiol 483 (Pt 3):621-640.

Halliday DM, Rosenberg JR, Amjad AM, Breeze P, Conway BA, Farmer SF (1995) A framework for the analysis of mixed time series/point process data--theory and application to the study of physiological tremor, single motor unit discharges and electromyograms. Prog Biophys Mol Biol 64:237-278.

Halliday DM, Conway BA, Farmer SF, Rosenberg JR (1999) Load-independent contributions from motor-unit synchronization to human physiological tremor. J Neurophysiol 82:664-675.

Hammond C, Bergman H, Brown P (2007) Pathological synchronization in Parkinson's disease: networks, models and treatments. Trends Neurosci 30:357-364.

Hariz MI, Krack P, Melvill R, Jorgensen JV, Hamel W, Hirabayashi H, Lenders M, Wesslen N, Tengvar M, Yousry TA (2003) A quick and universal method for stereotactic

visualization of the subthalamic nucleus before and after implantation of deep brain stimulation electrodes. Stereotact Funct Neurosurg 80:96-101.

Hassler R, Dieckmann G (1967) Arrest reaction, delayed inhibition and unusual gaze behavior resulting from stimulation of the putamen in awake, unrestrained cats. Brain Res 5:504-508.

Hjorth B (1975) An on-line transformation of EEG scalp potentials into orthogonal source derivations. Electroencephalogr Clin Neurophysiol 39:526-530.

Hoover JE, Strick PL (1999) The organization of cerebellar and basal ganglia outputs to primary motor cortex as revealed by retrograde transneuronal transport of herpes simplex virus type 1. J Neurosci 19:1446-1463.

Hoshi E, Tanji J (2007) Distinctions between dorsal and ventral premotor areas: anatomical connectivity and functional properties. Curr Opin Neurobiol 17:234-242.

Hutcheon B, Miura RM, Puil E (1996) Subthreshold membrane resonance in neocortical neurons. J Neurophysiol 76:683-697.

Hutcheon B, Yarom Y (2000) Resonance, oscillation and the intrinsic frequency preferences of neurons. Trends Neurosci 23:216-222.

Jenkins IH, Jahanshahi M, Jueptner M, Passingham RE, Brooks DJ (2000) Self-initiated versus externally triggered movements. II. The effect of movement predictability on regional cerebral blood flow. Brain 123 (Pt 6):1216-1228.

Jenkinson N, Nandi D, Miall RC, Stein JF, Aziz TZ (2004) Pedunculopontine nucleus stimulation improves akinesia in a Parkinsonian monkey. Neuroreport 15:2621-2624.

Jenkinson N, Nandi D, Oram R, Stein JF, Aziz TZ (2006) Pedunculopontine nucleus electric stimulation alleviates akinesia independently of dopaminergic mechanisms. Neuroreport 17:639-641.

Jenner P (2003) Oxidative stress in Parkinson's disease. Ann Neurol 53 Suppl 3:S26-S36

Jensen O, Gelfand J, Kounios J, Lisman JE (2002) Oscillations in the alpha band (9-12 Hz) increase with memory load during retention in a short-term memory task. Cereb Cortex 12:877-882.

Kaminski MJ, Blinowska KJ (1991) A new method of the description of the information flow in the brain structures. Biol Cybern 65:203-210.

Kempf F, Kuhn AA, Kupsch A, Brucke C, Weise L, Schneider GH, Brown P (2007) Premovement activities in the subthalamic area of patients with Parkinson's disease and their dependence on task. Eur J Neurosci 25:3137-3145.

Kilner JM, Baker SN, Salenius S, Jousmaki V, Hari R, Lemon RN (1999) Task-dependent modulation of 15-30 Hz coherence between rectified EMGs from human hand and forearm muscles. J Physiol 516 (Pt 2):559-570.

Kilner JM, Baker SN, Salenius S, Hari R, Lemon RN (2000) Human cortical muscle coherence is directly related to specific motor parameters. J Neurosci 20:8838-8845.

Klein C, Schlossmacher MG (2007) Parkinson disease, 10 years after its genetic revolution: multiple clues to a complex disorder. Neurology 69:2093-2104.

Klimesch W (1999) EEG alpha and theta oscillations reflect cognitive and memory performance: a review and analysis. Brain Res Brain Res Rev 29:169-195.

Kojima J, Yamaji Y, Matsumura M, Nambu A, Inase M, Tokuno H, Takada M, Imai H (1997) Excitotoxic lesions of the pedunculopontine tegmental nucleus produce contralateral hemiparkinsonism in the monkey. Neurosci Lett 226:111-114.

Korzeniewska A, Manczak M, Kaminski M, Blinowska KJ, Kasicki S (2003) Determination of information flow direction among brain structures by a modified directed transfer function (dDTF) method. J Neurosci Methods 125:195-207.

Kraft E, Chen AW, Flaherty AW, Blood AJ, Kwong KK, Jenkins BG (2007) The role of the basal ganglia in bimanual coordination. Brain Res 1151:62-73

Kuhn AA, Williams D, Kupsch A, Limousin P, Hariz M, Schneider GH, Yarrow K, Brown P (2004) Event-related beta desynchronization in human subthalamic nucleus correlates with motor performance. Brain 127:735-746.

Kuhn AA, Trottenberg T, Kivi A, Kupsch A, Schneider GH, Brown P (2005) The relationship between local field potential and neuronal discharge in the subthalamic nucleus of patients with Parkinson's disease. Exp Neurol 194:212-220.

Kuhn AA, Doyle L, Pogosyan A, Yarrow K, Kupsch A, Schneider GH, Hariz MI, Trottenberg T, Brown P (2006) Modulation of beta oscillations in the subthalamic area during motor imagery in Parkinson's disease. Brain 129:695-706.

Kuhn AA, Kupsch A, Schneider GH, Brown P (2006) Reduction in subthalamic 8-35 Hz oscillatory activity correlates with clinical improvement in Parkinson's disease. Eur J Neurosci 23:1956-1960.

Kurtzer I, Herter TM, Scott SH (2005) Random change in cortical load representation suggests distinct control of posture and movement. Nat Neurosci 8(4):498-504.

Lai YY, Siegel JM (1990) Muscle tone suppression and stepping produced by stimulation of midbrain and rostral pontine reticular formation. J Neurosci 10:2727-2734.

Lalo E, Gilbertson T, Doyle L, Lazzaro VD, Cioni B, Brown P (2006) Phasic increases in cortical beta activity are associated with alterations in sensory processing in the human. Exp Brain Res 177(1):137-45.

Leblois A, Boraud T, Meissner W, Bergman H, Hansel D (2006) Competition between feedback loops underlies normal and pathological dynamics in the basal ganglia. J Neurosci 26:3567-3583.

Leblois A, Meissner W, Bioulac B, Gross CE, Hansel D, Boraud T (2007) Late emergence of synchronized oscillatory activity in the pallidum during progressive Parkinsonism. Eur J Neurosci 26:1701-1713.

Leonard CT (1998) The neuroscience of human movement. Mosby, St. Louis, MO, USA.

Levy R, Hutchison WD, Lozano AM, Dostrovsky JO (2000) High-frequency synchronization of neuronal activity in the subthalamic nucleus of parkinsonian patients with limb tremor. J Neurosci 20:7766-7775.

Levy R, Ashby P, Hutchison WD, Lang AE, Lozano AM, Dostrovsky JO (2002) Dependence of subthalamic nucleus oscillations on movement and dopamine in Parkinson's disease. Brain 125:1196-1209.

Li X, Yao X, Fox J, Jefferys JG (2006) Interaction dynamics of neuronal oscillations analysed using wavelet transforms. J Neurosci Methods 160(1):178-85.

Limousin P, Pollak P, Benazzouz A, Hoffmann D, Broussolle E, Perret JE, Benabid AL (1995) Bilateral subthalamic nucleus stimulation for severe Parkinson's disease. Mov Disord 10:672-674.

Llinas RR, Grace AA, Yarom Y (1991) In vitro neurons in mammalian cortical layer 4 exhibit intrinsic oscillatory activity in the 10- to 50-Hz frequency range. Proc Natl Acad Sci U S A 88:897-901.

Loukas C, Brown P (2004) Online prediction of self-paced hand-movements from subthalamic activity using neural networks in Parkinson's disease. J Neurosci Methods 137:193-205.

Magarinos-Ascone C, Buno W, Garcia-Austt E (1992) Activity in monkey substantia nigra neurons related to a simple learned movement. Exp Brain Res 88:283-291.

Magill PJ, Bolam JP, Bevan MD (2000) Relationship of activity in the subthalamic nucleus-globus pallidus network to cortical electroencephalogram. J Neurosci 20:820-833.

Magill PJ, Bolam JP, Bevan MD (2001) Dopamine regulates the impact of the cerebral cortex on the subthalamic nucleus-globus pallidus network. Neuroscience 106:313-330.

Magill PJ, Sharott A, Bolam JP, Brown P (2004) Brain state-dependency of coherent oscillatory activity in the cerebral cortex and basal ganglia of the rat. J Neurophysiol 92:2122-2136.

Magill PJ, Sharott A, Bolam JP, Brown P (2004) Delayed synchronization of activity in cortex and subthalamic nucleus following cortical stimulation in the rat. J Physiol 574:929-946.

Marceglia S, Foffani G, Bianchi AM, Baselli G, Tamma F, Egidi M, Priori A (2006) Dopamine-dependent non-linear correlation between subthalamic rhythms in Parkinson's disease. J Physiol 571:579-591.

Marsden JF, Ashby P, Limousin-Dowsey P, Rothwell JC, Brown P (2000) Coherence between cerebellar thalamus, cortex and muscle in man: cerebellar thalamus interactions. Brain 123 (Pt 7):1459-1470.

Marsden JF, Limousin-Dowsey P, Ashby P, Pollak P, Brown P (2001) Subthalamic nucleus, sensorimotor cortex and muscle interrelationships in Parkinson's disease. Brain 124:378-388.

Mattay VS, Weinberger DR (1999) Organization of the human motor system as studied by functional magnetic resonance imaging. Eur J Radiol 30:105-114.

Martin JP (1967) The basal ganglia and posture. Lippincott, Philadelphia.

Masimore B, Schmitzer-Torbert NC, Kakalios J, Redish AD (2005) Transient striatal gamma local field potentials signal movement initiation in rats. Neuroreport 16:2021-2024.

Matsumura M (2005) The pedunculopontine tegmental nucleus and experimental parkinsonism. A review. J Neurol 252 Suppl 4:IV5-IV12.

Maurice N, Deniau JM, Degos B, Windels F, Carcenac C, Poupard A, Savasta M (2005) High Frequency Stimulation of the Subthalamic Nucleus. In: Bolam JP, Ingham CA, Magill PJ (Editors), The Basal Ganglia VIII. Springer Science and Business Media, New York, pp 243-253.

Mazzone P, Lozano A, Stanzione P, Galati S, Scarnati E, Peppe A, Stefani A (2005) Implantation of human pedunculopontine nucleus: a safe and clinically relevant target in Parkinson's disease. Neuroreport 16:1877-1881.

Mazzone P, Insola A, Lozano A, Galati S, Scarnati E, Peppe A, Stanzione P, Stefani A (2007) Peripeduncular and pedunculopontine nuclei: a dispute on a clinically relevant target. Neuroreport 18:1407-1408.

McAuley JH, Rothwell JC, Marsden CD (1997) Frequency peaks of tremor, muscle vibration and electromyographic activity at 10 Hz, 20 Hz and 40 Hz during human finger

muscle contraction may reflect rhythmicities of central neural firing. Exp Brain Res 114:525-541.

McFarland NR, Haber SN (2000) Convergent inputs from thalamic motor nuclei and frontal cortical areas to the dorsal striatum in the primate. J Neurosci 20:3798-3813.

Meissner W, Leblois A, Hansel D, Bioulac B, Gross CE, Benazzouz A, Boraud T (2005) Subthalamic high frequency stimulation resets subthalamic firing and reduces abnormal oscillations. Brain 128:2372-2382.

Mena-Segovia J, Giordano M (2003) Striatal dopaminergic stimulation produces c-Fos expression in the PPT and an increase in wakefulness. Brain Res 986:30-38.

Mena-Segovia J, Bolam JP, Magill PJ (2004) Pedunculopontine nucleus and basal ganglia: distant relatives or part of the same family? Trends Neurosci 27:585-588.

Mena-Segovia J, Ross H, Magill P, Bolam J (2005) The Pedunculopontine Nucleus. In: Bolam JP, Ingham CA, Magill PJ (Editors), The Basal Ganglia VIII. Springer Science and Business Media, New York, pp 533-544.

Mima T, Hallett M (1999) Electroencephalographic analysis of cortico-muscular coherence: reference effect, volume conduction and generator mechanism. Clin Neurophysiol 110:1892-1899.

Mima T, Steger J, Schulman AE, Gerloff C, Hallett M (2000) Electroencephalographic measurement of motor cortex control of muscle activity in humans. Clin Neurophysiol 111:326-337.

Mima T, Matsuoka T, Hallett M (2001) Information flow from the sensorimotor cortex to muscle in humans. Clin Neurophysiol 112:122-126.

Mink JW (2003) The basal ganglia. In: Squire LR, Bloom FE, Connell SK, Roberts JL, Spitzer NC, Zigmond MJ (Editors), Fundamental Neuroscience. Academic Press, CA, USA, pp 816-834.

Mitra PP, Pesaran B (1999) Analysis of dynamic brain imaging data. Biophys J 76:691-708.

Moritz CH, Meyerand ME, Cordes D, Haughton VM (2000) Functional MR imaging activation after finger tapping has a shorter duration in the basal ganglia than in the sensorimotor cortex. AJNR Am J Neuroradiol 21:1228-1234.

Moritz CT, Christou EA, Meyer FG, Enoka RM (2005) Coherence at 16-32 Hz can be caused by short-term synchrony of motor units. J Neurophysiol 94:105-118.

Moro E, Esselink RJ, Xie J, Hommel M, Benabid AL, Pollak P. (2002) The impact on Parkinson's disease of electrical parameter settings in STN stimulation. Neurology 59:706–713.

Muir RB, Lemon RN (1983) Corticospinal neurons with a special role in precision grip. Brain Res 261:312-316.

Murthy VN, Fetz EE (1992) Coherent 25- to 35-Hz oscillations in the sensorimotor cortex of awake behaving monkeys. Proc Natl Acad Sci U S A 89:5670-5674.

Murthy VN, Fetz EE (1996) Synchronization of neurons during local field potential oscillations in sensorimotor cortex of awake monkeys. J Neurophysiol 76:3968-3982.

Murthy VN, Fetz EE (1996) Oscillatory activity in sensorimotor cortex of awake monkeys: synchronization of local field potentials and relation to behavior. J Neurophysiol 76:3949-3967.

Nambu A (2004) A new dynamic model of the cortico-basal ganglia loop. Prog Brain Res 143:461-466.

Nambu A, Tachibana Y, Kaneda K, Tokuno H, Takada M (2005) Dynamic Model of Basal Ganglia Functions and Parkinson's Disease. In: Bolam JP, Ingham CA, Magill PJ (Editors), The Basal Ganglia VIII. Springer Science and Business Media, New York, pp 307-312.

Nandi D, Aziz TZ, Giladi N, Winter J, Stein JF (2002a) Reversal of akinesia in experimental parkinsonism by GABA antagonist microinjections in the pedunculopontine nucleus. Brain 125:2418-2430.

Nandi D, Liu X, Winter JL, Aziz TZ, Stein JF (2002b) Deep brain stimulation of the pedunculopontine region in the normal non-human primate. J Clin Neurosci 9:170-174.

Nicola SM, Surmeier J, Malenka RC (2000) Dopaminergic modulation of neuronal excitability in the striatum and nucleus accumbens. Annu Rev Neurosci 23:185-215.

Obeso JA, Rodriguez-Oroz M, Marin C, Alonso F, Zamarbide I, Lanciego JL, Rodriguez-Diaz M (2004) The origin of motor fluctuations in Parkinson's disease: importance of dopaminergic innervation and basal ganglia circuits. Neurology 62:S17-S30.

Okuma Y (2006) Freezing of gait in Parkinson's disease. J Neurol 253 Suppl 7:VII27-VII32.

Oldfield RC (1971) The assessment and analysis of handedness: the Edinburgh inventory. Neuropsychologia 9:97-113.

Pahapill PA, Lozano AM (2000) The pedunculopontine nucleus and Parkinson's disease. Brain 123 (Pt 9):1767-1783.

Palva S, Palva JM (2007) New vistas for alpha-frequency band oscillations. Trends Neurosci 30:150-158.

Paradiso G, Cunic D, Saint-Cyr JA, Hoque T, Lozano AM, Lang AE, Chen R (2004) Involvement of human thalamus in the preparation of self-paced movement. Brain 127:2717-2731.

Parent A, Hazrati LN (1995) Functional anatomy of the basal ganglia. II. The place of subthalamic nucleus and external pallidum in basal ganglia circuitry. Brain Res Brain Res Rev 20:128-154.

Parent A, Hazrati LN (1995) Functional anatomy of the basal ganglia. I. The cortico-basal ganglia-thalamo-cortical loop. Brain Res Brain Res Rev 20:91-127.

Passingham RE, Stephan KE, Kotter R (2002) The anatomical basis of functional localization in the cortex. Nat Rev Neurosci 3:606-616.

Pavese N, Evans AH, Tai YF, Hotton G, Brooks DJ, Lees AJ, Piccini P (2006) Clinical correlates of levodopa-induced dopamine release in Parkinson disease: a PET study. Neurology 67:1612-1617

Penny WD, Harrison L (2006) Multivariate autoregressive models. In K. Friston, J. Ashburner, S. Kiebel, T. Nichols, and W. Penny (editors) Statistical Parametric Mapping: The analysis of functional brain images. Elsevier, London, UK.

Penny WD, Roberts SJ (2002) Bayesian Multivariate Autoregresive Models with structured priors. IEE Proceedings on Vision, Image and Signal Processing 149:33-41.

Pfurtscheller G (1981) Central beta rhythm during sensorimotor activities in man. Electroencephalogr Clin Neurophysiol 51:253-264.

Pfurtscheller G (1989) Functional topography during sensorimotor activation studied with event-related desynchronization mapping. J Clin Neurophysiol 6:75-84.

Pfurtscheller G, Neuper C, Kalcher J (1993) 40-Hz oscillations during motor behavior in man. Neurosci Lett 164:179-182.

Pfurtscheller G, Flotzinger D, Neuper C (1994) Differentiation between finger, toe and tongue movement in man based on 40 Hz EEG. Electroencephalogr Clin Neurophysiol 90:456-460.

Pfurtscheller G, Stancak A, Jr., Neuper C (1996) Post-movement beta synchronization. A correlate of an idling motor area? Electroencephalogr Clin Neurophysiol 98:281-293.

Pfurtscheller G, Pichler-Zalaudek K, Ortmayr B, Diez J, Reisecker F (1998) Postmovement beta synchronization in patients with Parkinson's disease. J Clin Neurophysiol 15:243-250.

Pfurtscheller G, Lopes da Silva FH (1999) Event-related EEG/MEG synchronization and desynchronization: basic principles. Clin Neurophysiol 110:1842-1857.

Pfurtscheller G, Graimann B, Huggins JE, Levine SP, Schuh LA (2003) Spatiotemporal patterns of beta desynchronization and gamma synchronization in corticographic data during self-paced movement. Clin Neurophysiol 114:1226-1236.

Picard N, Strick PL (2001) Imaging the premotor areas. Curr Opin Neurobiol 11:663-672.

Plaha P, Gill SS (2005) Bilateral deep brain stimulation of the pedunculopontine nucleus for Parkinson's disease. Neuroreport 16:1883-1887.

Pogosyan A, Kuhn AA, Trottenberg T, Schneider GH, Kupsch A, Brown P (2006) Elevations in local gamma activity are accompanied by changes in the firing rate and

information coding capacity of neurons in the region of the subthalamic nucleus in Parkinson's disease. Exp Neurol 202:271-279.

Porter R, Lemon RG (1993) Corticospinal function and voluntary movement. Oxford, Oxford University Press, UK.

Priori A, Foffani G, Pesenti A, Bianchi A, Chiesa V, Baselli G, Caputo E, Tamma F, Rampini P, Egidi M, Locatelli M, Barbieri S, Scarlato G (2002) Movement-related modulation of neural activity in human basal ganglia and its L-DOPA dependency: recordings from deep brain stimulation electrodes in patients with Parkinson's disease. Neurol Sci 23 Suppl 2:S101-S102.

Priori A, Foffani G, Pesenti A, Tamma F, Bianchi AM, Pellegrini M, Locatelli M, Moxon KA, Villani RM (2004) Rhythm-specific pharmacological modulation of subthalamic activity in Parkinson's disease. Exp Neurol 189:369-379.

Puil E, Meiri H, Yarom Y (1994) Resonant behavior and frequency preferences of thalamic neurons. J Neurophysiol 71:575-582.

Quinn NP (2003) Movement disorders. In: Fowler TJ, Scadding JW (Editors), Clinical Neurology. Arnold, London, pp 225-245.

Raz A, Vaadia E, Bergman H (2000) Firing patterns and correlations of spontaneous discharge of pallidal neurons in the normal and the tremulous 1-methyl-4-phenyl-1,2,3,6-tetrahydropyridine vervet model of parkinsonism. J Neurosci 20:8559-8571.

Reichenbach JR, Feiwell R, Kuppusamy K, Bahn M, Haacke EM (1998) Functional magnetic resonance imaging of the basal ganglia and cerebellum using a simple motor paradigm. Magn Reson Imaging 16:281-287.

Riddle CN, Baker SN (2005) Manipulation of peripheral neural feedback loops alters human corticomuscular coherence. J Physiol 566:625-639.

Riddle CN, Baker SN (2006) Digit displacement, not object compliance, underlies task dependent modulations in human corticomuscular coherence. Neuroimage 33:618-627.

Richter W, Andersen PM, Georgopoulos AP, Kim SG (1997) Sequential activity in human motor areas during a delayed cued finger movement task studied by time-resolved fMRI. Neuroreport 8:1257-1261.

Rizzolatti G, Luppino G (2001) The cortical motor system. Neuron 31:889-901.

Rubia K, Russell T, Overmeyer S, Brammer MJ, Bullmore ET, Sharma T, Simmons A, Williams SC, Giampietro V, Andrew CM, Taylor E (2001) Mapping motor inhibition: conjunctive brain activations across different versions of go/no-go and stop tasks. Neuroimage 13:250-261.

Rubino D, Robbins KA, Hatsopoulos NG (2006) Propagating waves mediate information transfer in the motor cortex. Nat Neurosci 9:1549-1557.

Sadato N, Ibanez V, Deiber MP, Campbell G, Leonardo M, Hallett M (1996) Frequency-dependent changes of regional cerebral blood flow during finger movements. J Cereb Blood Flow Metab 16:23-33.

Salenius S, Salmelin R, Neuper C, Pfurtscheller G, Hari R (1996) Human cortical 40 Hz rhythm is closely related to EMG rhythmicity. Neurosci Lett 213:75-78.

Salenius S, Portin K, Kajola M, Salmelin R, Hari R (1997) Cortical control of human motoneuron firing during isometric contraction. J Neurophysiol 77:3401-3405.

Salenius S, Avikainen S, Kaakkola S, Hari R, Brown P (2002) Defective cortical drive to muscle in Parkinson's disease and its improvement with levodopa. Brain 125:491-500.

Samar VJ, Bopardikar A, Rao R, Swartz K (1999) Wavelet analysis of neuroelectric waveforms: a conceptual tutorial. Brain Lang 66:7-60.

Samuel M, Williams SC, Leigh PN, Simmons A, Chakraborti S, Andrew CM, Friston KJ, Goldstein LH, Brooks DJ (1998) Exploring the temporal nature of hemodynamic responses of cortical motor areas using functional MRI. Neurology 51:1567-1575.

Sanes JN, Donoghue JP (1993) Oscillations in local field potentials of the primate motor cortex during voluntary movement. Proc Natl Acad Sci U S A 90:4470-4474.

Sanes JN, Donoghue JP (2000) Plasticity and primary motor cortex. Annu Rev Neurosci 23:393-415.

Sauve K (1999) Gamma-band synchronous oscillations: recent evidence regarding their functional significance. Conscious Cogn 8:213-224.

Schatton W, Lyssy, R. (2000) Parkinsonism Treatment. Ullmann's Encyclopedia of Industrial Chemistry, 1-21.

Schieber MH, Baker JF (2003) Descending control of movement. In: Squire LR, Bloom FE, Connell SK, Roberts JL, Spitzer NC, Zigmond MJ (Editors), Fundamental Neuroscience. Academic Press, CA, USA, pp 792-813.

Schnitzler A, Gross J (2005) Normal and pathological oscillatory communication in the brain. Nat Rev Neurosci 6:285-296.

Schnitzler A, Gross J (2005) Normal and pathological oscillatory communication in the brain. Nat Rev Neurosci 6:285-296.

Schoffelen JM, Oostenveld R, Fries P (2005) Neuronal coherence as a mechanism of effective corticospinal interaction. Science 308:111-113.

Schoffelen JM, Oostenveld R, Fries P (2005) Neuronal coherence as a mechanism of effective corticospinal interaction. Science 308:111-113.

Sharott A, Magill PJ, Harnack D, Kupsch A, Meissner W, Brown P (2005) Dopamine depletion increases the power and coherence of beta-oscillations in the cerebral cortex and subthalamic nucleus of the awake rat. Eur J Neurosci 21:1413-1422.

Silberstein P, Kuhn AA, Kupsch A, Trottenberg T, Krauss JK, Wohrle JC, Mazzone P, Insola A, Di L, V, Oliviero A, Aziz T, Brown P (2003) Patterning of globus pallidus local field potentials differs between Parkinson's disease and dystonia. Brain 126:2597-2608.

Silberstein P, Oliviero A, Di L, V, Insola A, Mazzone P, Brown P (2005) Oscillatory pallidal local field potential activity inversely correlates with limb dyskinesias in Parkinson's disease. Exp Neurol 194:523-529.

Smith Y, Kieval JZ (2000) Anatomy of the dopamine system in the basal ganglia. Trends Neurosci 23:S28-S33.

Sochurkova D, Rektor I (2003) Event-related desynchronization/synchronization in the putamen. An SEEG case study. Exp Brain Res 149:401-404.

Stefani A, Lozano AM, Peppe A, Stanzione P, Galati S, Tropepi D, Pierantozzi M, Brusa L, Scarnati E, Mazzone P (2007) Bilateral deep brain stimulation of the pedunculopontine and subthalamic nuclei in severe Parkinson's disease. Brain 130:1596-1607.

Strafella AP, Lozano AM, Ballanger B, Poon YY, Lang AE, Moro E (2008) rCBF changes associated with PPN stimulation in a patient with Parkinson's disease: A PET study. Mov Disord. In Press

Strambi SK, Rossi B, De MG, Sello S (2004) Effect of medication in Parkinson's disease: a wavelet analysis of EMG signals. Med Eng Phys 26:279-290.

Tallon-Baudry C, Bertrand O (1999) Oscillatory gamma activity in humans and its role in object representation. Trends Cogn Sci 3:151-162.

Tatton WG, Lee RG (1975) Evidence for abnormal long-loop reflexes in rigid parkinsonian patients. Brain Res 100:671-676.

Terman D, Rubin JE, Yew AC, Wilson CJ (2002) Activity patterns in a model for the subthalamopallidal network of the basal ganglia. J Neurosci 22:2963-2976.

Tisch S, Silberstein P, Limousin-Dowsey P, Jahanshahi M (2004) The basal ganglia: anatomy, physiology, and pharmacology. Psychiatr Clin North Am 27:757-799.

Toma K, Nakai T (2002) Functional MRI in human motor control studies and clinical applications. Magn Reson Med Sci 1:109-120.

Torrence, C and Combo, G. P. (1998) A practical guide to wavelet analysis. Bull Am Meteorol Soc 79: 61-78.

Trottenberg T, Fogelson N, Kuhn AA, Kivi A, Kupsch A, Schneider GH, Brown P (2006) Subthalamic gamma activity in patients with Parkinson's disease. Exp Neurol 200:56-65.

Trottenberg T, Kupsch A, Schneider GH, Brown P, Kuhn AA (2007) Frequency-dependent distribution of local field potential activity within the subthalamic nucleus in Parkinson's disease. Exp Neurol 205:287-291.

Ward LM (2003) Synchronous neural oscillations and cognitive processes. Trends Cogn Sci 7:553-559.

Weinberger M, Mahant N, Hutchison WD, Lozano AM, Moro E, Hodaie M, Lang AE, Dostrovsky JO (2006) Beta oscillatory activity in the subthalamic nucleus and its relation to dopaminergic response in Parkinson's disease. J Neurophysiol 96:3248-3256.

Weinberger M, Hamani C, Hutchison WD, Moro E, Lozano AM, Dostrovsky JO (2008) Pedunculopontine nucleus microelectrode recordings in movement disorder patients. Exp Brain Res. In Press

Wennberg RA, Lozano AM (2003) Intracranial volume conduction of cortical spikes and sleep potentials recorded with deep brain stimulating electrodes. Clin Neurophysiol 114:1403-1418.

Whittington MA, Traub RD (2003) Interneuron diversity series: inhibitory interneurons and network oscillations in vitro. Trends Neurosci 26:676-682.

Wichmann T, Bergman H, DeLong MR (1994) The primate subthalamic nucleus. III. Changes in motor behavior and neuronal activity in the internal pallidum induced by subthalamic inactivation in the MPTP model of parkinsonism. J Neurophysiol 72:521-530.

Wichmann T, DeLong MR (2003) Functional neuroanatomy of the basal ganglia in Parkinson's disease. Adv Neurol 91:9-18.

Wichmann T, DeLong MR (2003) Functional neuroanatomy of the basal ganglia in Parkinson's disease. Adv Neurol 91:9-18.

Wichmann, T., Gatev, P. G., and Kliem, M. A. (2006) Neuronal discharge in the basal ganglia is correlated with EEG in normal and Parkinsonian primates. Mov Disord. 17(Suppl 5): 155.

Williams D, Tijssen M, Van BG, Bosch A, Insola A, Di L, V, Mazzone P, Oliviero A, Quartarone A, Speelman H, Brown P (2002) Dopamine-dependent changes in the functional connectivity between basal ganglia and cerebral cortex in humans. Brain 125:1558-1569.

Williams D, Kuhn A, Kupsch A, Tijssen M, Van BG, Speelman H, Hotton G, Yarrow K, Brown P (2003) Behavioural cues are associated with modulations of synchronous oscillations in the human subthalamic nucleus. Brain 126:1975-1985.

Williams D, Kuhn A, Kupsch A, Tijssen M, Van BG, Speelman H, Hotton G, Loukas C, Brown P (2005) The relationship between oscillatory activity and motor reaction time in the parkinsonian subthalamic nucleus. Eur J Neurosci 21:249-258.

Wingeier B, Tcheng T, Koop MM, Hill BC, Heit G, Bronte-Stewart HM (2006) Intra-operative STN DBS attenuates the prominent beta rhythm in the STN in Parkinson's disease. Exp Neurol 197:244-251.

Womelsdorf T, Schoffelen JM, Oostenveld R, Singer W, Desimone R, Engel AK, Fries P (2007) Modulation of neuronal interactions through neuronal synchronization. Science 316:1609-1612.

Wooten GF (2003) Agonists vs levodopa in PD: the thrilla of whitha. Neurology 60:360-362.

Yelnik J (2002) Functional anatomy of the basal ganglia. Mov Disord 17 Suppl 3:S15-S21.

Yelnik J (2007) PPN or PPD, what is the target for deep brain stimulation in Parkinson's disease? Brain 130:e79.

Zrinzo L, Zrinzo LV, Hariz M (2007) The peripeduncular nucleus: a novel target for deep brain stimulation? Neuroreport 18:1301-1302.

Zeitler M, Fries P, Gielen S (2006) Assessing neuronal coherence with single-unit, multi-unit, and local field potentials. Neural Comput 18(9):2256-81.